# QUANTITATIVE ANALYSIS OF SOLID SURFACES BY AUGER ELECTRON SPECTROSCOPY

Aleksander Jabłoński

Institute of Physical Chemistry
of the Polish Academy of Sciences

http://rcin.org.pl

A-21-2
A-21-7
A-21-15
K-k-219 R-g-161
H-66

INSTITUTE OF PHYSICAL CHEMISTRY
OF THE POLISH ACADEMY OF SCIENCES
DEPARTMENT OF CATALYSIS ON METALS

# QUANTITATIVE ANALYSIS OF SOLID SURFACES BY AUGER ELECTRON SPECTROSCOPY

by

Aleksander Jabłoński

Warszawa, 1982

Biblioteka Instytutu Chemii Fizycznej PAN
F-B.229/83

http://rcin.org.pl

Copyright © Institute of Physical Chemistry
Polish Academy of Sciences
01-224 Warszawa, ul.Kasprzaka 44/52

All rights Reserved. No part of this publication may be reproduced, stored in a retrieval system or transmitted in any form or by any means: electronic, electrostatic, magnetic tape, mechanical, photocopying, recording or otherwise, without permission in writing from the publishers.

First edition 1982

Printed in Poland

B 229/83

http://rcin.org.pl

The author would like to thank
Professor W. Palczewska for
stimulating discussions, support
and encouragement throughout the
course of this work

http://rcin.org.pl

Contents

1. Introduction 1

2. Notation 4

3. Assumptions of quantitative Auger electron spectroscopy 8

4. Mathematical formalism of Auger electron spectroscopy 12

4.1. Electron probe microanalysis 12

4.2. Auger electron spectroscopy 15

5. Correcting factors of quantitative Auger electron spectroscopy 22

5.1. The backscattering factor 22

5.1.1. Experimental methods for determining the backscattering factor 26

5.1.1.1. Method of Gallon 26
5.1.1.2. Method of Gerlach and DuCharme 27
5.1.1.3. Method of Goto et al. 28
5.1.1.4. Method of Meyer and Vrakking 30

5.1.2. Theoretical methods for determining the backscattering factor 30

5.1.2.1. Method based on Everhart's theory 31
5.1.2.2. The Monte Carlo method 32

5.1.3. Compilation of the values of the backscattering factor 35

5.1.4. The relation between the backscattering factor in AES and the function $\phi(0)$ in EPMA 44

5.1.5. The effect of the Coster-Kronig transitions on the value of the backscattering factor 59

5.1.6. The dependence of the backscattering factor on the composition of solids 62

5.1.7. Conclusions 63

5.2. The inelastic mean free path 66

5.2.1. The experimental values of the inelastic mean free path 67

http://rcin.org.pl

5.2.2. The theoretical values of the inelastic mean free path 70

5.2.3. The dependence of the inelastic mean free path on the composition of solids 72

5.2.4. Conclusions 75

5.3. The number of atoms in unit volume and the monolayer thickness 76

6. Experimental aspects of quantitative Auger electron spectroscopy 79

6.1. Electron energy analysers 79

6.1.1. The retarding field analyser (RFA) 79

6.1.2. The cylindrical mirror analyser (CMA) 80

6.2. The measure for the Auger electron current 83

6.3. Experimental procedures 87

6.3.1. Relative sensitivity factor approach 88

6.3.2. Direct comparison with a standard 92

7. Proposition of an universal algorithm for calculating the surface composition of binary alloys 94

7.1. Section A 96

7.2. Section B 96

7.3. Section C 98

7.4. Section D 99

7.5. Input and output data 101

8. Examples of calculations 106

9. Concluding remarks 119

Appendix 122

References 138

http://rcin.org.pl

http://rcin.org.pl

## 1. Introduction

In recent years the Auger electron spectroscopy has become a well established technique for studies of solid surfaces. The physical basis for this technique is the so-called Auger transition. The Auger process is a radiationless reorganization of an ionized atom. When the ionized shell is filled by an electron from the outer shell, the released energy may ionize another shell in the atom. As a result, an electron is ejected from the atom with energy characteristic for the atomic number and the atomic shells involved in transition. Both the deactivation process and the ejected electron are named after their discoverer (Auger, 1925a,b).

First analytical applications of the Auger effect were started in fifties by works of Lander (1953) and Harrower (1956). They were studying the fine structure of the energy distribution of electrons backscattered from a solid. Both authors identified Auger features on a slowly varying background of secondary electrons. Lander (1953) suggested that the excitation of Auger transitions in a solid by a beam of monoenergetic electrons provides an interesting technique for surface analysis. He pointed out that, due to the high attenuation of electrons in solid, the technique enables the qualitative analysis of a surface region with thickness of several atom layers. However, the fast development of Auger electron spectroscopy began in late sixties. Harris (1968) has shown that the Auger features in the energy spectra become more prominent on differentation. He has indicated that the Auger electron spectroscopy is well suited for detection of surface contaminations and for investigation of surface processes such as surface migration, segregation and diffusion.

http://rcin.org.pl

Tharp and Scheibner (1967), Weber and Peria (1967) and Palmberg (1968) pointed out that the low energy electron diffraction (LEED) optics may be used in recording the Auger electron spectra (the retarding field analyzer). The cylindrical mirror analyser, introduced to Auger electron spectroscopy by Palmberg et al. (1969), made possible obtaining the high quality spectra. The bibliographies of papers on Auger electron spectroscopy published up to early 1972 list by then over three hundred items (Haas et al., 1971, Chang, 1974). The fundamentals, experimental aspects and analytical possibilities of Auger electron spectroscopy have been discussed in books and extensive review papers (Ertl and Küppers, 1974b, Chang, 1974, Joshi et al., 1975, Chattarji, 1976). The tables of the Auger electron spectra were compiled to facilitate the identification of elements, and thus, the qualitative analysis of the surface region (Palmberg et al., 1972, McGuire, 1979).

The possibility of quantitative analysis of the solid surfaces by AES has already been mentioned by Harris (1968). The growing interest of research and industrial laboratories in surface studies has stimulated the rapid progress in quantitative Auger electron spectroscopy over the last few years (Holloway, 1978, Shimizu and Ichimura, 1981). AES as a quantitative technique requires a simple formula relating the Auger electron current collected by the analyzer to the concentration of a given element in the surface region. The formalism, widely used at the present time, involves accurate measurements of the Auger electron current, a knowledge of the inelastic mean free path of Auger electrons, and a knowledge of some measure accounting for the influence of backscattered electrons on the Auger electron yield.

Palmberg (1973) has pointed out that physical similarities

http://rcin.org.pl

exist between Auger electron spectroscopy and electron probe microanalysis (EPMA). In both cases the sample is bombarded with a beam of electrons to ionize the solid atoms, and the products of deactivation are analysed, Auger electrons or X-ray quanta. Thus, one can expect that the same formalism applies to both methods. The electron probe microanalysis is now the routine quantitative technique for determining the composition of solids. The accuracy is usually better than 2% within the sampling depth of this technique, i.e. several micrometers (Reed, 1975a). For this reason EPMA is not considered to be surface sensitive. The calculations of concentration in EPMA are based on a system of four corrections accounting for phenomena that influence the X-ray yield, i.e. the electron backscattering, the X-ray absorption, the stopping power and the fluorescence. A correction approach is also applied in quantitative AES. The corrections take into account similar effects as in EPMA, i.e. the electron backscattering, attenuation of Auger electrons and the variations in atomic density. The accuracy of quantitative AES at present is lower than the accuracy of EPMA. The errors in determining the surface composition may reach 20%. Such errors are mainly due to uncertainties in determining the corrections, and to other factors affecting the Auger electron yield which are difficult to control, e.g. the surface roughness, the diffraction effects, etc.

The objective of the present work is to discuss the mathematical formalism of quantitative AES, to review the methods for determining the correcting factors and, basing on recent results, to propose the universal algorithm for calculations of the surface composition. Also, the present work summarizes the contribution of the author to the field of quantitative AES.

http://rcin.org.pl

## 2. Notation

The mathematical formalism of quantitative Auger electron spectroscopy involves a number of parameters, which in general may depend on the composition of solid under investigation (the matrix) and the Auger transitions chosen for analysis. Let us denote such a parameter by $Q$. In the presented formalism each quantity $Q$ will be accompanied by the superscript and the subscript according to the following rules:

$$Q^{\mu}_{\nu}$$

Superscript $\mu$ specifies the matrix, i.e. the chemical surrounding of a given region in solid. The following symbols are encountered.

i - the matrix is an almost pure i-th element.

o - the quantity $Q$ is independent of a matrix.

blank - the matrix is an alloy.

s - the quantity $Q$ is associated with the surface region.

b - the quantity $Q$ is associated with the bulk.

The usual experimental techniques of quantitative analysis involve the choice of one Auger transition for each elemental constituent of an alloy. Thus, the atomic species and the Auger transition can be denoted by the same index. Therefore, the subscript $\nu$ denotes the Auger transition or elements determining the quantity $Q$. The following indexes are met with:

http://rcin.org.pl

i,j - refer to chosen Auger transitions in i-th and j-th elements, respectively.

i - refers to a chosen Auger transition in i-th element, or to the i-th element.

blank - refers to a chosen Auger transition (or a given element), or the quantity Q is independent of a chosen Auger transition (or a given element).

The parameters Q of the presented formalism are listed below with exemplary indexes.

$A^o$ - the atomic mass.

$A_i^o$ - the atomic mass of i-th element.

C - the mass fraction.

$C^s$ - the mass fraction of a given element in the surface region.

$C_i^s$ - the mass fraction of i-th element in the surface region.

d - the inelastic mean free path of Auger electrons associated with a given Auger transition.

$d_i^j$ - the inelastic mean free path of Auger electrons associated with Auger transition in i-th element in a matrix being almost pure j-th element.

$H_i$ - the Auger electron intensity corresponding to Auger transition in i-th element, recorded from a given alloy.

$H_i^i$ - the Auger electron intensity recorded from pure i-th element.

$k_i^o$ - the spectrometer constant for Auger transition in i-th element.

M - the total number of atoms per unit volume of an alloy.

$M^i$ - the total number of atoms per unit volume of pure i-th element.

N - the number of atoms of a given element in unit volume of an alloy.

http://rcin.org.pl

$P_{i,j}$ - the relative sensitivity factor associated with Auger transitions in i-th and j-th elements, respectively.

$r$ - the backscattering factor for an alloy corresponding to a given Auger transition.

$r_i^j$ - the backscattering factor corresponding to Auger transition in i-th element in a matrix being almost pure j-th element.

$S_i^o$ - the analyzer function for Auger transition in i-th element.

$t$ - the monolayer thickness.

$t^i$ - the monolayer thickness for a pure i-th element.

$X$ - the atom fraction.

$X_i^s$ - the atom fraction of i-th element in the surface region.

$\rho$ - the density of an alloy.

$\rho^i$ - the density of pure i-th element.

The fundamental physical constants have their usual notation

$a_o$ - the Bohr radius.

$e$ - the elementary charge.

$\hbar$ - the Planck constant.

$m$ - the electron rest mass.

$N_o$ - the Avogadro constant.

Other, more important symbols are the following

$E$ - the electron energy.

$E_o$ - the primary electron energy.

$E_A$ - the Auger electron energy.

$E_c$ - the ionization energy.

$I_o$ - the current of primary electrons.

$I_A$ - the Auger electron current collected by the analyser.

$I_X$ - the X-ray intensity collected by the analyzer.

http://rcin.org.pl

$P_A$ - the probability that Auger transition follows the ionization.

$P_X$ - the probability that X-ray ejection follows the ionization.

$U = E/E_c$ - the reduced energy for a given electron.

$U_o = E_o/E_c$ - the reduced energy for primary electrons.

$W = E/E_o$ - the fractional energy.

Z - the atomic number.

$\alpha$ - the escape angle, i.e. the angle between a given direction and the surface normal.

$\eta$ - the backscattering coefficient, i.e. the fraction of the primary current reflected from a solid with energy exceeding 50 eV.

$\mu$ - the mass attenuation coefficient for X-rays in units of $cm^2/g$.

$\sigma(E)$ - the ionization cross section at the electron energy E .

$\phi(\rho z)$ - the function determining the density of ionizations versus the distance from the surface, z .

$\phi(0)$ - the surface ionization function in electron probe microanalysis.

$\psi$ - the take-off angle, i.e. the angle between a given direction and the surface plane.

$\Delta\Omega$ - the solid angle subtended by the analyser.

The symbols of remaining parameters, of auxiliary character in the present considerations, are explained in the text.

http://rcin.org.pl

## 3. Assumptions of quantitative Auger electron spectroscopy

The assumptions on which the quantitative analysis is based may be systematized into several groups:

I. The assumptions specifying the geometry and physical properties of the solid under investigation.

The following assumptions are made here:

I A. The surface of the solid is ideally flat.

The surface roughness has been found to influence the Auger electron yield (Chang, 1974, Holloway, 1975a). There is a number of effects caused by the surface roughness: the variation in the local incidence angle, the excitation and detector shielding,the reflection of escaping electrons, and the recapture of energetic electrons. These effects decrease the detected Auger electron current. To make the assumption I A valid, it is necessary to polish the surfaces to be analysed. In cases when it is impossible, e.g. analysis of powders, fractured surfaces etc., the surface roughness should be similar in all samples investigated. Then, the effect of the surface roughness on the Auger electron yield may be assumed to be similar for each sample, and thus it may be partially cancelled when taking the ratio of Auger electron intensities.

I B. The solid is a set of randomly distributed atoms (randium).

Random distribution of atoms in solid should result in avoiding the diffraction effects (Dejardin-Horgues et al., 1976). In other words, the Auger yield is supposed not to be affected by

http://rcin.org.pl

the diffraction effects. There are two processes that may influence the spatial distribution of electrons (Chang, 1975).
(i) the diffraction of the primary beam;
(ii) the diffraction of the ejected Auger electrons.
The intensity of Auger electrons originating from single crystal surfaces may have rather complicated space structure being the function of the polar and azimuthal angles and the atomic number of solid (McDonnell et al., 1975, Noonan et al., 1976, Allié et al., 1976, Weeks and Liebsch, 1977). Such spatial distribution of Auger electrons is difficult to account for in quantitative analysis. For this reason the quantitative approach applies rather to polycrystalline materials, since such materials resemble the model of randium. The spatial distribution of Auger electrons ejected from surfaces of polycrystalline samples is much simpler than in the case of single crystals (Harris, 1969, Matsudaira and Onchi, 1978); it seems to follow the cosine law (Matsudaira and Onchi, 1978).

I C. The solid is a binary alloy or a pure material.

The limitation imposed by the assumption I C is due to the present lack of the experimental and theoretical data on correcting factors for multicomponent alloys. Most of the published data on corrections, e.g. the backscattering correction or the inelastic mean free path, refer to pure elements. The composition dependence of both corrections is discussed only in few papers, but the discussion is restricted to binary alloys (Holloway, 1977, Jabłoński, 1978, 1979b, 1980a, Streubel et al., 1978, Berndt et al. 1980).

The quantitative analysis of multicomponent systems is also

http://rcin.org.pl

possible at present. When one of the components is in prevalence the corrections can be calculated for the pure prevalent component (Hall and Morabito, 1979). Also, the corrections may be omitted in quantitative analysis (Palmberg et al., 1972). In the latter case the omission of the correcting procedure may introduce significant errors.

II. The assumption specifying the model of the surface region.

The models of the surface region are discussed in section 4 (assumptions II A and II B).

III. The assumptions simplifying the definitions and the determination of the correcting factors.

The relevant assumptions are formulated and discussed in section 5.1 (assumptions III A, III B and III C) and in section 5.3 (assumptions III D).

IV. The assumptions specifying the geometry and physical properties of Auger electron production.

The assumptions of this group form the physical basis for the formalism of quantitative Auger electron spectroscopy (Jabłoński, 1979a,b, 1980a).

IV A. The number of ionizations produced by an electron in the solid, dn, per increment of electron path length, dx, is given by the formula

$$dn = N\,\sigma(E)\,dx$$

http://rcin.org.pl

IV B. The Auger electron emission from the parent atom is isotropic.

IV C. The attenuation of Auger electrons follows the Beer law

$$I' = I \exp(-\text{const} \cdot x)$$

where $I$ and $I'$ are intensities before and after passing a thickness $x$ of a solid.

IV D. The primary electrons are bombarding the solid surface at the normal incidence angle.

Identical assumptions, with X-ray intensity instead of Auger electron intensity, are made in the case of electron probe microanalysis.

The assumption IV D facilitates the calculations of the surface composition, since most of the published data on correcting factors, especially concerning the electron backscattering, were determined at the normal incidence of the primary beam. Moreover, the cylindrical mirror analyzer, often used in quantitative analysis, is usually equipped with the coaxial electron gun. That geometry is very convenient in analysis at the normal incidence.

http://rcin.org.pl

## 4. The mathematical formalism of Auger electron spectroscopy

As it has been mentioned earlier, similarities exist between Auger electron spectroscopy and electron microprobe analysis. Since the physical basis for AES and EPMA is identical (assumptions IV),we shall expect that similar formalism can be used for both techniques. The analytical potential of EPMA has been developed since early fifties, and it is possible that some problems of quantitative analysis will also apply to AES. Thus, it seems to be advantageous to discuss here the basic aspects of EPMA. At the beginning we shall consider the mathematical formalism of EPMA and find the relation with the formalism of AES. Also, we shall compare the correction procedure in both techniques.

### 4.1. Electron probe microanalysis

The quantitative analysis requires knowledge of an expression relating the measured intensity of X-ray quanta or Auger electrons to the concentration of a given element in the solid. This expression should account for all the physical factors affecting the X-ray or Auger yield. The formalism of EPMA is based on a concept of a function $\phi(\rho z)$ that provides the density of X-ray production as a function of the distance from the surface, z (in mass-thickness units). This function is usually defined as a ratio of X-ray intensity generated in a thin layer of mass-thickness $d(\rho z)$ at a depth $\rho z$ in a bulk specimen to the intensity generated in an isolated thin film of the same mass-thickness (Vignes and Dez, 1968, Love et al., 1974). The above definition follows from the experimental method for determining the function $\phi(\rho z)$ called the "tracer technique" (Castaing and Henoc, 1966,

http://rcin.org.pl

Vignes and Dez, 1968). From this definition and the assumption IV A we obtain

$$\int_0^{\infty} \Phi(\rho z)\, d(\rho z) = N_X / [P_X I_o N \sigma(E_o)/\rho] \qquad (4.1)$$

where $N_X$ is the total number of X-rays produced. The density $\rho$ appears in the right side of eq (4.1) when the dimension of N is $1/cm^3$.

Suppose that an ideally flat solid surface is bombarded with a beam of monoenergetic electrons. Let us determine the number of X-ray quanta, $I_X$, collected by the analyser subtending the solid angle $\Delta\Omega$ at the take-off angle $\Psi$. Taking into account the assumptions IV B, IV C and eq (4.1) we obtain the following formula for the X-ray intensity, $I_X$ (in absence of fluorescence)

$$I_X = \frac{\Delta\Omega}{4\pi} \int_0^{\infty} P_X I_o N\, \sigma(E_o) \frac{1}{\rho}\, \Phi(\rho z) \exp(-\mu\rho z \operatorname{cosec}\Psi)\, d(\rho z) \qquad (4.2)$$

where $\mu$ is the mass attenuation coefficient in units of $cm^2/g$.

In the ZAF method, which is usually applied in quantitative analysis of EPMA, eq (4.2) is rearranged into the product of three correcting factors (Bishop, 1968, Ruste and Gantois, 1975)

$$I_X = \left(- I_o \frac{\Delta\Omega}{4\pi} P_X \frac{N_A}{A^o}\right) C\, f(\chi)\ \ R\, \frac{1}{S} \qquad (4.3)$$

The corrections $f(\chi)$, R and $\frac{1}{S}$ account for processes affecting the X-ray yield, i.e. X-ray absorption, electron backscattering, and electron energy loss, respectively.

The corrections are given by the formulas:

(i) absorption correction

http://rcin.org.pl

$$f(\chi) = \frac{\int_0^\infty \phi(\rho z) \exp(-\chi \rho z)\, d(\rho z)}{\int_0^\infty \phi(\rho z)\, d(\rho z)} \qquad (4.4)$$

where $\chi = \mu \operatorname{cosec} \psi$ ;

(ii) backscattering correction

$$R = 1 - \frac{\int_{E_c}^{E_o} \eta(E)\, \sigma(E) [d(\rho x)/dE]\, dE}{\int_{E_c}^{E_o} \sigma(E) [d(\rho x)/dE]\, dE} \qquad (4.5)$$

where

$$\eta(E) = \int_{E}^{E_o} (d\eta/dE)\, dE$$

and $d\eta/dE$ is the energy distribution of backscattered electrons;

(iii) stopping power correction

$$\frac{1}{S} = \int_{E_c}^{E_o} \sigma(E) [d(\rho x)/dE]\, dE \qquad (4.6)$$

The calculation of correcting factors $f(\chi)$, $R$ and $1/S$ is a routine procedure at present (Reed, 1975b). The ZAF approach can be applied to materials with low X-ray absorption. In the case of long wavelength X-rays the absorption can be considerable (Leroux, 1961). For this case Duncumb and Melford (1966) proposed

http://rcin.org.pl

the so-called "thin film approximation". Let us consider the limit of high absorption coefficients. From eq (4.2) we have

$$\lim_{\chi \to \infty} I_X \chi =$$

$$= \lim_{\chi \to \infty} \frac{\Delta\Omega}{4\pi} P_X I_o N\, \sigma(E_o) \frac{1}{\rho} \chi \int_0^{\infty} \phi(\rho z) \exp(-\chi \rho z)\, d(\rho z) =$$

$$= \frac{\Delta\Omega}{4\pi} P_X I_o N\, \sigma(E_o) \frac{1}{\rho} \int_0^{\infty} \phi(\rho z)\, \delta(\rho z)\, d(\rho z) = \tag{4.7}$$

$$= \frac{\Delta\Omega}{4\pi} P_X I_o N\, \sigma(E_o) \frac{1}{\rho} \phi(0)$$

where $\phi(0)$ is the value of the function $\phi(\rho z)$ at $\rho z = 0$. The quantity $\phi(0)$ is called the surface ionization function (Vignes and Dez, 1968, Reuter, 1972, Ruste and Gantois, 1975, Love et al., 1978b). It follows from the above equation that in the case of severe absorption the X-ray intensity is given by (Duncumb and Melford, 1966, Bishop, 1968, Ruste and Gantois,1975)

$$I_X \cong \left[ \frac{\Delta\Omega}{4\pi} P_X I_o\, \sigma(E_o) \frac{1}{\rho} \right] N \frac{\phi(0)}{\chi} =$$

$$= \left[ \frac{\Delta\Omega}{4\pi} P_X I_o\, \sigma(E_o) \frac{N_A}{A^0} \right] c \frac{\phi(0)}{\chi} \tag{4.8}$$

4.2. Auger electron spectroscopy

Electron probe microanalysis differs from Auger electron spectroscopy in escape depth of a signal. Auger electron spectroscopy samples much smaller depth of a solid than EPMA, 5-30 Å as

http://rcin.org.pl

compared with micrometers, because the attenuation of Auger electrons in solid is much stronger than attenuation of X-ray quanta. The attenuation in AES is usually expressed by the inelastic mean free path of Auger electrons, d . The mean free path may be defined as a distance in which the number of electrons with a given energy diminishes by a factor of e = 2.718. The mean free path so defined is related to the mass attenuation coefficient

$$\mu = 1/(\rho d) \tag{4.9}$$

The other difference between EPMA and AES is in acceptance angle of the analyser. In the case of AES this angle may be significant (e.g. retarding field analyser, section 6.1.1) and calculation of the current collected by the analyser involves integration over the solid angle, subtended by the analyser. Introducing eq (4.9) into eq (4.2) and replacing $P_X$ with the probability of Auger transition $P_A$ we should obtain the formula describing the Auger electron current collected by the analyser

$$I_A = \frac{\Delta\Omega}{4\pi} \int_0^\infty P_A I_o N\, \sigma(E_o)\, \frac{1}{\rho}\, \phi(\rho z)\, \exp\left[-z/(d \cos\alpha)\right] d(\rho z), \tag{4.10}$$

where $\alpha = \pi/2 - \Psi$ is the so-called escape angle, i.e. the angle between escaping Auger electron and the surface normal. In the case of large acceptance angle, i.e. when the escape angle of Auger electrons entering the analyser varies considerably, the Auger electron current is given by

$$I_A = \frac{1}{4\pi} \int_{\Delta\Omega} \int_0^\infty P_A I_o N\, \sigma(E_o)\, \frac{1}{\rho}\, \phi(\rho z)\, \exp\left[-z/(d \cos\alpha)\right] d(\rho z)\, d\Omega \tag{4.11}$$

http://rcin.org.pl

Since the extent of surface segregation in binary alloys is comparable with the sampling depth of Auger electrons (Williams and Nason, 1974, McDavid and Fain, 1975), the number of atoms of element under analysis in unit volume can be a strongly varying function of the distance $\rho z$ in the surface region. We rewrite eqs (4.10) and (4.11) in the form

$$I_A = \frac{\Delta\Omega}{4\pi} P_A I_o \sigma(E_o) \frac{1}{\rho} \int_0^\infty N(\rho z)\, \phi(\rho z)\, \exp\left[-z/(d\cos\alpha)\right] d(\rho z) \tag{4.12}$$

and, more generally

$$I_A = \frac{1}{4\pi} P_A I_o \sigma(E_o) \frac{1}{\rho} \int_{\Delta\Omega} \int_0^\infty N(\rho z)\, \phi(\rho z)\, \exp\left[-z/(d\cos\alpha)\right] d(\rho z) d\Omega \tag{4.13}$$

In any correction approach the equation describing the measured intensity is transformed into the product of concentration of element under analysis, corrections depending in general on composition of the sample, and the constant independent of composition. Eq (4.13) is the physical basis for the correction procedure in AES. It is convenient to base the correction procedure on an idealized model of Auger electron production. This model has the following properties (Jabłoński, 1979a,b)

(i) only primary electrons contribute to the production of Auger electrons in the surface region.

(ii) primary electron trajectory is linear in the surface region.

(iii) primary electron does not change its energy in the surface region.

Instytut Chemii Fizycznej PAN BIBLIOTEKA

http://rcin.org.pl

In that idealized model the function describing the distribution of Auger electron production with the distance from the surface has the simple form

$$\Phi^{(id)}(\rho z) \equiv 1$$

Thus, from eq (4.13) we obtain

$$I_A^{(id)} = \frac{1}{4\pi} P_A I_o \sigma(E_o) \frac{1}{\rho} \int_{\Delta\Omega} \int_0^{\infty} N(\rho z) \exp\left[-z/(d \cos\alpha)\right] d(\rho z) d\Omega \qquad (4.14)$$

The difference between the actual Auger electron current, $I_A$, and the current $I_A^{(id)}$ given by eq (4.14) is accounted for by the correction called the backscattering factor. This correction is defined as a ratio of the Auger electron current recorded by the analyser to the current that would be recorded in the idealized case characterized by the properties (i) - (iii)

$$r = I_A/I_A^{(id)} \qquad (4.15)$$

Substitution of eq (4.14) into eq (4.15) gives

$$I_A = \frac{1}{4\pi} P_A I_o \sigma(E_o) \frac{1}{\rho} r \int_{\Delta\Omega} \int_0^{\infty} N(\rho z) \exp\left[-z/(d \cos\alpha)\right] d(\rho z) d\Omega \qquad (4.16)$$

Obviously, determination of the surface concentration from the measured Auger electron intensities requires knowledge of the function $N(\rho z)$. Further derivation requires at this point the discussion of the model of the surface region.

The calculations based on the regular solution model showed that the concentration of a given element is different in the surface region and in the bulk of metal alloys (Williams and Nason, 1974, Overbury et al., 1975, Jabłoński, 1977). Also, this

http://rcin.org.pl

effect has been found in numerous experimental studies. Both theory (Williams and Nason, 1974) and experiment (McDavid and Fain, 1975) indicate that composition may be different for each atom layer in the surface region approaching eventually the bulk composition. However, the largest difference in composition was found between the first and second atom layers. The surface region in which the concentration variation was noticeable did not exceed 3-4 atom layers. In quantitative AES the model of the surface region has to be considerably simplified. Two assumptions specifying the surface region are made most frequently:

II A. Uniform composition of the surface region within the sampling depth of Auger electrons.

In that case the function $N(\rho z)$ has the simple form

$N(\rho z) = N^s = \text{const.}$

This model can be assumed when the extent of surface segregation is close to the escape depth of Auger electrons.

II B. Uniform composition of the surface region limited to first monolayer. Further layers have the bulk composition.

We have then

$$N(\rho z) = \begin{cases} N^s & \text{for} \quad 0 < z < t \\ N^b & \text{for} \quad t < z \end{cases}$$

where $t$ is the monolayer thickness.

Assumption of this model is justified when the escape depth of Auger electrons is larger than the surface segregation region.

Eq (4.16) has the following form for the model of uniform composition of the surface region

http://rcin.org.pl

$$I_A = \left[ \frac{1}{4\pi} P_A I_o \sigma(E_o) \int_{\Delta\Omega} \cos\alpha \, d\Omega \right] N^s r \, d \qquad (4.17)$$

or, for small variation in the escape angle

$$I_A = \left[ \frac{\Delta\Omega}{4\pi} P_A I_o \sigma(E_o) \cos\alpha \right] N^s r \, d \qquad (4.18)$$

For the case of segregation limited to the first monolayer we obtain from eq (4.16)

$$I_A = \left[ \frac{1}{4\pi} P_A I_o \sigma(E_o) \right] r \, d \int_{\Delta\Omega} \cos\alpha \left\{ N^s \left[ 1 - \exp(-t/(d\cos\alpha)) \right] + \right. \\ \left. + N^b \exp(-t/(d\cos\alpha)) \right\} d\Omega \qquad (4.19)$$

or

$$I_A = \left[ \frac{\Delta\Omega}{4\pi} P_A I_o \sigma(E_o) \cos\alpha \right] r \, d \left\{ N^s \left[ 1 - \exp(-t/(d\cos\alpha)) \right] + \right. \\ \left. + N^b \exp(-t/(d\cos\alpha)) \right\} \qquad (4.20)$$

Since the number of atoms in unit volume $N^s$ can be written as $M^s X^s$, eqs (4.17) - (4.20) relate the surface concentration $X^s$ to the current of Auger electrons collected by the analyser. The parameters in square brackets in eqs (4.17)-(4.20) depend on the Auger transition chosen for analysis ($P_A$, $\sigma(E_o)$), geometry of the experimental setup ($\Delta\Omega$, $\alpha$), and the instrument settings ($I_o$, $E_o$). The product of these parameters is practically independent of the composition of the sample. Remaining parameters, i.e. M, r, d, and t may in general depend on the solid composition. The knowledge of these parameters as well as their composition dependence is necessary in quantitative analysis. They can

http://rcin.org.pl

be considered as correcting factors. One can see that different sampling depth of EPMA and AES resulted in different correction procedure even if the derivation is based on the same general formula (eqs (4.2) and (4.11)).

In the next sections we discuss the present state of art in determining the corrections of AES.

http://rcin.org.pl

# 5. Correcting factors of quantitative Auger electron spectroscopy

## 5.1. The backscattering factor

The backscattering correction accounts for the effect of backscattered electrons on the Auger electron yield. This correction was introduced to quantitative AES analysis by Bishop and Rivière (1969), who were also the first to estimate its numerical value for several elements.

Introducing eqs (4.13) and (4.14) into eq (4.15) we obtain

$$r = \frac{\int_{\Delta\Omega} \int_0^{\infty} N(\rho z)\, \phi(\rho z)\, \exp\left[-z/(d\cos\alpha)\right] d(\rho z)\, d\Omega}{\int_{\Delta\Omega} \int_0^{\infty} N(\rho z)\, \exp\left[-z/(d\cos\alpha)\right]\, d(\rho z)\, d\Omega} \qquad (5.1)$$

The depth of penetration of exciting electrons at energies usually applied in AES is of the order of 1000 Å, which is much greater than the extent of surface segregation. It is then reasonable to assume that the concentration variations of a given element in the surface region do not affect the electron trajectories in the solid. This is equivalent to assumption that the backscattering factor is a bulk property (Bishop and Rivière, 1969) and is independent of the shape of function $N(\rho z)$ in the surface region. Let the function $N(\rho z)$ be constant in the layer contributing to the Auger electron current. Eq (5.1) has then the form (Jabłoński, 1979a,b, 1980a)

http://rcin.org.pl

$$r = \frac{\int_{\Delta\Omega}\int_0^\infty \phi(\rho z)\,\exp[-z/(d\cos\alpha)]\,d(\rho z)\,d\Omega}{\int_{\Delta\Omega}\int_0^\infty \exp[-z/(d\cos\alpha)]\,d(\rho z)\,d\Omega} = \frac{\int_{\Delta\Omega}\int_0 \phi(\rho z)\,\exp[-z/(d\cos\alpha)]\,d(\rho z)\,d\Omega}{\rho d \int_{\Delta\Omega} \cos\alpha\,d\Omega} \tag{5.2}$$

Calculation of the backscattering factor from eq (5.2) requires knowledge of function $\phi(\rho z)$ . However, eq (5.2) is considerably simplified under assumptions discussed below.

The function $\phi(\rho z)$ can be expressed by means of the angular and energy distribution of electrons in the solid, $I(E,\theta;\rho z)$

$$\phi(\rho z) = \frac{\int_{E_c}^{E_o}\int_0^\pi I(E,\theta;\rho z)\,\sigma(E)\,\sec\theta\,d\theta\,dE}{I_o\,\sigma(E_o)} \tag{5.3}$$

Let us assume (Jabłoński, 1979b, 1980a)

III A. The energy and angular distribution is not a function of the distance $\rho z$ in the surface region

$$I(E,\theta;\rho z) = I(E,\theta) \tag{5.4}$$

This is equivalent to assumption that the function $\phi(\rho z)$ does

http://rcin.org.pl

not vary in the region sampled by Auger electrons [cf. eq (5.3)].
From eqs (5.2), (5.3) and (5.4) we obtain

$$r = \frac{1}{I_o\, \sigma(E_o)} \int_{E_c}^{E_o} \int_0^{\pi} I(E, \theta)\, \sigma(E) \sec\theta \, d\theta \, dE \qquad (5.5)$$

The backscattering factor thus defined becomes independent of the solid angle $\Delta\Omega$ .

III B. All electrons in the surface region have constant energy and direction

$$I(E, \theta) = I_o\, \delta(E - E_o)\, \delta(\theta - \theta_o) + I_B(E, \theta) \qquad (5.6)$$

where $\delta(x)$ is the Dirac function, and $I_B(E,\theta)$ is the energy and angular distribution of electrons leaving the solid.
Substitution of eq (5.6) into eq (5.5) gives

$$r = 1 + \frac{1}{I_o\, \sigma(E_o)} \int_{E_c}^{E_o} \int_0^{\pi} I_B(E,\alpha)\, \sigma(E) \sec\alpha \, d\alpha \, dE \qquad (5.7)$$

where $\alpha = \pi - \theta$ is the escape angle.

III C. In the case of normal incidence of the primary beam the angular distribution of the backscattered electrons is independent of energy distribution and follows the cosine distribution (Gallon, 1972, Gerlach and DuCharme, 1972).

$$I_B(E,\alpha) = I_B(E)\, f(\alpha) \qquad (5.8)$$

where $I_B(E)$ is energy distribution of electrons leaving the solid, and

$$f(\alpha) = 2 \sin\alpha \cos\alpha \qquad (5.9)$$

http://rcin.org.pl

There are two ways to account for the cosine distribution

(i) Introduction of eqs (5.8) and (5.9) into eq (5.7) gives

$$r = 1 + \frac{2}{I_o\, \sigma(E_o)} \int_{E_c}^{E_o} I_B(E)\, \sigma(E)\, dE \qquad (5.10)$$

(ii) The cosine distribution, i.e. the function (5.9) has maximum at $\alpha = \pi/4$ . One can assume that all backscattered electrons leave the solid at this angle. In that case

$$f(\alpha) = \delta(\alpha - \pi/4)$$

and

$$r = 1 + \frac{\sec \pi/4}{I_o\, \sigma(E_o)} \int_{E_c}^{E_o} I_B(E)\, \sigma(E)\, dE \qquad (5.11)$$

There are some experimental proofs for the cosine distribution of backscattered electrons (Kanter, 1957, Sommerkamp, 1970). Also, the cosine distribution was obtained from Monte Carlo calculations (Murata et al., 1971, Shimizu et al., 1971a).

Equations (5.5), (5.7), (5.10) and (5.11) are usually used in the literature to define the backscattering factor (Bishop and Rivière, 1969, Gallon, 1972, Meyer and Vrakking, 1972, 1974, Palmberg, 1973, 1976, Smith and Gallon, 1974, Jabłoński, 1978).

Gergely et al. (1980a) proposed to separate the term corresponding to elastically reflected electrons in the definition of the backscattering factor, because the fraction of elastically reflected electrons in the total backscattered current may be significant at low primary energies. However, at primary energies usually applied in AES this fraction is rather small. The contribution of the elastically reflected electrons to the backscattered

http://rcin.org.pl

current at primary energy 2.2 keV does not exceed 2% for all atomic numbers (Gergely et al., 1980a,b, Gergely, 1981). This contribution decreases rapidly with the primary energy increase (Gergely et al., 1980b).

### 5.1.1. Experimental methods for determining the backscattering factor

Much attention has been devoted to the problem of determining the backscattering factor. The experimental methods published in the literature will be briefly discussed in this section. The reader is referred to original papers for details.

#### 5.1.1.1. Method of Gallon

Gallon (1972) and Smith and Gallon (1974) proposed an experimental method that makes possible the simultaneous determination of the backscattering factor and the shape of the ionization cross-section energy dependence. The experimental data can be obtained using a standard LEED/Auger spectrometer provided with a retarding field analyser (section 6.1.1.). The experiment involves measurements of the energy distribution of backscattered electrons at different primary energies, and the primary energy dependence of the Auger electron current. Introducing eq (5.10) into eq (4.17) we obtain the following integral equation

$$I_A(E_o)/I_o = D\,\sigma(E_o) + 2\int_{E_c}^{E_o}[I_B(E;\,E_o)/I_o]\,D\,\sigma(E)\;dE \qquad (5.12)$$

where the constant

$$D = \frac{1}{4\pi}\,P_A N^s d\int_{\Delta\Omega}\cos\alpha\;d\Omega$$

http://rcin.org.pl

is independent of the primary energy.
The notation $I_A(E_o)$ and $I_B(E; E_o)$ means that the Auger electron current and the energy distribution are functions of the primary energy. Solving the integral equation (5.12) will provide the function $D\,\sigma(E_o)$ . The backscattering factor can be calculated from eq (5.12) written in the form

$$r = [I_A(E_o)/I_o]/D\,\sigma(E_o) \tag{5.13}$$

The results obtained from Gallon's method were shown to be affected by the use of the simplified definition of the backscattering factor in derivation of the integral equation (5.12) (Jabłoński and Hartweck, 1981). In the case of Auger transitions following the ionization of the $L_3$ shell the error in the ionization cross-section and the backscattering factor reaches 10% and 4%, respectively (Jabłoński and Hartweck, 1981). Larger errors are probable for Auger transitions involving higher shells.

5.1.1.2. Method of Gerlach and DuCharme

Gerlach and DuCharme (1972) assumed that the backscattered electron energy distribution is uniform in the range $E_c < E < E_o$. In that case

$$I_B(E) = I_s/(E_o - E_c) \tag{5.14}$$

where $I_s$ is the current of backscattered electrons with energy higher than $E_c$ .
Introducing eq (5.14) into defining formula (5.10) we obtain

$$r = 2\,\eta_s\,[\,\bar{\sigma}(E_o)/\,\sigma(E_o)] \tag{5.15}$$

where

http://rcin.org.pl

$$\bar{\sigma}(E_o) = \frac{1}{E_o - E_c} \int_{E_c}^{E_o} \sigma(E)\, dE$$

and $\eta_s = I_s/I_o$ is the fraction of primary current backscattered with energy exceeding $E_c$ . The function $\bar{\sigma}(E_o)/\sigma(E_o)$ can be calculated using semiempirical or theoretical expressions for ionization cross-sections (Powell, 1976). The Gerlach and DuCharme method is probably less accurate than Gallon's method due to simplification of the energy distribution.

5.1.1.3. Method of Goto et al.

The method of Goto et al. (1975) requires simultaneous determination of the Auger electron current $I_A$ and the reflection coefficient $\eta$ , i.e. the fraction of primary current reflected with energy exceeding 50 eV. The element under investigation is evaporated on a substrate of considerably larger atomic number. The Auger electron current is then plotted against the reflection coefficient at different thicknesses of the overlayer. As the overlayer thickness increases, the Auger electron current, after passing a maximum, decreases roughly linearly down to the bulk value (fig. 1). The authors postulated that the linear part of the plot extrapolated to $\eta = 0$ should give the Auger electron current produced only by primary electrons. The ratio of the Auger electron current from the bulk of overlayer material to the extrapolated value of the current gives the backscattering factor.

The accuracy of the method of Goto et al. is difficult to estimate. It seems that better results would be obtained if the value of Auger electron current were plotted against the fraction of primary current backscattered with energy exceeding the

http://rcin.org.pl

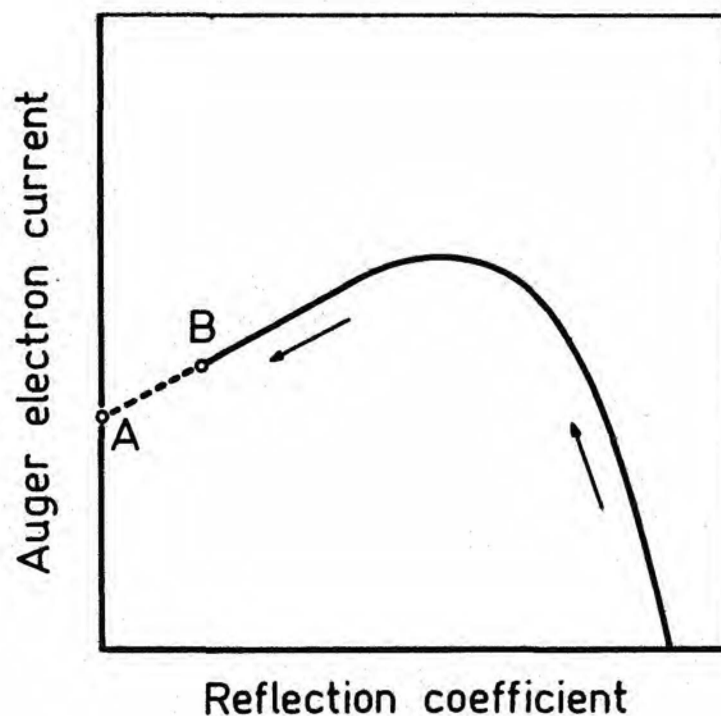


Fig. 1. Sketch of the dependence of the Auger electron yield on the reflection coefficient for overlayers. Arrows indicate the direction of increasing overlayer thickness. Point B: the Auger electron yield from the bulk material; point A: the Auger electron yield corresponding to primary electrons [figure taken from Jabłoński (1979b)].

http://rcin.org.pl

ionization energy, i.e. against the fraction effective in producing ionizations.

#### 5.1.1.4. Method of Meyer and Vrakking

In principle, the backscattering factor can be determined directly from eq (4.17) provided all the remaining parameters are known. This approach was proposed by Meyer and Vrakking (1972) and Vrakking and Meyer (1975).

Experiment involves measurements of the absolute Auger electron current, the primary current, and the surface concentration of a given element. The method of Meyer and Vrakking is subject to large systematic and experimental errors, since the absolute values of all parameters are required. Some of them are known with limited accuracy, e.g. the error in the value of $\sigma(E)$ reaches 15%.

### 5.1.2. Theoretical methods for determining the backscattering factor

The theoretical determination of the backscattering factor requires knowledge of the ionization cross-section energy dependence and the angular and energy distribution of backscattered electrons [cf. eqs (5.7), (5.10), (5.11)]. The theoretical approach to the problem is based on calculation of both functions using existing theoretical or semiempirical methods. As follows from eqs (5.7), (5.10) and (5.11), the absolute value of the ionization cross-section is not necessary in calculations of the backscattering factor. It is sufficient to use the relative values, i.e. the values normalized with respect to the maximum value, so only the shape of the energy dependence is important. The experimental data indicate

http://rcin.org.pl

that the dependence of the ionization cross-section on the reduced energy, $U_o = E_o/E_c$ , has a similar shape for ionization of K, $L_{23}$ and $M_{45}$ shells (Glupe and Mehlhorn, 1967, 1971, Meyer and Vrakking, 1973, Vrakking and Meyer, 1973, 1975). The experimental data also compare well with the theoretical and semiempirical expressions describing the ionization cross-section energy dependence (Powell, 1976). The Gryziński (1965) theoretical formula was used in calculations of the backscattering factor described below.

5.1.2.1. Method based on Everhart's theory

The semiempirical approach of Everhart makes possible the calculation of the angular and energy distribution of electrons backscattered from low atomic number materials ($Z < 40 - 45$) (Everhart, 1960, Archard, 1961). The energy spectra resulting from the theory are found to be in reasonable agreement with the experimental data (McAfee, 1976, Iafrate et al., 1976). Everhart's theory is based on the following assumptions:

(i) Electrons passing through the solid undergo a continuous energy loss, which is a function of the distance traversed.

(ii) An electron changes its direction as a result of scattering by a Coulomb field of bare nucleus.

(iii) Electrons scattered through an angle less than $\pi/2$ are treated as if they are not scattered at all. Those scattered through an angle greater than $\pi/2$ are leaving the target.

If the Thomson-Whiddington law is used to express the continuous energy loss, the angular and energy distribution of backscattered electrons has the form (Jabłoński, 1978)

http://rcin.org.pl

$$I_B(E,\alpha) = \frac{4\ a\ I_o E}{E_o^2} \left(1 - \frac{\cos\alpha}{1 + \cos\alpha}\ w\right)^{a-1} \frac{\sin\alpha \cos\alpha}{(1 + \cos\alpha)^3} \qquad (5.16)$$

where $w = 1 - (E/E_o)^2$ and $a = 0.045\ Z$ . Substituting eq (5.16) into eq (5.7) we obtain the following expression (Jabłoński,1978)

$$r = 1 + \frac{4a}{U_o^2\ \sigma(U_o)} \int_1^{U_o} U\ \sigma(U)\ \Phi(a,\ w)\ dU \qquad (5.17)$$

where

$$\Phi(a,\ w) = \frac{w(a + 1) - 1 - (1 - w/2)^a \left[w(a/2 + 1) - 1\right]}{w^2 a(a + 1)}$$

The integral in the right-hand side of eq (5.17) is easily calculated using the Gaussian quadrature method.

### 5.1.2.2. The Monte Carlo method

The Monte Carlo method was widely used to simulate the scattering of kilovolt electrons in solid targets (Green, 1963, Bishop, 1965, 1967, Reimer, 1968, Murata et al., 1971, 1972, Shimizu and Murata, 1971, Shimizu et al., 1972a,b, 1975, 1976, Matsukawa et al., 1973, Murata, 1974, 1976, Jabłoński, 1979a,1980a, Shimizu and Ichimura, 1981). This method has also been proved to be a useful tool in calculations of the backscattering factor (Bishop and Rivière, 1969, Kirschner, 1977, El Gomati et al., 1979, Jabłoński, 1979a, 1980a, Shimizu and Ichimura, 1981). The Monte Carlo approach involves generating a number of individual electron trajectories consisting of linear steps, at the end of which the energy and the direction of an electron are suddenly changed. Several Monte Carlo schemes published so far differ

http://rcin.org.pl

in calculation of the basic factors of electron trajectory, i.e. in calculation of the scattering angle, the step length and the electron energy loss along the trajectory. The schemes can be roughly divided into two groups: the multiple scattering schemes (Green, 1963, Bishop, 1965, 1967, Shimizu and Murata, 1971, Shimizu et al., 1972a,b) and the single scattering schemes (Reimer, 1968, Murata et al., 1971, 1972, Matsukawa et al., 1973, Murata, 1974, 1976, Shimizu et al., 1975, 1976, Shimizu and Ichimura, 1981). In the multiple scattering scheme one step summarizes the effect of a considerable number of elastic collisions, while in the case of the single scattering scheme one scattering event takes place in one step. The latter scheme provides an electron trajectory closer to the real one and is thus considered to be more accurate (Murata et al., 1972, Matsukawa et al., 1973). On the other hand it requires much more computer time (Shimizu et al., 1972a,b). The main features of the single scattering scheme for an elemental solid are briefly sketched below. The electron scattering is usually described by the screened Rutherford cross-section

$$\frac{d\,\sigma(\theta)}{d\Omega} = \frac{Z^2e^4}{p^2v^2}\,\frac{1}{(1-\cos\theta+2\beta)^2} \tag{5.18}$$

where $p$ and $v$ is momentum and velocity of an electron, respectively,

$$\beta = \frac{1}{4}\left[\mu(\hbar/p)\,(Z^{1/3}/0.885a_o)\right]^2$$

and $\mu$ is the screening parameter (Jabłoński, 1981a). The step length is calculated from the formula

$$s = 1/(N\,\sigma_t) \tag{5.19}$$

http://rcin.org.pl

where $\sigma_t$ is the total scattering cross-section.

The energy loss is given by the Bethe stopping-power formula

$$\frac{dE}{dx} = - \frac{2\pi e^4 N Z}{E} \ln \frac{1.166 E}{J} \tag{5.20}$$

where J is the mean excitation energy.

This Monte Carlo algorithm was extensively used by Murata et al. (1971, 1972), Murata (1974, 1976) and Matsukawa et al. (1973) in calculations associated with electron probe microanalysis.

The single scattering Monte Carlo scheme makes possible calculations of the backscattering factor from the general formula (5.2). For the case of the cylindrical mirror analyser this formula may be transformed into (Jabłoński, 1979a, 1980a)

$$\bar{r} = \frac{1}{d \cos \alpha_1 \; \sigma(E_o)} \lim_{n \to \infty} \frac{1}{n} \sum_{i=1}^{n} \int_0^{\ell_i} \sigma[E(x)] \; \exp\left[-z_i(x)/(d \cos \alpha_1)\right] dx \tag{5.21}$$

where n is the number of trajectories, $\alpha_1 = 42.3^o$ is the acceptance angle of CMA, $\ell_i$ is the length of i-th trajectory and $z_i(x)$ is the dependence of the distance z on the distance x measured along the i-th trajectory. Eq (5.10) may also be used in calculations; it can be written in the form (Jabłoński, 1979a, 1980a)

$$r_o = 1 + \frac{2}{\sigma(E_o)} \lim_{n \to \infty} \frac{1}{n} \sum_{j=1}^{n_B} \sigma(E_j) \tag{5.22}$$

where $n_B$ is the number of backscattered electrons and $E_j$ is energy of j-th backscattered electron. It turned out that it is necessary to generate about 10000-30000 trajectories to obtain accuracy of 1% (Jabłoński, 1979a, 1980a).

http://rcin.org.pl

The introduced single scattering Monte Carlo algorithm was estimated by Murata et al. (1971) and Murata (1974) to be valid for electron energies exceeding 500 eV. Thus it can be applied only to Auger transitions involving ionization energy higher than this value.

### 5.1.3. Compilation of the values of the backscattering factor

In general, the value of the backscattering factor is characteristic for the incident electron energy and a given Auger electron transition. However, as it will be shown below, the values of $r$ for different Auger transitions in a given element at a given reduced energy are considered to be the same even if ionization energies corresponding to these transitions differ considerably.

Almost all theoretical and semiempirical expressions describing the ionization cross-section can be written in the form (Powell, 1976)

$$\sigma(E)E_c^2 = \text{const} \cdot g(U)$$

where $g(U)$ is a function of reduced energy.
On the other hand, the fractional energy distribution of backscattered electrons, $I_B'(W) = I_B'(E/E_0)$, is practically independent of the incident electron energy. Sternglass (1954) found this to be true in the energy range from 400 eV to 2000-3000 eV for carbon, iron, tantalum and platinum. For such an energy range the defining formula (5.10) transforms into (Jabłoński, 1979a,b)

$$r = 1 + \frac{2}{I_0 g(U_0)} \int_{1/U_0}^{1} I'(W)\, g(WU_0)\, dW \qquad (5.23)$$

http://rcin.org.pl

Thus, the backscattering factor is a function of the reduced energy only. Eq (5.23) justifies plotting the values of the backscattering factor against the reduced energy.

Experimental data on the backscattering factor are rather limited at the moment. They are listed in table 1. These data indicate that the backscattering factor increases with the reduced energy and the atomic number of element. There is substantial discrepancy between results of different authors (e.g. silicon). This can be due to systematic and experimental errors which are different for different experimental methods. The method of Gallon is probably most accurate since it does not involve additional simplifying assumptions or postulates.

Values of the backscattering factor calculated from method based on Everhart's theory are listed in table 2. The calculated values are found to be in reasonable agreement with the experimental data for beryllium, carbon, and silicon (fig. 2). They also well compare with values of Bishop and Rivière (1969) obtained from Monte Carlo calculations (fig. 3).

At present, among theoretical methods, the Monte Carlo method seems to be most accurate, because it is based on more realistic scattering law and energy loss law than Everhart's theory, and accounts for multiple scattering of electrons in solid. The single scattering Monte Carlo algorithm has been used in calculations of the reflection coefficient and the angular and energy distribution of backscattered electrons for elements with atomic number up to $Z = 82$ providing fair agreement with experimental data (Murata et al., 1971, 1972, Matsukawa et al., 1973, Murata, 1974, 1976). However, this method can be recommended in calculations of $r$ for Auger transitions involving rather high ioniza-

http://rcin.org.pl

Table 1. Compilation of the experimental values of the backscattering factor [table taken from Jabłoński (1979b)].

| Element | Atomic number | Auger electron energy[a] eV | Primary energy eV | Reduced energy | Experimental method | Backscattering factor | References |
|---|---|---|---|---|---|---|---|
| 1 | 2 | 3 | 4 | 5 | 6 | 7 | 8 |
| Be | 4 | 104 | 800<br>1000<br>1500<br>2000 | | Goto et al. | 1.1<br>1.2<br>1.2<br>1.25 | Goto et al., 1975 |
| C | 6 | 272 | | 2<br>3<br>4<br>5 | Gallon | 1.11[b]<br>1.15[b]<br>1.18 ± 0.03[b]<br>1.21[b] | Smith and Gallon, 1974 |
| Si | 14 | 120 - 510<br>C, N, O, P, S, Cl on Si single crystals | | 3.33-10 | Meyer Vrakking | 1.2 ± 0.1 | Meyer and Vrakking, 1972 |
| Si | 14 | 510<br>O on Si (100)<br><br>152<br>S on Si (100) | | 1.88<br>2.82<br>4.69<br>4.55<br>12.20 | Meyer Vrakking | 1.26 ± 0.10<br>1.30 ± 0.10<br>1.32 ± 0.10<br>1.51 ± 0.10<br>1.62 ± 0.10 | Vrakking and Meyer, 1975 |



http://rcin.org.pl

Table 1. Continued (i)

| 1 | 2 | 3 | 4 | 5 | 6 | 7 | 8 |
|---|---|---|---|---|---|---|---|
| Si | 14 | 92 | | 3<br>4<br>5<br>6<br>7<br>8<br>9<br>10 | Gallon | 1.32[b]<br>1.38[b]<br>1.42[b]<br>1.47[b]<br>1.51[b]<br>1.55[b]<br>1.58[b]<br>1.60[b] | Smith and Gallon, 1974 |
| Ge | 32 | 120 - 510<br>C, N, O, P, S, Cl<br>on Ge single crystals | | 3.33-10 | Meyer Vrakking | 1.3 ± 0.1 | Meyer and Vrakking, 1972 |
| Se | 34 | 99 | | 2<br>3<br>4<br>5<br>6 | Gallon | 1.27[b]<br>1.38[b]<br>1.46[b]<br>1.53[b]<br>1.59[b] | Smith and Gallon, 1974 |



http://rcin.org.pl

Table 1. Continued (ii)

| 1 | 2 | 3 | 4 | 5 | 6 | 7 | 8 |
|---|---|---|---|---|---|---|---|
| Ag | 47 | 351 , 356 | | 2<br>3<br>4<br>5 | Gallon | 1.34[b]<br>1.45[b]<br>1.51[b]<br>1.55[b] | Smith and Gallon, 1974 |
| Gd | 64 | 138 | | 3<br>4<br>5 | Gallon | 1.53[b]<br>1.66[b]<br>1.82[b] | Smith and Gallon, 1974 |
| W | 74 | 272<br>C on W (100) | | 1.06<br>1.41<br>1.76<br>2.46<br>3.52<br>4.23<br>5.29 | Gerlach DuCharme | 1.06[d]<br>1.20[d]<br>1.26[d]<br>1.34[d]<br>1.36[d]<br>1.40[d]<br>1.52[d] | Gerlach and DuCharme, 1972 |
| Au | 79 | 69 | | 1.5[c]<br>2[c]<br>3[c]<br>4[c] | Gallon | 1.28[b]<br>1.52[b]<br>1.77[b]<br>1.88 $\pm$ 0.05[b] | Smith and Gallon, 1974 |



http://rcin.org.pl

Table 1. Continued (iii)

| 1 | 2 | 3 | 4 | 5 | 6 | 7 | 8 |
|---|---|---|---|---|---|---|---|
| Au | 79 | 69 | 2000 | | Gallon | 1.94 ± 0.08 | Shaw and Fain, 1977 |

[a] Energies reported in Palmberg et al. (1972).

[b] Values taken from the plot.

[c] Scaled using the ionization energy of $N_{4,5}$ shell, i.e. 352 eV.

[d] The relation between the parameter $\gamma_B$ of Gerlach and DuCharme and r given by eq (5.10) has the form: $r = 1 + 2\gamma_B$ .



http://rcin.org.pl

Table 2. Values of the backscattering factor calculated from the method based on Everhart's theory of electron backscattering [eq (5.17)].

| $U_0$ | Beryllium | Carbon | Aluminum | Silicon | Titanium | Copper | Selenium |
|---|---|---|---|---|---|---|---|
| 1.1 | 1.010 | 1.015 | 1.032 | 1.035 | 1.054 | 1.072 | 1.084 |
| 1.5 | 1.040 | 1.059 | 1.127 | 1.136 | 1.211 | 1.274 | 1.318 |
| 2.0 | 1.064 | 1.096 | 1.203 | 1.218 | 1.335 | 1.433 | 1.501 |
| 2.5 | 1.082 | 1.122 | 1.258 | 1.277 | 1.423 | 1.544 | 1.628 |
| 3 | 1.096 | 1.143 | 1.301 | 1.322 | 1.491 | 1.629 | 1.724 |
| 4 | 1.117 | 1.174 | 1.364 | 1.390 | 1.591 | 1.755 | 1.866 |
| 5 | 1.132 | 1.196 | 1.410 | 1.440 | 1.664 | 1.846 | 1.969 |
| 6 | 1.144 | 1.214 | 1.446 | 1.478 | 1.720 | 1.916 | 2.048 |
| 7 | 1.154 | 1.229 | 1.476 | 1.510 | 1.766 | 1.973 | 2.112 |
| 8 | 1.162 | 1.241 | 1.500 | 1.536 | 1.804 | 2.020 | 2.165 |
| 9 | 1.169 | 1.251 | 1.521 | 1.558 | 1.837 | 2.060 | 2.210 |
| 10 | 1.175 | 1.260 | 1.539 | 1.577 | 1.865 | 2.095 | 2.249 |



http://rcin.org.pl

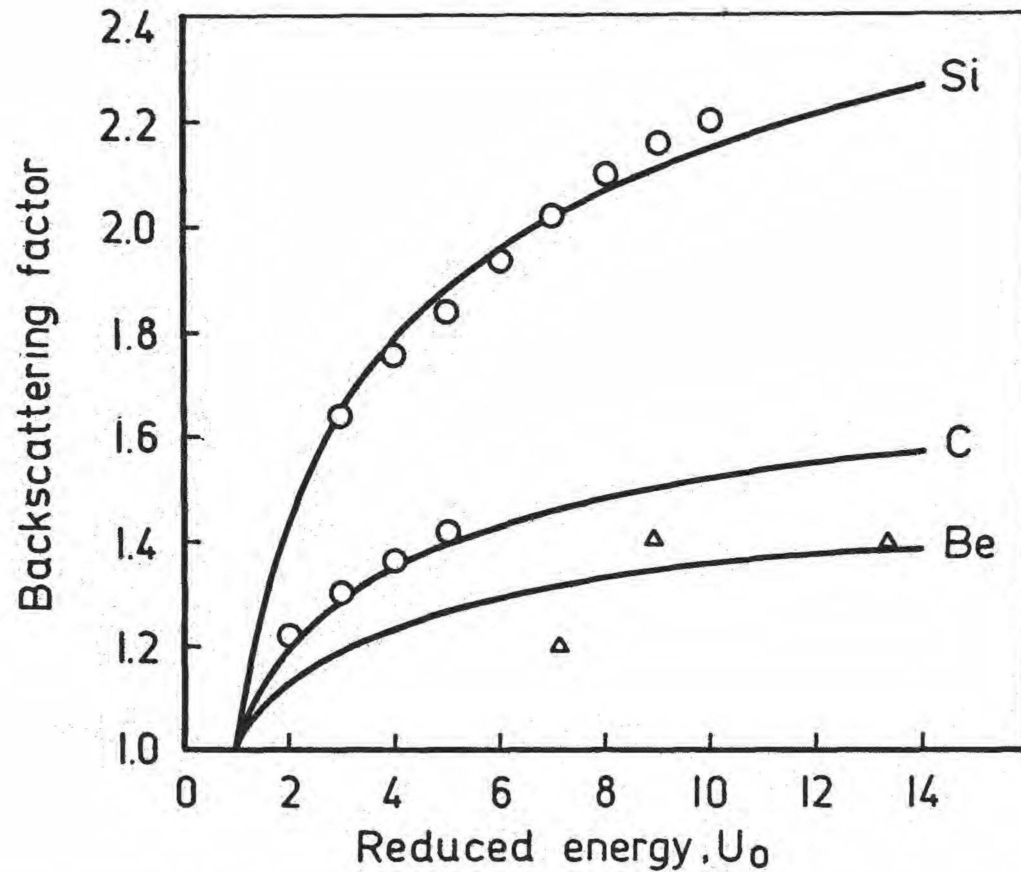


Fig. 2. The reduced energy dependence of the backscattering factor for beryllium, carbon and silicon. Solid line: values calculated from the method based on Everhart s theory; circles: experimental values of Smith and Gallon (1974); triangles: experimental values of Goto et al. (1975) [figure taken from Jabłoński (1979b)].



http://rcin.org.pl

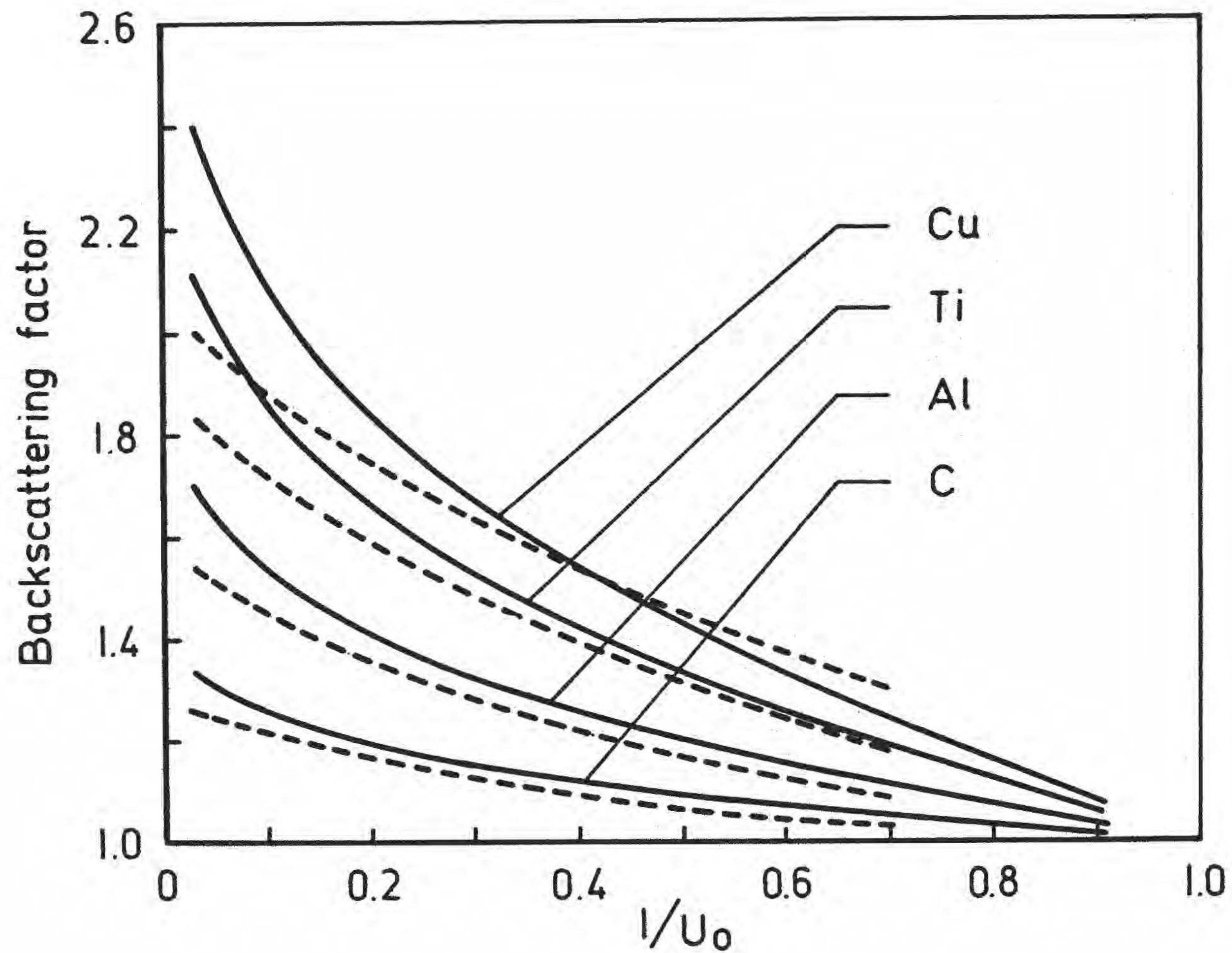


Fig. 3. The reduced energy dependence of the backscattering factor for carbon, aluminium, titanium and copper. Solid line: values calculated from the method based on Everhart's theory; dashed line: multiple scattering Monte Carlo calculations of Bishop and Rivière (1969) [figure taken from Jabłoński (1978)].

http://rcin.org.pl

tion energy, in excess of 500-1000 eV, because the Monte Carlo algorithm is not valid in the range of low electron energies. Using the Monte Carlo method it is possible to estimate the effect of simplifying assumptions III A-III C on the value of the backscattering factor. It is sufficient to compare values $\bar{r}$ and $r_o$ calculated from eqs (5.21) and (5.22). In fact, such calculation has been made for KLL and $L_3MM$ Auger transitions (Jabłoński, 1979a, 1980a). Results are shown in tables 3 and 4. In can be seen that the values of the backscattering factors, resulting from defining formulas (5.2) and (5.10), coincide at sufficiently high primary energies. They start to diverge substantially at reduced energies below 1.5 - 2 in the case of KLL Auger transitions, and at primary energies below 4000-5000 eV in the case of $L_3MM$ Auger transitions.

### 5.1.4. The relation between the backscattering factor in AES and the function $\phi(0)$ in EPMA

Due to small sampling depth of Auger electron spectroscopy as compared with electron probe microanalysis, the formalism of AES should be identical with the "thin film model" of EPMA (section 4). Indeed, remembering that $\chi = \mu \operatorname{cosec} \psi$ and $\mu = 1/(\rho d)$ we can see that eqs (4.8) and (4.18) are equivalent if $\phi(0) \equiv r$ (Jabłoński, 1980b). In fact, the equation defining the function $\phi(0)$ (Bishop, 1968, Ruste and Gantois, 1975) is identical with eq (5.11) although they refer to different primary energies, 10 - 30 keV in the case of EPMA and 1 - 10 keV in the case of AES. Inasmuch as the backscattering factor can be scaled over wide range of primary energies [cf. eq (5.23)] there is a possibility of using the published expressions for the function $\phi(0)$ in

http://rcin.org.pl

Table 3. The values of the backscattering factors $r_o$ and $\bar{r}$ calculated for KLL Auger transitions in carbon, magnesium, aluminum and silicon [table taken from Jabłoński (1979a)].

| $E_o$ | Carbon | | Magnesium | | Aluminum | | Silicon | |
|---|---|---|---|---|---|---|---|---|
| | $r_o$ | $\bar{r}$ | $r_o$ | $\bar{r}$ | $r_o$ | $\bar{r}$ | $r_o$ | $\bar{r}$ |
| 500 | 1.033±.002 | 1.014±.003 | | | | | | |
| 1000 | 1.104±.005 | 1.116±.006 | | | | | | |
| 1500 | 1.134±.007 | 1.143±.008 | 1.003±.001 | .909±.001 | | | | |
| 2000 | 1.152±.008 | 1.153±.009 | 1.037±.003 | 1.029±.003 | 1.015±.002 | .978±.002 | 1.0012±.003 | .8512±.0003 |
| 2500 | 1.169±.008 | 1.166±.010 | 1.075±.004 | 1.079±.005 | 1.053±.003 | 1.053±.004 | 1.030±.002 | 1.016±.003 |
| 3000 | 1.178±.009 | 1.172±.011 | 1.103±.005 | 1.099±.006 | 1.085±.004 | 1.091±.006 | 1.061±.004 | 1.060±.004 |
| 3500 | 1.186±.009 | 1.183±.013 | 1.127±.006 | 1.126±.008 | 1.111±.005 | 1.115±.007 | 1.094±.004 | 1.097±.006 |
| 4000 | 1.191±.010 | 1.179±.013 | 1.157±.006 | 1.156±.008 | 1.137±.006 | 1.144±.008 | 1.121±.005 | 1.119±.007 |
| 4500 | 1.193±.008 | 1.190±.012 | 1.171±.006 | 1.163±.007 | 1.155±.005 | 1.155±.006 | 1.142±.005 | 1.140±.006 |
| 5000 | 1.195±.008 | 1.182±.011 | 1.188±.006 | 1.182±.008 | 1.176±.006 | 1.174±.007 | 1.163±.005 | 1.162±.007 |
| 5500 | 1.199±.009 | 1.184±.011 | 1.199±.006 | 1.192±.008 | 1.187±.006 | 1.185±.008 | 1.184±.006 | 1.181±.007 |



http://rcin.org.pl

Table 4. The values of the backscattering factors $r_o$ and $\bar{r}$ calculated for $L_3MM$ Auger transitions in: (a) vanadium, chromium and manganese; (b) iron, cobalt and nickel; (c) copper, zinc and germanium [table taken from Jabłoński (1980a)].

(a)

| $E_o$ | Vanadium | | Chromium | | Manganese | |
|---|---|---|---|---|---|---|
| | $r_o$ | $\bar{r}$ | $r_o$ | $\bar{r}$ | $r_o$ | $\bar{r}$ |
| 3000 | 1.581±.015 | 1.668±.020 | 1.580±.014 | 1.687±.020 | 1.581±.014 | 1.716±.020 |
| 4000 | 1.637±.016 | 1.683±.022 | 1.643±.016 | 1.720±.022 | 1.636±.015 | 1.704±.021 |
| 5000 | 1.661±.017 | 1.657±.022 | 1.670±.017 | 1.705±.023 | 1.676±.017 | 1.704±.024 |
| 7000 | 1.711±.019 | 1.692±.025 | 1.697±.018 | 1.707±.026 | 1.709±.018 | 1.709±.025 |
| 10000 | 1.720±.020 | 1.661±.026 | 1.731±.019 | 1.702±.026 | 1.743±.019 | 1.708±.026 |



http://rcin.org.pl

Table 4. Continued (i)

(b)

| $E_o$ | Iron | | Cobalt | | Nickel | |
|---|---|---|---|---|---|---|
| | $r_o$ | $\bar{r}$ | $r_o$ | $\bar{r}$ | $r_o$ | $\bar{r}$ |
| 3000 | $1.577 \pm .014$ | $1.718 \pm .019$ | $1.553 \pm .013$ | $1.748 \pm .020$ | $1.562 \pm .013$ | $1.762 \pm .019$ |
| 4000 | $1.631 \pm .015$ | $1.737 \pm .021$ | $1.639 \pm .015$ | $1.754 \pm .021$ | $1.626 \pm .014$ | $1.762 \pm .021$ |
| 5000 | $1.679 \pm .016$ | $1.745 \pm .023$ | $1.674 \pm .016$ | $1.749 \pm .022$ | $1.665 \pm .015$ | $1.744 \pm .022$ |
| 7000 | $1.722 \pm .018$ | $1.738 \pm .025$ | $1.726 \pm .017$ | $1.743 \pm .024$ | $1.719 \pm .017$ | $1.735 \pm .023$ |
| 10000 | $1.760 \pm .019$ | $1.735 \pm .025$ | $1.761 \pm .019$ | $1.760 \pm .027$ | $1.766 \pm .018$ | $1.740 \pm .025$ |



http://rcin.org.pl

Table 4. Continued (ii)

(c)

| $E_o$ | Copper | | Zinc | | Germanium | |
|---|---|---|---|---|---|---|
| | $r_o$ | $\bar{r}$ | $r_o$ | $\bar{r}$ | $r_o$ | $\bar{r}$ |
| 3000 | 1.541±.013 | 1.747±.018 | 1.532±.012 | 1.722±.018 | 1.496±.012 | 1.663±.016 |
| 4000 | 1.632±.014 | 1.781±.021 | 1.624±.014 | 1.756±.020 | 1.577±.013 | 1.688±.018 |
| 5000 | 1.668±.015 | 1.752±.021 | 1.662±.015 | 1.743±.021 | 1.648±.014 | 1.725±.020 |
| 7000 | 1.734±.017 | 1.778±.024 | 1.725±.016 | 1.745±.022 | 1.721±.016 | 1.755±.023 |
| 10000 | 1.789±.018 | 1.781±.025 | 1.770±.018 | 1.747±.024 | 1.784±.017 | 1.777±.024 |



http://rcin.org.pl

quantitative AES. A question arises: what errors are committed in such a case?

Two analytical expressions for the function $\phi(0)$ are used in EPMA: the formula of Reuter (1972)

$$\phi(0) = 1 + 2.8\,(1 - 0.9/U_o)\eta \tag{5.24}$$

and the formula of Love et al. (1978b)

$$\phi(0) = 1 + [\eta/(\eta + 1)]\,[I(U_o) + G(U_o)\ln(1 + \eta)] \tag{5.25}$$

where $I(U_o)$ and $G(U_o)$ are polynomials of $1/U_o$ .

$$I(U_o) = 3.43378 - 10.78720/U_o + 10.97628/U_o^2 - 3.62286/U_o^3 \,,$$

$$G(U_o) = -0.59299 + 21.55329/U_o - 30.55248/U_o^2 + 9.59218/U_o^3 \,.$$

Numerous experimental data on the reflection coefficient $\eta$ have been published in the literature (Sternglass, 1954, Weinryb and Philibert, 1964, Bishop, 1966, Wittry, 1966, Heinrich, 1966, Colby et al., 1967, Drescher et al., 1970, Darlington and Cosslett, 1972, Hunger and Küchler, 1979). Also, several analytical formulas were published expressing $\eta$ in terms of the atomic number of solid (Reuter, 1972, Love and Scott, 1978, Hunger and Küchler, 1979). In the following analysis the Reuter (1972) expression was used

$$\eta = -0.0254 + 0.016\,Z - 0.000186\,Z^2 + 8.3 \cdot 10^{-7}\,Z^3$$

Let us compare the analytical formulas for the surface ionization function $\phi(0)$ with the experimental and theoretical data on the backscattering factor. We will limit the analysis to the data that are most accurate and numerous. For this reason we will use the values of the backscattering factor from four different

http://rcin.org.pl

sources: the experimental data of Smith and Gallon (1974), Monte Carlo calculations of Bishop and Rivière (1969), Monte Carlo calculations for KLL Auger transitions (Jabłoński, 1979a) and Monte Carlo calculations for $L_3MM$ transitions (Jabłoński, 1980a). Fig. 4 compares the experimental data of Smith and Gallon (1974) with the functions $\phi(0)$ . Let us choose the relative difference $100(r - \phi(0))/r$ as a measure of deviation of $\phi(0)$ from $r$ . The histograms of such relative differences are shown in figs. 5 - 8. The standard deviations on the values of the relative difference for all the data considered are listed in table 5. Since the standard deviation is a measure of the scatter in values of the relative differences, the function $\phi(0)$ of Love et al. (1978b) seems to be generally in better agreement with values of $r$ than the function $\phi(0)$ of Reuter (1972).

The quantitative Auger electron spectroscopy involves the ratios of the backscattering factor rather than the absolute values (cf. section 6.3). Let us consider the diluted binary alloy. Comparison of the Auger electron current from the diluted component with the current from the pure diluent (standard) involves knowledge of the ratio of backscattering factors for pure components, both taken at the same reduced energy. Similarly as above, let us choose the relative difference $100(S - F)/S$ as a measure of the deviation of the ratio $F = \phi_i^j(0)/\phi_i^i(0)$ from the ratio $S = r_i^j/r_i^i$ . The histograms of the relative differences between the ratios of the Smith and Gallon data and the ratios of functions $\phi(0)$ are shown in fig. 9. The standard deviations corresponding to such histograms are listed in table 5.

Two conclusions result from the table 5. The expression of Love et al. (1978b) better compares with the theoretical and experimental values of the backscattering factor in practically all

http://rcin.org.pl

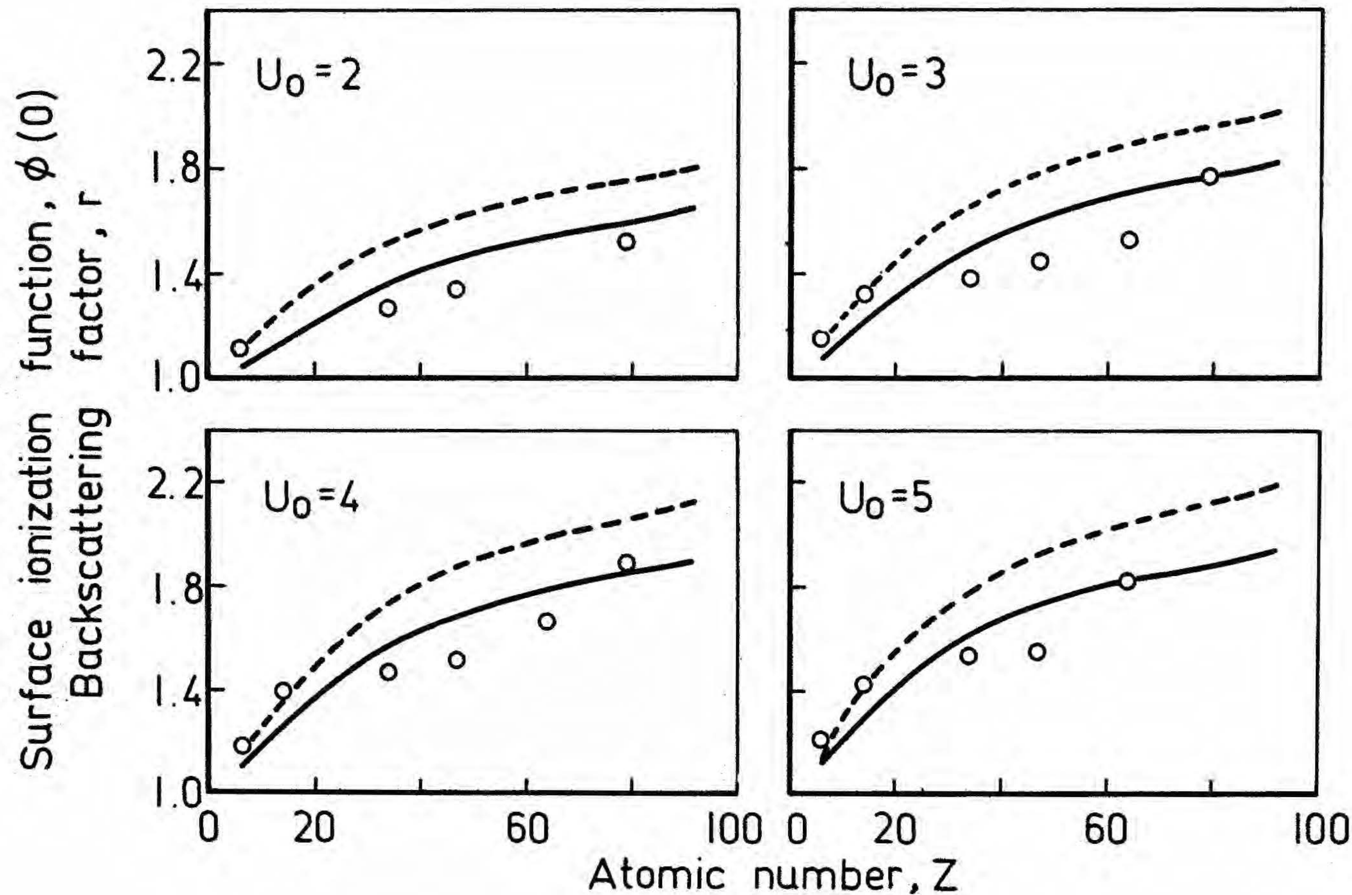


Fig. 4. Comparison of the experimental data on the backscattering factor with functions $\phi(0)$ . Solid line: function $\phi(0)$ of Love et al. (1978b); dashed line: function $\phi(0)$ of Reuter (1972); circles: experimental values of Smith and Gallon (1974).



http://rcin.org.pl

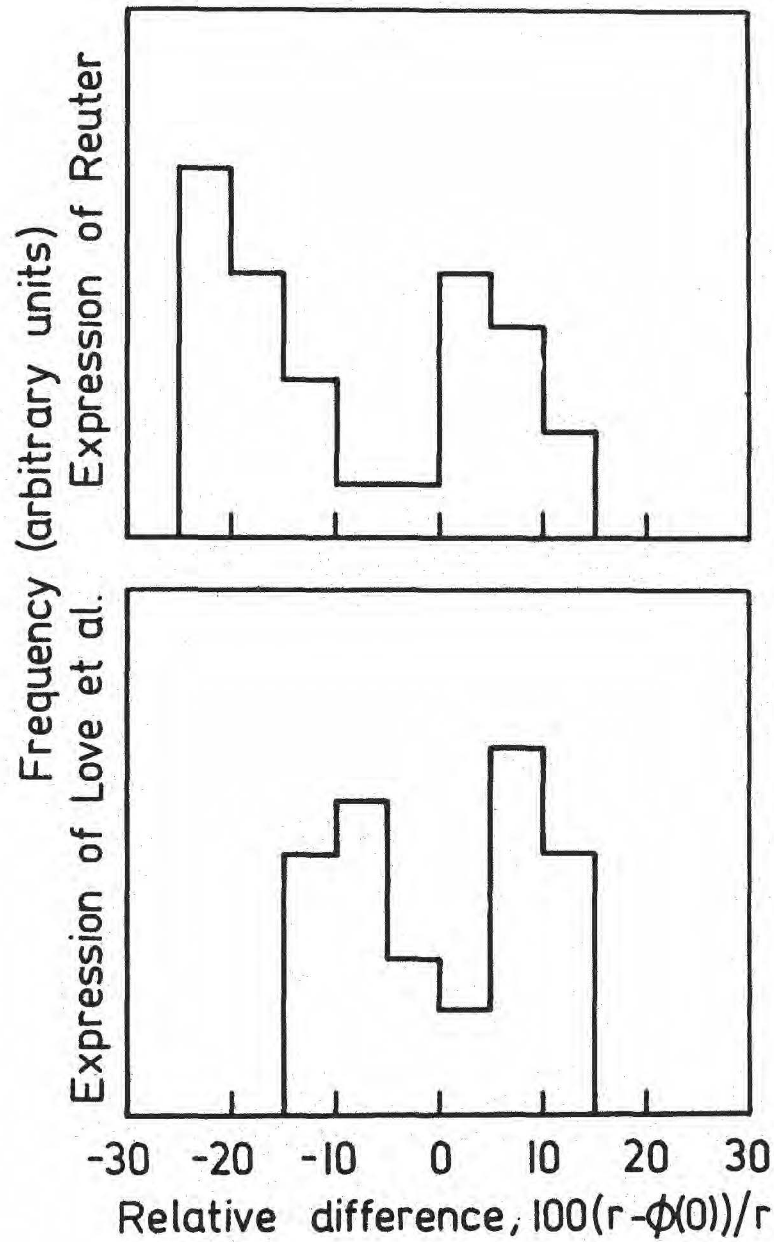


Fig. 5. Histograms of relative differences, $100(r - \Phi(0))/r$ , between experimental values of the backscattering factor taken from Smith and Gallon (1974) and the functions $\Phi(0)$ [figure taken from Jabłoński (1980b)].

http://rcin.org.pl

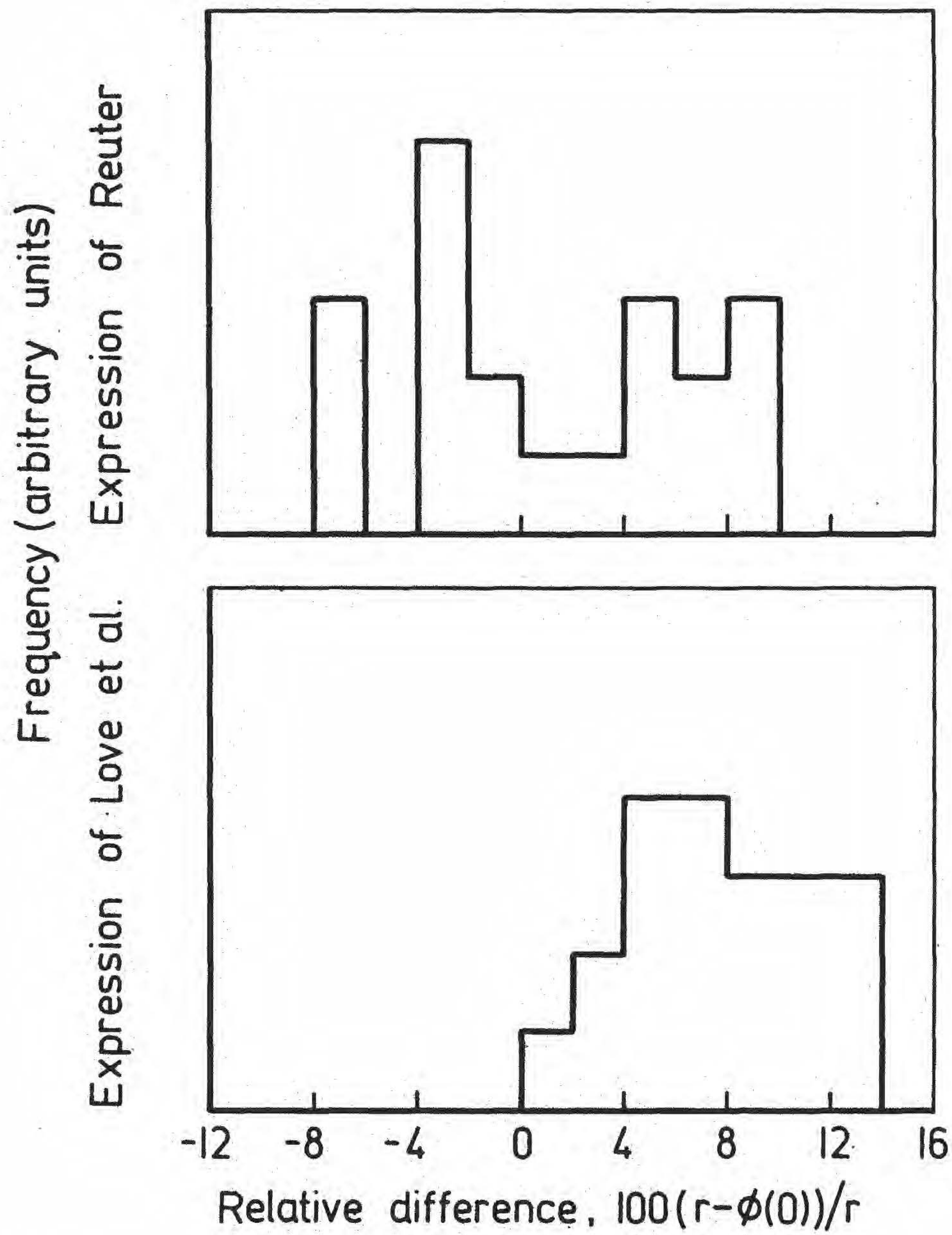


Fig. 6. Histograms of relative differences, $100(r - \phi(0))/r$, between calculated values of the backscattering factor taken from Bishop and Rivière (1969) and the functions $\phi(0)$ .

http://rcin.org.pl

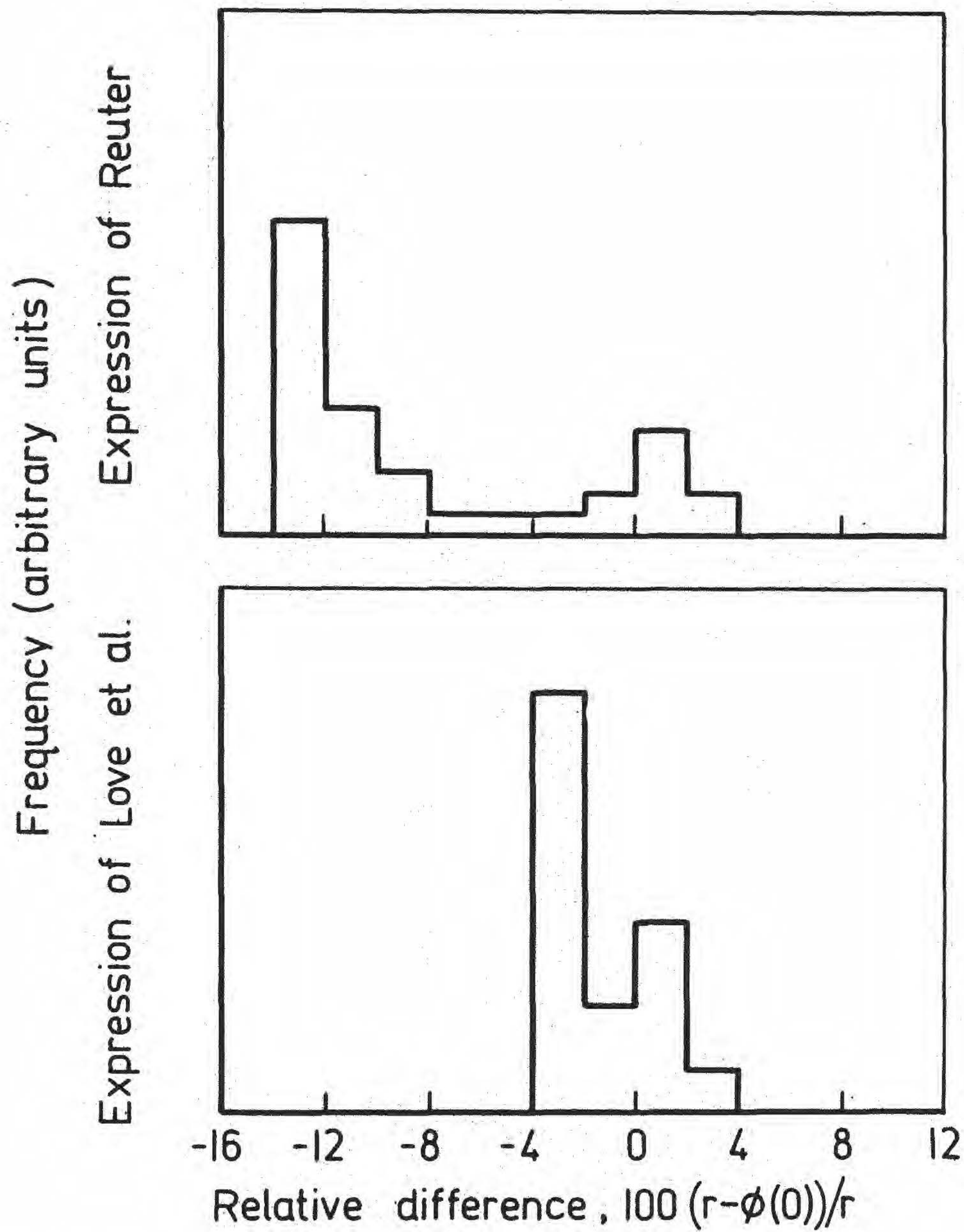


Fig. 7. Histograms of relative differences, $100(r - \phi(0))/r$, between calculated values of the backscattering factor taken from Jabłoński (1979a) and the functions $\phi(0)$.

http://rcin.org.pl

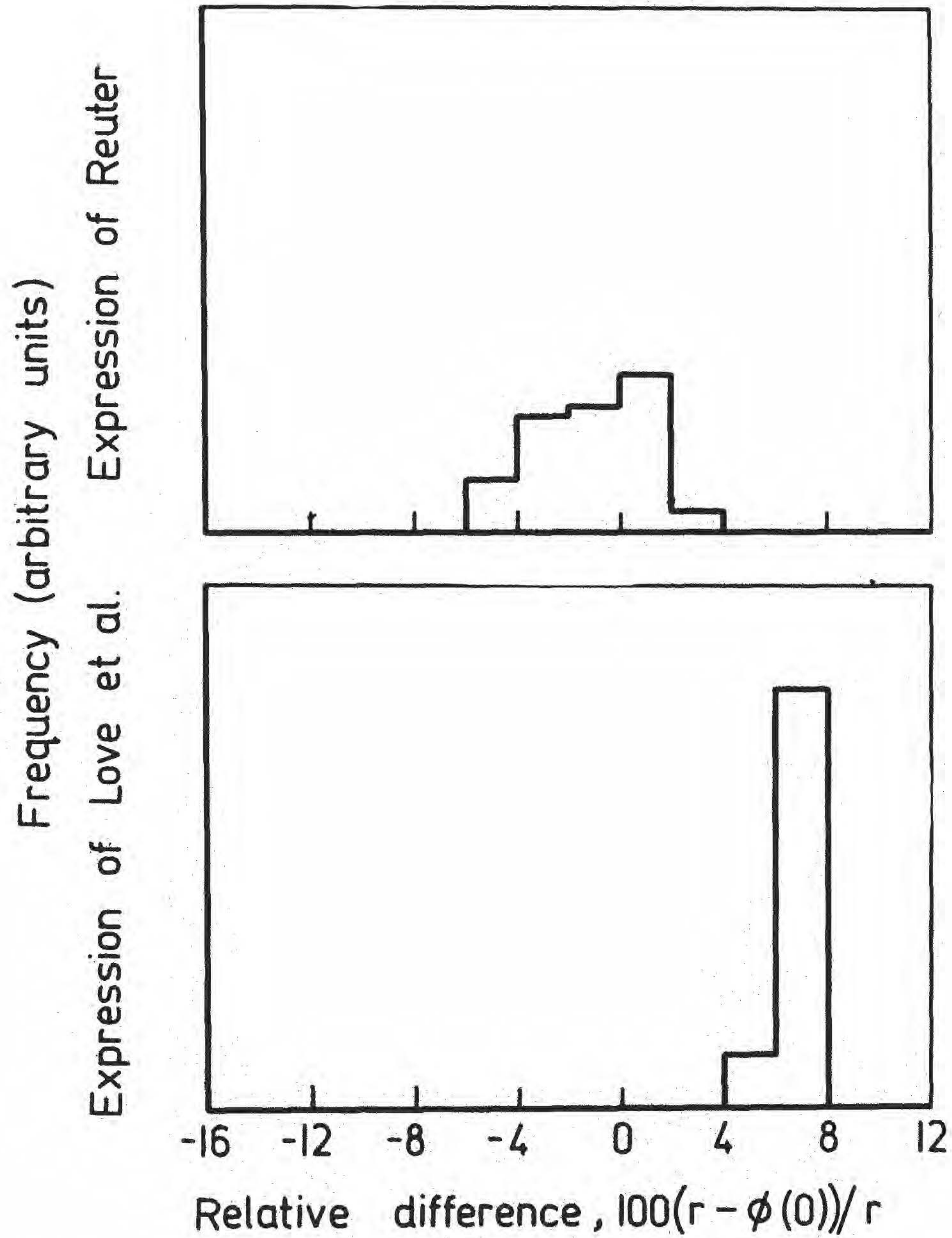


Fig. 8. Histograms of relative differences, 100(r - $\phi$(0))/r, between calculated values of the backscattering factor taken from Jabłoński (1980a) and the functions $\phi$(0) .

http://rcin.org.pl

Table 5. The standard deviations on the relative differences $100(r - \Phi(0))/r$ and $100(S - F)/S$ [table taken from Jabłoński (1980b)].

| r | $\Phi(0)$ | Standard deviation | |
|---|---|---|---|
| | | $100(r - \Phi(0))/r$ | $100(S - F)/S$ |
| Smith and Gallon | Reuter | 12.45 | 15.25 |
| | Love et al. | 9.06 | 12.18 |
| Bishop and Rivière | Reuter | 5.32 | 2.83 |
| | Love et al. | 3.65 | 5.33 |
| Jabłoński KLL | Reuter | 5.85 | 5.33 |
| | Love et al. | 1.83 | 2.47 |
| Jabłoński $L_3MM$ | Reuter | 2.01 | 0.94 |
| | Love et al. | 0.43 | 0.40 |



http://rcin.org.pl

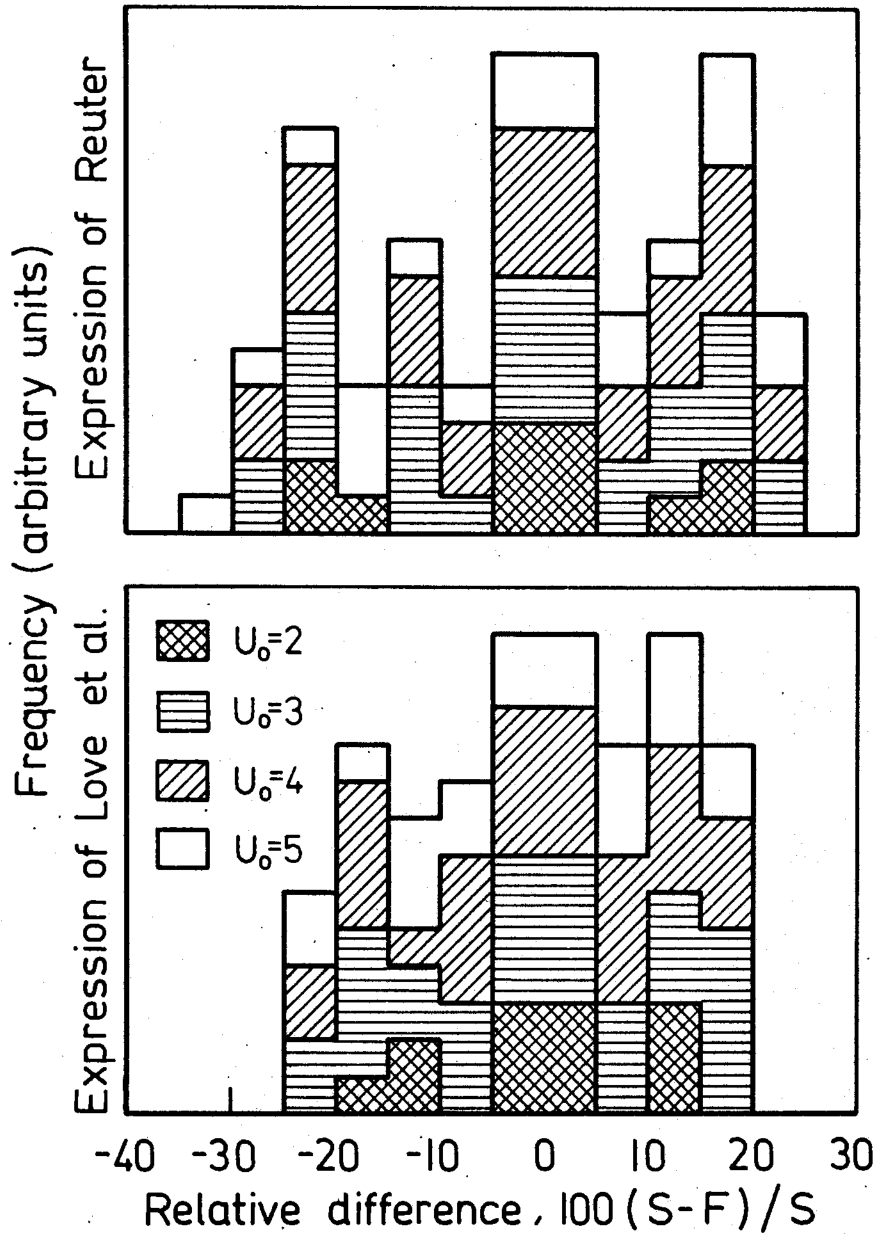


Fig. 9. Histograms of relative differences, 100(S - F)/S, between experimental values of the backscattering factor taken from Smith and Gallon (1974) and the functions $\phi(0)$
[$S = r_i^j/r_i^i$ ; $F = \phi_i^j(0)/\phi_i^i(0)$; figure taken from Jabłoński (1980b)].

http://rcin.org.pl

cases considered. It is possible that the Reuter expression is less accurate than the expression of Love et al. In fact, a number of objections were risen against the experimental method of Reuter (Love et al., 1978b). Secondly, the values of $r$ obtained from Monte Carlo calculations are generally in better agreement with both functions $\phi(0)$ than the experimental values. This stems from the fact that the experimental data of Smith and Gallon (1974) were determined at lower energies (300-1500 eV) than the calculated values (1000-10000 eV), thus the latter being closer in energy to EPMA. The severe differences between functions $\phi(0)$ and $r$ at low primary energies can be caused by the strong dependence of the reflection coefficient $\eta$ on the primary energy in the range below ~3000 eV (Darlington and Cosslett, 1972). The reflection coefficient becomes practically independent of $E_0$ above 5000 eV (Darlington and Cosslett, 1972). The application of primary energies in AES higher than 5000 eV also has another advantage. The backscattering factor $r$ resulting from the usual definition [eq(5.10)] represents in that case the true enhancement of the Auger electron yield due to backscattering (Jabłoński, 1979a, 1980a).

The backscattering factor $R$ in the ZAF formalism of EPMA is defined similarly as this factor in AES (Bishop, 1968). It is a ratio of the number of ionizations produced in the whole solid to the number of ionizations that would be produced in the case of no backscattering. The similar definition of the backscattering factor in AES involves only the region sampled by Auger electrons. However, the numerical values of $R$ and $r$ differ significantly. $R$ is always smaller than unity, and its value decreases with primary energy increase (Bishop, 1968, Love et al., 1978a), in

http://rcin.org.pl

contrast with the backscattering factor in AES. For this reason the values of $R$ cannot be used in quantitative AES analysis.

### 5.1.5. The effect of the Coster-Kronig transitions on the value of the backscattering factor

It follows from eqs (5.24) and (5.25) that the function $\Phi(0)$ (or the backscattering factor in AES) can be related to the reflection coefficient. Several other relations of this kind were published in the literature (Janssen et al., 1977, Jabłoński, 1979b). In all these relations the backscattering factor was expressed in terms of the reflection coefficient and the reduced energy, $U_o = E_o/E_c$ . It is pertinent at this point to discuss the effect of the so-called Coster-Kronig transitions on the value of the backscattering factor since these transitions can introduce an uncertainity in determining the reduced energy.

One of the radiationless processes that follow the ionization of the atom are the transitions that move the vacancy from one subshell to another within the same shell. The freed energy may be taken by an outer electron and an atom becomes doubly ionized. Such processes are called the Coster-Kronig transitions. They may be denoted as of the XXY type. The Coster-Kronig transitions are much faster than Auger transitions and take place in certain regions of atomic numbers. These regions are tabulated by Sevier (1972a). Let us consider the $L$ shell as an example. All three subshells, $L_1$, $L_2$ and $L_3$, are ionized in some specific ratio. The vacancies originally created in $L_1$ and $L_2$ subshells can move to $L_3$ shell with certain probability before the $L_3MM$ Auger transition takes place. The Coster-Kronig probabilities were compiled by Fink et al. (1966). Two effects are caused by the Coster-

http://rcin.org.pl

-Kronig transitions

(i) The relative Auger electron intensities within L shell are changed.

(ii) The $L_3MM$ Auger electron intensity has contributions due to ionization of $L_1$ and $L_2$ subshells.

We should ascribe to a given Auger transition the ionization of such subshell which contributes predominantly to the observed Auger electron yield. The subshells may differ considerably in ionization energy. Let us consider the N shell in gold. The pronounced Auger transition at 69 eV is usually assigned the $N_7O_{4,5}O_{4,5}$ subshells (Smith and Gallon, 1974, Wood and Wise, 1975, Jabłoński et al., 1977) since the ionization energy of $N_7$ subshell is equal to 84.1 eV. However, Smith and Gallon (1974) found that the reduced energy dependence of the ionization cross--section is closer to theoretical prediction when the reduced energy is scaled with respect to the ionization energy of the $N_4$ subshell, i.e. 352 eV. The significant contribution of $N_{4,5}$ subshell ionization to the intensity of 69 eV gold peak has also been postulated by Holloway (1976). Fortunately, the quantitative AES involves ratios of backscattering factors, and these ratios are rather weak functions of the reduced energy. We shall demonstrate the effect of variations in the value of the ionization energy on the ratio of backscattering factors for 69 eV transition in gold. Let us consider the ratio of the backscattering factors for a diluted gold alloy and for the pure gold, and let us use in calculations the function $\phi(0)$ of Love et al.(1978b). Results for the AuNi and AuPd binary alloys are shown in table 6. One can see that the change of the ionization energy from 84.1 eV to 352 eV affects the ratio $r_i^j/r_i^i$ in a minor degree.

http://rcin.org.pl

Table 6. The values of the ratio of backscattering factors, $r_i^j/r_i^i$ , for 69 eV Auger transition in gold.

| $E_o$ eV | Au Ni | | Au Pd | |
|---|---|---|---|---|
| | $E_c$ = 84.1 eV | $E_c$ = 352 eV | $E_c$ = 84.1 eV | $E_c$ = 352 eV |
| 500 | 0.8182 | 0.8541 | 0.9171 | 0.9290 |
| 1000 | 0.8330 | 0.8045 | 0.9261 | 0.9075 |
| 2000 | 0.8425 | 0.8171 | 0.9317 | 0.9164 |
| 3000 | 0.8460 | 0.8265 | 0.9337 | 0.9222 |
| 4000 | 0.8478 | 0.8322 | 0.9348 | 0.9256 |
| 5000 | 0.8488 | 0.8360 | 0.9354 | 0.9278 |
| 6000 | 0.8496 | 0.8386 | 0.9359 | 0.9294 |
| 7000 | 0.8501 | 0.8405 | 0.9362 | 0.9305 |



http://rcin.org.pl

### 5.1.6. The dependence of the backscattering factor on the composition of solids

One can expect that the backscattering factor in AES for a given Auger transitions is a function of the bulk composition of solids. The reflection coefficient, being related to the backscattering factor, was found to vary with composition; almost linear dependence on the mass fraction was observed for the AuCu alloy (Bishop, 1966, Murata et al., 1972). The energy distribution of backscattered electrons also depends on the composition of solids (Matsukawa et al., 1973). It has been postulated in several papers that the backscattering factor is a monotonic function of the binary alloy composition, increasing from the component with lower atomic number to component with higher atomic number (Jabłoński et al., 1977, Kuijers et al., 1978). Quantitative AES requires the actual concentration dependence of $r$. Unfortunately, there are only few experimental data on the backscattering factor for alloys. Shaw and Fain (1977) determined the backscattering factor for the 69 eV gold transition in $Cu_3Au$ alloy. The authors used the experimental method of Gallon. They found, rather unexpectedly, that the backscattering factor, equal to 1.94 ± 0.08, is the same as in the case of pure gold. The monotonic dependence of $r$ on concentration was confirmed experimentally by Berndt et al. (1980) for CuPd alloy.

The backscattering factor for low atomic number binary alloys was estimated on the basis of Everhart's theory (Jabłoński,1978). It has been shown that the backscattering factor can be calculated from eq (5.17) with parameter a given by

$$a = 0.045 \frac{A_i^o Z_i X_i + A_j^o Z_j X_j}{A_i^o X_i + A_j^o X_j} \tag{5.26}$$

http://rcin.org.pl

The concentration dependence of the backscattering factor was calculated for $L_3MM$ Auger transitions in a number of alloys using the single scattering Monte Carlo algorithm (Jabłoński, 1980a). The Monte Carlo calculations, as well as the method based on Everhart's theory, indicate that the backscattering factor is a linear function of concentration when plotted against the mass fraction of a given component (figs 10 and 11). Fig. 10 compares the concentration dependence of the backscattering factor obtained from both theoretical approaches. The Everhart's theory provides the values of $r$ larger by 10-20% than the values of $r_o$. This may be due to the fact that the angular distribution of backscattered electrons resulting from Everhart's theory overestimates the contribution of electrons backscattered at large escape angles as compared with the cosine distribution (Murata, 1976). Fig. 11 shows the effect of alloying on the backscattering factor for the $L_3MM$ transition of Ni in AuNi, CuNi and NiPd binary alloys.

### 5.1.7. Conclusions

In summary, the present compilation shows that much more experimental and theoretical work is still necessary to attain better accuracy in determining the backscattering factor. Although a knowledge of backscattering effects is vital in quantitative AES analysis, especially when components of the sample differ significantly in atomic number, the existing experimental or theoretical data are insufficient to recommend an accurate and universal method for determining the backscattering correction. As follows from the brief survey of experimental methods, the Gallon method seems to be most reliable in providing the values of the back-

http://rcin.org.pl

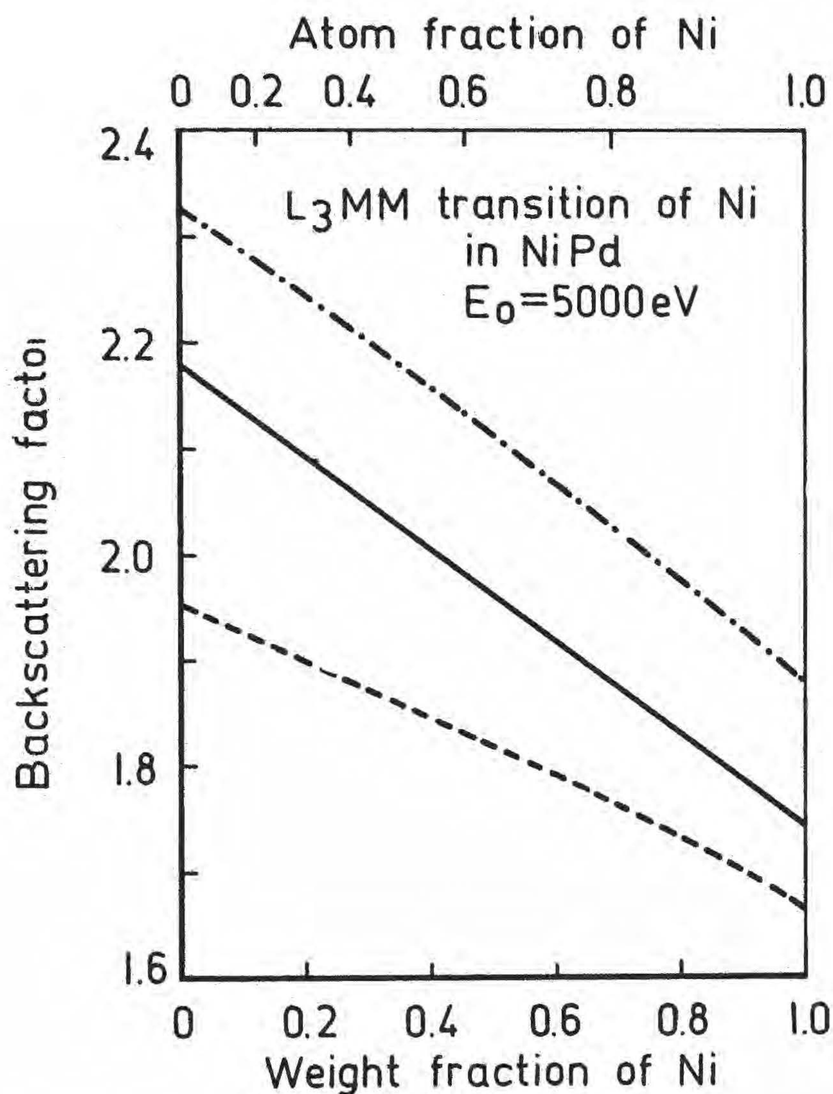


Fig. 10. Concentration dependence of the backscattering factor for the $L_3$MM Auger transition of nickel in NiPd binary alloy. Dot-dash line: the backscattering factor calculated on the basis of Everhart's theory [eqs (5.17) and (5.26)]; solid line: the backscattering factor $\bar{r}$ calculated from eq (5.21); dashed line: the backscattering factor $r_0$ calculated from eq (5.22) [figure taken from Jabłoński (1980a)].

http://rcin.org.pl

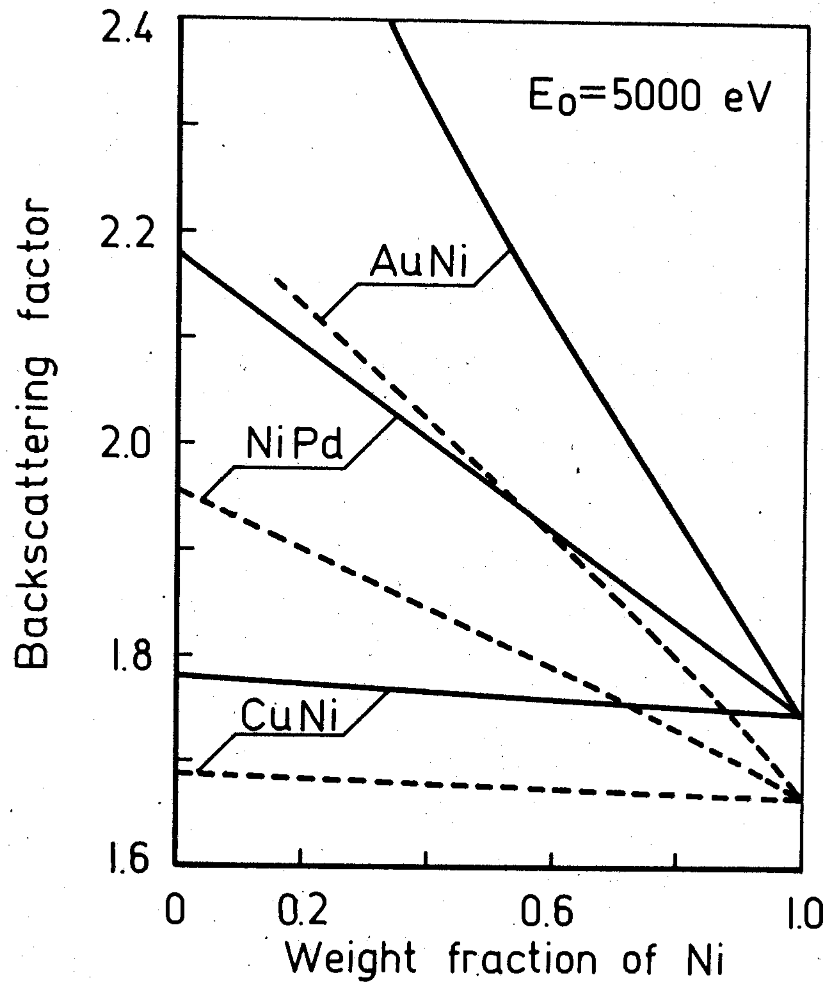


Fig. 11. Concentration dependence of the backscattering factor calculated for the $L_3MM$ transition of nickel in Au Ni, Cu Ni and Ni Pd binary alloys. Solid line: the backscattering factor $\bar{r}$ calculated from eq (5.21); dashed line: the backscattering factor $r_o$ calculated from eq (5.22) [figure taken from Jabłoński (1980a)].

http://rcin.org.pl

scattering factor. The single scattering Monte Carlo scheme is recommended for calculations of $r$ in the case of high energy Auger transitions, involving the ionization energy in excess of 500-1000 eV. The backscattering factor can be also calculated from the expressions providing the function $\phi(0)$ in electron probe microanalysis. Deviations of the values $\phi(0)$ from the experimental and theoretical data on $r$ reach 15%.

In the present compilation the dependence of the backscattering factor on the angle of incidence of the primary beam has not been discussed. An interested reader is referred to the literature (Vrakking and Meyer, 1975, Jabłoński, 1979a, Shimizu and Ichimura, 1981).

## 5.2. The inelastic mean free path

The next correcting factor in eqs (4.17) - (4.20) is the inelastic mean free path of electrons in the solid. This parameter can be considered as a mean value of distances $\ell$ travelled by an electron with a given energy between inelastic collisions. The energy loss process is in reality the Poisson process (Shimizu et al., 1976), so the distances between inelastic collisions should follow the exponential distribution

$$f(\ell) = (1/d)\exp(-\ell/d)$$

Hence

$$E(\ell) = \int_0^{\infty} (\ell/d)\exp(-\ell/d)\,d\ell = d$$

The following processes may decrease the electron energy in the solid (Ritchie et al., 1969).

http://rcin.org.pl

(i) Interaction with the solid lattice.

(ii) Collision with an electron in the conduction band.

(iii) Excitation of the volume plasmon.

(iv) Excitation of the surface plasmon.

(v) Excitation of the core level electrons.

Each of the above processes has certain energy loss cross section (per one atom of solid). The total inelastic excitation cross section is given by

$$\sigma_T = \sum_k \sigma_{(k)} \tag{5.27}$$

where summation is extended over all energy loss processes. Since the inelastic mean free path for a particular excitation is related to the cross section by

$$d_{(k)} = 1/(N\,\sigma_{(k)})$$

we obtain for the total inelastic mean free path (Koval et al., 1978 )

$$1/d = \sum_k 1/d_{(k)} \tag{5.28}$$

In the next sections we will discuss the methods for determining the values of $d$ .

5.2.1. The experimental values of the inelastic mean free path

Besides quantitative AES, the values of the inelastic mean free path are also of interest to other electron spectroscopies, e.g. XPS or UPS. For this reason much attention has been paid to the problem of determining the values of $d$ . The experimental

http://rcin.org.pl

techniques for determining the inelastic mean free path were briefly reviewed by Powell (1974). The overlayer technique seems to be applied most frequently. This technique consists in evaporating the material under investigation on the substrate and in measuring the dependence of the Auger electron intensity (or photoelectron intensity) on the overlayer thickness. The system for investigation and the evaporation conditions should be selected such that the overlayer material does not agglomerate or diffuse into a substrate. The other experimental problem inherent in this technique is the reliable determination of the overlayer thickness. Suppose that the uniform overlayer "i" is evaporated on the substrate "j", both materials with similar backscattering properties. In that case the Auger electron intensity from substrate is proportional to $\exp(-T/d_j^i \cos\alpha)$ ,where $T$ is the overlayer thickness [cf. eq (4.20)]. Similarly, the Auger electron intensity from overlayer is proportional to $1 - \exp(-T/d_i^i \cos\alpha)$ . Thus, determination of the mean free paths $d_j^i$ and $d_i^i$ in the considered case is a simple matter. However, the substantial difference in backscattering from substrate and overlayer results in more complicated dependence of the Auger electron intensity on the overlayer thickness (Tarng and Wehner, 1973, Tokutaka et al., 1977).

The experimental data on the inelastic mean free paths in electron energy range of interest for Auger electron spectroscopy have been compiled by several authors (Lindau and Spicer, 1974, Brundle, 1974, Powell, 1974, Seah and Dench, 1979). It turned out that the inelastic mean free path was dependent primarily on the electron energy. The mean free path has minimum value at electron energy around 100 eV and then increases with energy roughly as

http://rcin.org.pl

square root. The dependence on the atomic number is not significant, and in earlier papers it was neglected. The existence of the universal curve has been postulated, i.e. the dependence of the mean free path on the electron energy only (Palmberg, 1973, Chang, 1974, 1975, Ertl and Küppers, 1974a). Chang (1975) proposed a simple expression for the mean free path,

$$d = 0.2\ E^{1/2}\ \text{monolayers} \qquad (E\ \text{in eV}) \qquad (5.29\ a)$$

which was fitted to the high energy part of the universal curve, i.e. it is valid for electron energies exceeding 100 eV. Similar expression has been postulated by Pons et al. (1977b)

$$d = 0.44\ E^{1/2}\ \text{Å} \qquad (E\ \text{in eV}) \qquad (5.29\ b)$$

A comprehensive bibliography on the inelastic mean free path of electron in solid has been recently published by Seah and Dench (1979). The authors compiled nearly 350 experimental values of $d$ in the energy range between 0 and 10 keV. They fitted the following relation to the experimental data

$$d = \frac{A}{E^2} + B\ E^{1/2}$$

and then looked for a correlation between the deviation of the experimental values from the curve and the atom size, conduction band electron density, and the number of conduction band electrons per atom. Seah and Dench (1979) found that the correlation exists between the deviations and the atom size (or monolayer thickness). They proposed the following equations for the inelastic mean free path for elements

$$d = \frac{538}{E^2} + 0.41\ (t\ E)^{1/2} \qquad (5.30)$$

http://rcin.org.pl

The energy is expressed in electronvolts. This equation is considered to be most accurate at the moment.

### 5.2.2. The theoretical values of the inelastic mean free path

The early theoretical works on calculating the inelastic mean free path of electron in solid are reviewed by Ritchie et al. (1969). Since then a number of theoretical papers on that subject were published ( Powell, 1974, Shelton, 1974, Penn, 1976a,b,c, Ashley et al., 1979, Tung et al., 1979 ).

Penn (1976a,b,c) proposed an universal method for calculating the inelastic mean free path in the energy range from a few hundred to a few thousand electronvolts. In that energy range the electron energy loss is mainly due to the valence band excitations, which include the plasmon excitation and the electron--electron collisions (Penn, 1976a). For this reason the inelastic mean free path is determined by the valence band structure rather than by the atomic number of the solid. The excitation of core electrons has also been taken into account in determining the mean free path since it reduces its value by about 10%. The Penn theory is applicable for free-electron-like materials, i.e. for materials which exhibit plasmons with frequency close to frequency of a free electron plasma

$$\omega_p = (4\pi n_{el} e^2/m)^{1/2} ,$$

where $n_{el}$ is the concentration of valence electrons. The solids which do not contain transition metals, or noble metals can be considered as the free-electron-like materials. In the considered case the total inelastic mean free path is determined by the collisions with core electrons and valence electrons. Eq (5.28) has

http://rcin.org.pl

the form

$$1/d = 1/d_{(c)} + 1/d_{(v)} \tag{5.31}$$

Penn (1976c) has shown that the mean free path associated with plasmon excitation, $d_{(v)}$, is given by

$$d_{(v)} = E/\left[a_v(\ln E + b_v)\right] \tag{5.32}$$

where $a_v$ and $b_v$ are functions of the parameter $r_s$ defined by

$$r_s = \left( \frac{3}{4\pi} \frac{1}{n_{el}} \right)^{1/3} \frac{1}{a_o}$$

The values of $a_v$ and $b_v$ may be determined from the universal plot presenting both parameters in terms of $r_s$ (Penn, 1976c). The contribution to the inelastic mean free path due to the core electrons excitation is calculated from the theory published by Powell (1974).

$$d_{(c)} = E/\left[a_c(\ln E + b_c)\right] \tag{5.33}$$

where

$$a_c = 392\,(\rho N_{el}/A^{o}\,\Delta E) \tag{5.33a}$$

$$b_c = -\ln \Delta E/4 \tag{5.33b}$$

$N_{el}$ is the number of electrons in the highest core level, and $\Delta E$ is the average excitation energy of electrons from highest core level expressed in electronvolts. The excitation energies $\Delta E$ were estimated from binding energies $E_c$ according to formula

http://rcin.org.pl

$$\Delta E = \begin{cases} 2\,E_c & \text{if} \quad E_c < 70 \text{ eV} \\ E_c + 70 & \text{if} \quad E_c > 70 \text{ eV} \end{cases}$$

Penn (1976c) compiled the values of $N_{el}$ , $\Delta E$ , $a_c$ and $b_c$ for a number of elements. From eqs (5.31) - (5.33) one obtains

$$d = E/[a(\ln E + b)] \qquad (5.34)$$

where

$$a = a_v + a_c$$

$$b = (a_v\, b_v + a_c\, b_c)/(a_v + a_c)$$

Table 7 lists the values of parameters $a$ and $b$ taken from Penn (1976c). Eq (5.34) was used by Penn (1976c) in tabulating the inelastic mean free paths for elements in energy range from 200 to 2400 eV and atomic numbers varying from 3 to 83. The author indicated that even if the theory does not apply to transition and noble metals, still it gives fair estimate of the ratio of mean free paths. As it will be shown in section 6.3, the quantitative AES involves the ratios of the mean free paths rather than absolute values. On the other hand, Seah and Dench (1979) indicated that their semiempirical expression for elements [eq. (5.30)] much better compares with the experimental data on the mean free path than the expression of Penn [eq. (5.34)] .

5.2.3. The dependence of the inelastic mean free path on the composition of solids

The values of the inelastic mean free paths discussed so far were determined for pure elements. Similarly as in the case of

http://rcin.org.pl

Table 7. The parameters a and b taken from Penn (1976c) for calculating the total inelastic mean free path from eq (5.34). The dimensions of a and b are such that energy is expressed in eV and d in Å.

| Z | a | b | Z | a | b |
|---|---|---|---|---|---|
| 3 | 4.97 | -1.23 | 40 | 11.5 | -2.10 |
| 4 | 11.7 | -2.32 | 41 | 14.2 | -2.37 |
| 5 | 10.8 | -2.70 | 42 | 16.9 | -2.56 |
| 6 | 18.3 | -2.95 | 43 | 18.5 | -2.72 |
| 7 | 4.66 | -1.05 | 44 | 19.9 | -2.85 |
| 11 | 4.84 | -1.25 | 45 | 20.6 | -2.94 |
| 12 | 7.74 | -1.77 | 46 | 20.6 | -2.98 |
| 13 | 10.2 | -2.16 | 47 | 19.5 | -2.95 |
| 14 | 10.7 | -2.19 | 48 | 17.4 | -2.81 |
| 19 | 3.55 | -0.820 | 49 | 14.0 | -1.80 |
| 20 | 6.67 | -1.48 | 50 | 12.9 | -2.04 |
| 21 | 9.92 | -1.94 | 51 | 12.4 | -2.18 |
| 22 | 13.2 | -2.28 | 52 | 12.0 | -2.22 |
| 23 | 16.5 | -2.54 | 53 | 10.0 | -2.05 |
| 24 | 19.0 | -2.74 | 55 | 3.20 | -0.570 |
| 25 | 19.7 | -2.87 | 56 | 5.59 | -1.15 |
| 26 | 21.1 | -3.00 | 57 | 9.47 | -1.60 |
| 27 | 22.8 | -3.14 | 72 | 11.4 | -2.14 |
| 28 | 23.7 | -3.21 | 73 | 13.8 | -2.40 |
| 29 | 23.6 | -3.21 | 74 | 16.2 | -2.58 |
| 30 | 21.1 | -3.10 | 75 | 18.3 | -2.71 |
| 31 | 17.3 | -2.00 | 76 | 19.1 | -2.86 |
| 32 | 14.0 | -2.22 | 77 | 19.9 | -2.95 |
| 33 | 13.7 | -1.69 | 78 | 19.9 | -2.96 |
| 34 | 11.9 | -2.25 | 79 | 19.6 | -2.95 |
| 35 | 9.58 | -2.46 | 80 | 16.6 | -2.71 |
| 37 | 3.51 | -0.710 | 81 | 13.4 | -1.62 |
| 38 | 5.55 | -1.24 | 82 | 13.2 | -1.97 |
| 39 | 8.52 | -1.71 | 83 | 12.0 | -2.02 |

http://rcin.org.pl

the backscattering factor, the quantitative analysis of alloys or compounds requires knowledge of the composition dependence of the mean free path. Seah and Dench (1979) proposed the semiempirical expression for calculating the inelastic mean free path for inorganic compounds

$$d = \frac{2170}{E^2} + 0.72(t\,E)^{1/2} \quad \text{monolayers} \quad (E \text{ in eV}) \qquad (5.35)$$

The monolayer thickness $t$ is calculated from

$$t = \left(\frac{A^o}{\rho N_o\, n_a}\right)^{1/3}$$

where $n_a$ is the number of atoms in the molecule.

According to Seah and Dench (1979) the inelastic mean free path of electrons in organic compounds depends only on electron energy

$$d = \frac{10^3}{\rho}\left(\frac{49}{E^2} + 0.11\, E^{1/2}\right) \quad \text{nanometers} \qquad (5.36)$$

($E$ in eV, $\rho$ in kg/m$^3$)

As in the case of elements, eqs (5.35) and (5.36) give the smallest scatter of the experimental data on the inelastic mean free path for compounds.

Penn (1976c) generalized eq (5.34) for the case of compounds of a type $X_i\, Y_j$ . The total concentration of valence electrons is calculated from the formula

$$n_{el} = N_o\, z\, \rho / A_m \,,$$

where $z$ is the number of valence electrons in a compound, and $A_m$ is the molecular weight. Then, the parameters $a_v$ and $b_v$ are determined as in the case of pure elements, i.e. from the universal plot. The parameters $a_c$ and $b_c$ are given by genera-

http://rcin.org.pl

lized equations (5.33a) and (5.33b)

$$a_c = 392 \sum_i (N_{el,i}/\Delta E_i)(\rho/A_m) ,$$

$$b_c = - \sum_i (N_{el,i}/\Delta E_i) \ln(\Delta E_i/4) \Big/ \sum_i N_{el,i}/\Delta E_i ,$$

where subscript "i" denotes the type of atom. Eventually, the inelastic mean free path is calculated from eq (5.34).

Unfortunately, there is no experimental and theoretical data on inelastic mean free path for metal alloys. In AES analysis of binary alloys the concentration dependence of the inelastic mean free path is usually neglected, or linear dependence on concentration is assumed from one pure component to the other (Holloway, 1977, Berndt et al., 1980). Such assumptions are expected to introduce small error due to weak dependence of the inelastic mean free path on the atomic number. For the same reason the effect of the concentration variation at the solid surface on the mean free path is also usually neglected.

### 5.2.4. Conclusions

The most accurate values of the inelastic mean free path of electron in elements and compounds can be calculated from the semiempirical expressions of Seah and Dench (1979). These expressions were obtained from the statistical analysis of the experimental data on the mean free path. There is no data at present on the concentration variation of the mean free path in metal alloys, but neglecting the concentration dependence of $d$ in quantitative analysis should not introduce significant errors.

http://rcin.org.pl

## 5.3. The total number of atoms in unit volume and the monolayer thickness

The last two correcting factors in quantitative AES may be determined with relatively high accuracy for pure elements. The number of atoms in unit volume of pure element is usually calculated from the expression (Reed, 1975c)

$$M^i = N_o \rho^i / A_i^o \tag{5.37}$$

The monolayer thickness can be derived from the average volume of one atom (Seah and Dench, 1979)

$$t^i = (1/M^i)^{1/3} = (A_i^o / N_o \rho^i)^{1/3} \tag{5.38}$$

The monolayer thickness also can be determined from crystallographic considerations (Jabłoński et al., 1977).

The composition dependence of the total number of atoms and the monolayer thickness is also relatively easy to account for. According to Vegard's law, the lattice constant of the alloy forming continuous series of solid solutions is a linear function of concentration expressed in atom fractions (Pearson, 1958).

$$a = a^j + (a^i - a^j) X_i \tag{5.39}$$

where $a$, $a^i$ $a^j$ are the lattice constants for the alloy, i-th pure component and j-th pure component, respectively.
Let us base the determination of the total number of atoms and the monolayer thickness for alloys on the general assumption that:

III D. Vegard's law is valid in the case of investigated alloys.

http://rcin.org.pl

The number of atoms in unit volume of the alloy is then given by

$$M = K/a^3 \tag{5.40}$$

where $K$ is the number of atoms per unit cell.
From eqs (5.37), (5.39) and (5.40) we obtain eventually

$$(1/M)^{1/3} = (1/M^j)^{1/3} + \left[(1/M^i)^{1/3} - (1/M^j)^{1/3}\right] X_i \tag{5.41}$$

Taking into account eq (5.38) we have

$$t = t^j + (t^i - t^j)\, X_i \tag{5.42}$$

The Vegard law is of an approximate character. Deviations from that law are observed in majority of binary metal alloys (Gschneidner and Vineyard, 1962). These deviations should not introduce serious errors in quantitative AES analysis in most of the cases. However, it is advisable to check the validity of the Vegard's law in a binary system under investigation.

In the case of systems to which the Vegard law cannot be applied e.g. alloys with long range order, metallic compounds the total number of atoms may be calculated from (Reed, 1975c)

$$M = N_o \rho \left( \frac{C_i}{A_i^o} + \frac{C_j}{A_j^o} \right) \tag{5.43}$$

and the monolayer thickness from

$$t = (1/M)^{1/3} \tag{5.44}$$

Application of eqs (5.43) and (5.44) in quantitative AES requires knowledge of the density of studied alloys.

The effect of the changes of concentration in the surface region on the parameters $M$ and $t$ is usually neglected, especially in cases when the atom sizes of both constituents of

http://rcin.org.pl

binary alloy are similar. However, the change of the atom density at the surface can be significant, e.g. the alloy AuNi (Burton et al., 1976) and this effect should be accounted for in such a case.

http://rcin.org.pl

## 6. Experimental aspects of quantitative Auger electron spectroscopy

The current of Auger electrons leaving the solid is imposed on a much larger background of backscattered electrons. The ratio $I_A/I_o$ for KLL Auger transitions is of the order of $10^{-4}$ (Bishop and Rivière, 1969) while the reflection coefficient $\eta$ varies between 0.1 and 0.5 for majority of solids. For this reason the measurements of the absolute Auger electron current are rather difficult (Meyer and Vrakking, 1972, Staib and Kirschner, 1974) and in actual experimental practice the ratios of two intensities are measured. These intensities correspond to two different Auger transitions or to two different samples.

The Auger electron intensities are determined from the energy distributions of backscattered electrons, i.e. from the dependences $N(E)$ vs $E$ or $dN(E)/dE$ vs $E$. In these distributions the sharp peaks due to Auger transitions are imposed on a slowly varying background. Thus, the main unit of the Auger electron spectrometer is the electron energy analyser. The analysers most frequently used in AES are briefly described in the next section.

### 6.1. Electron energy analysers

#### 6.1.1. The retarding field analyser (RFA)

Palmberg (1967) indicated that the retarding field optics, designed for low energy electron studies, can be used in measurements of electron energy distributions. Scheibner and Tharp (1967), Tharp and Scheibner (1967), Weber and Peria (1967), Palmberg(1968) and Palmberg and Rhodin (1968), were first to use this analyser in determining the Auger electron spectra. The retarding field

http://rcin.org.pl

analyser is depicted in fig. 12. The analyser consists of a spherical collector with a system of four grids. The negative potential $V_o$ applied to the two inner grids separates electrons with energy lower than $E = eV_o$ from the backscattered current reaching the collector, $i(V_o)$ . We have

$$i(V_o) = \int_{eV_o}^{\infty} N(E)dE$$

The energy distribution $N(E)$ vs $E$ is obtained by differentiation of the function $i(V_o)$ : $N(E) \sim d[i(V_o)]/dV_o$ .
Similarly: $dN(E)/dE \sim d^2[i(V_o)]/dV_o^2$ .
The differentiation is usually performed electronically.

The retarding field analyser has rather large acceptance angle. It collects the backscattered electrons with escape angles between about $6^o$ and $60^o$. The energy resolution is about 1%.

6.1.2. The cylindrical mirror analyser (CMA)

The theoretical basis for the operation of the cylindrical mirror analyser was given by Zashkvara et al. (1966). This analysis was extended later by Sar-El (1967), Hafner et al. (1968), Aksela et al. (1970) and Frank (1976). The energy spectra were obtained by means of cylindrical mirror analyser already in fifties (Blaut, 1957). A number of constructions were published since then (Sar-El, 1967, Bishop et al., 1973, Vašina and Frank, 1979). Palmberg et al. (1969) indicated the advantages of using the cylindrical mirror analyser in Auger electron spectroscopy.

The analysing part of CMA is a system of two coaxial cylinders (fig. 13). The inner cylinder has the entrance and exit slits for electrons. A negative potential $V_o$ applied to the outer cylinder allows only electrons with a certain selected energy to reach the first dynode of the electron multiplier. There is a linear

http://rcin.org.pl

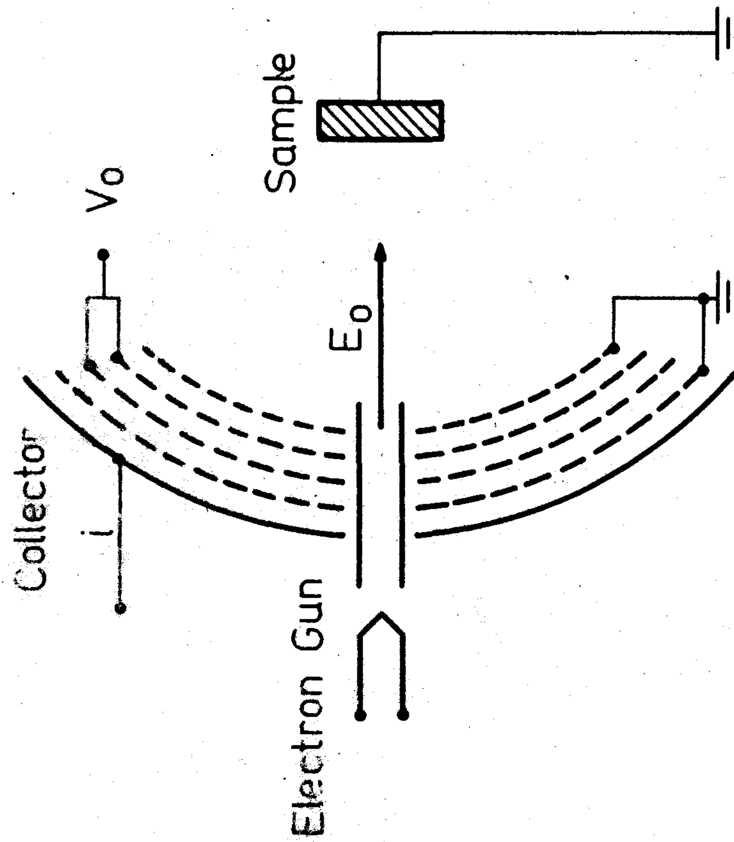


**Fig. 12. Scheme of the retarding field analyser.**

http://rcin.org.pl

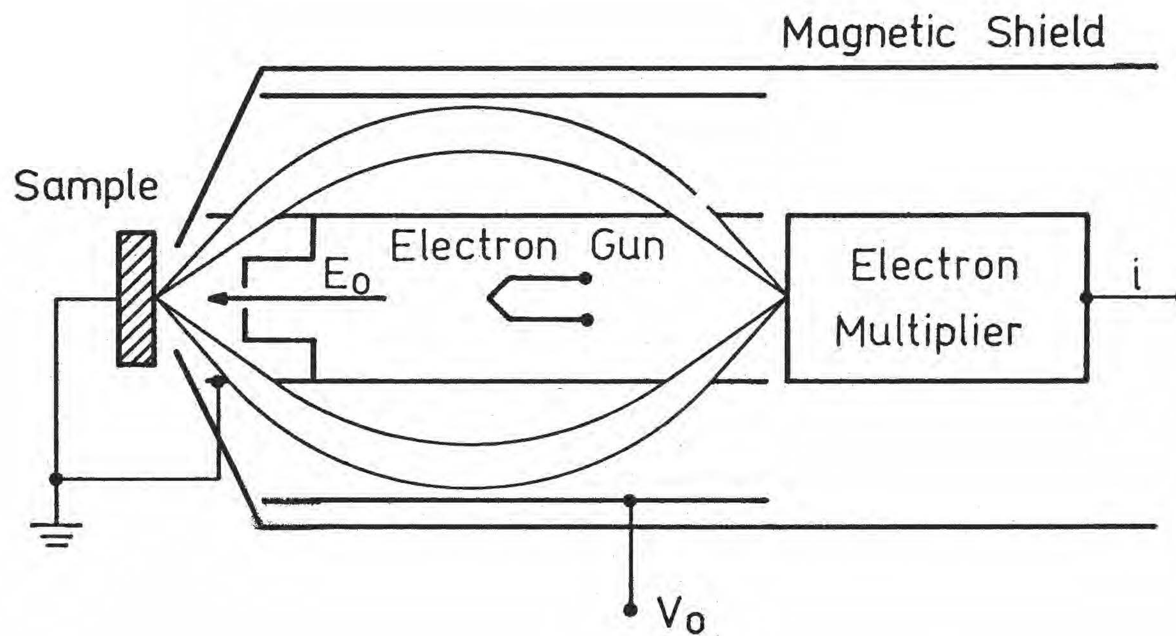


Fig. 13. Scheme of the cylindrical mirror analyser.



http://rcin.org.pl

dependence between the potential $V_0$ and the analysed energy $E$. The current leaving the electron multiplier is proportional to the product $E\,N(E)$. We have then

$$d[i(V_0)]/dV_0 \sim N(E) + E\,dN(E)/dE$$

However, the $N(E)$ term is small as compared with $E\,dN(E)/dE$, and it is usually assumed that differentiation of the signal $i(V_0)$ gives the distribution $dN(E)/dE$. The CMA operates in conditions of the second order focus. At the focal distance $L$ corresponding to the escape angle $\alpha = 42.3^o$ we have

$$dL/d\alpha = 0 \quad \text{and} \quad d^2L/d\alpha^2 = 0 .$$

The second order focus property increases the transmission of CMA. In most commercial instruments the transmission usually reaches 10% which corresponds to the acceptance angle $42^o \pm 6^o$. The energy resolution varies between 0.5% and 0.7%. The CMA collects the backscattered current in a narrow energy range, and that increases the signal to noise ratio by a factor of 100 as compared with RFA. For this reason the CMA may operate much faster than RFA or at much smaller primary currents.

### 6.2. The measure for the Auger electron current

Since the first publications the Auger electron spectra were recorded in the differential form, i.e. $dN(E)/dE$ vs $E$ (Weber and Peria, 1967, Harris, 1968). The derivative spectra are more convenient for two reasons. The function $N(E)$ is positive and the background current is much larger than the current associated with the Auger transition. Magnification of the Auger electron peak to a manegable size would involve high values of the back-

http://rcin.org.pl

ground. Secondly, the Auger electron peaks are relatively narrow features on the slowly varying background and become more pronounced on differentiation. The problems encountered in differentiation of the energy spectra were discussed in the literature (Taylor, 1969, Gerlach, 1972, Seah, 1979b). In the following we shall consider the question of features of the Auger electron peak that carry the quantitative information.

The usual measure of the Auger electron current is the distance between the most positive and most negative values of the spectra $dN(E)/dE$ vs $E$ (the peak-to-peak height). Taylor (1969) and Hall et al. (1977) have shown that the peak-to-peak height is proportional to the Auger electron current in the case of a Gaussian peak. The use of this criterion in quantitative analysis is justified when the Auger peak is symmetrical and its shape is independent of the chemical composition. Pons et al.(1977a) suggested selection of such Auger transitions for analysis which do not involve the valence electrons because the core electrons are much less affected by variations in the chemical state. Hall et al. (1977) indicated that the effect of peak broadening with changes of composition can be easily accounted for if the peak remains symmetrical. They have shown that the proper measure of the Auger electron current in the case of Gaussian peak is the product $H\delta^2$ where $H$ is the peak-to-peak height and $\delta$ is the measure of the peak width, e.g. the energy separation of maximum and minimum in the differentiated spectra. The corrected peak-to-peak height is then calculated from the formula

$$H_{corr} = H_{meas}(\delta / \delta_o)^2$$

where $\delta_o$ is the value of $\delta$ for pure material.

http://rcin.org.pl

Several authors proposed the area under the peak in the integral spectra, N(E) vs E , as a measure of the Auger electron current (Grant et al., 1973a,b, 1974, Houston, 1973, Leygraf et al., 1974, Staib and Kirschner, 1974, Fujinaga, 1977). The area has been proved to be less sensitive to the shape changes caused by the chemical surrounding than the peak-to-peak height (Grant et al., 1973a,b). The determination of the area under the peak requires subtracting the background and the corresponding techniques of background removal have been developed (Staib and Kirschner, 1974, Ishikawa and Tomida, 1978). An additional problem inherent in the integration of the dN(E)/dE vs E spectra is setting the integration limits. The value of the area does not approach a constant as integration limit expand, so the choice of the limits is somewhat arbitrary. Seah (1979a) discussed the prospects of using the differential and integral energy spectra in quantitative AES analysis. He pointed out that Auger electrons which suffered the characteristic energy losses rise the background of the low energy side of the Auger feature in the N(E) vs E spectra (fig. 14a). The integration may account for electrons originating from atom layers deeper than the inelastic mean free path. The proper measure of the Auger electron current is the shaded area in fig. 14a. Thus, only the high energy part of the Auger peak is informative about the Auger electron current from the outer atom layers. Seah (1979a) recommended the peak height between the negative minimum and the background level in the differential spectra as a measure of the Auger electron current, or the product $H\delta^2$ in the case of peak broadening (fig. 14b).

http://rcin.org.pl

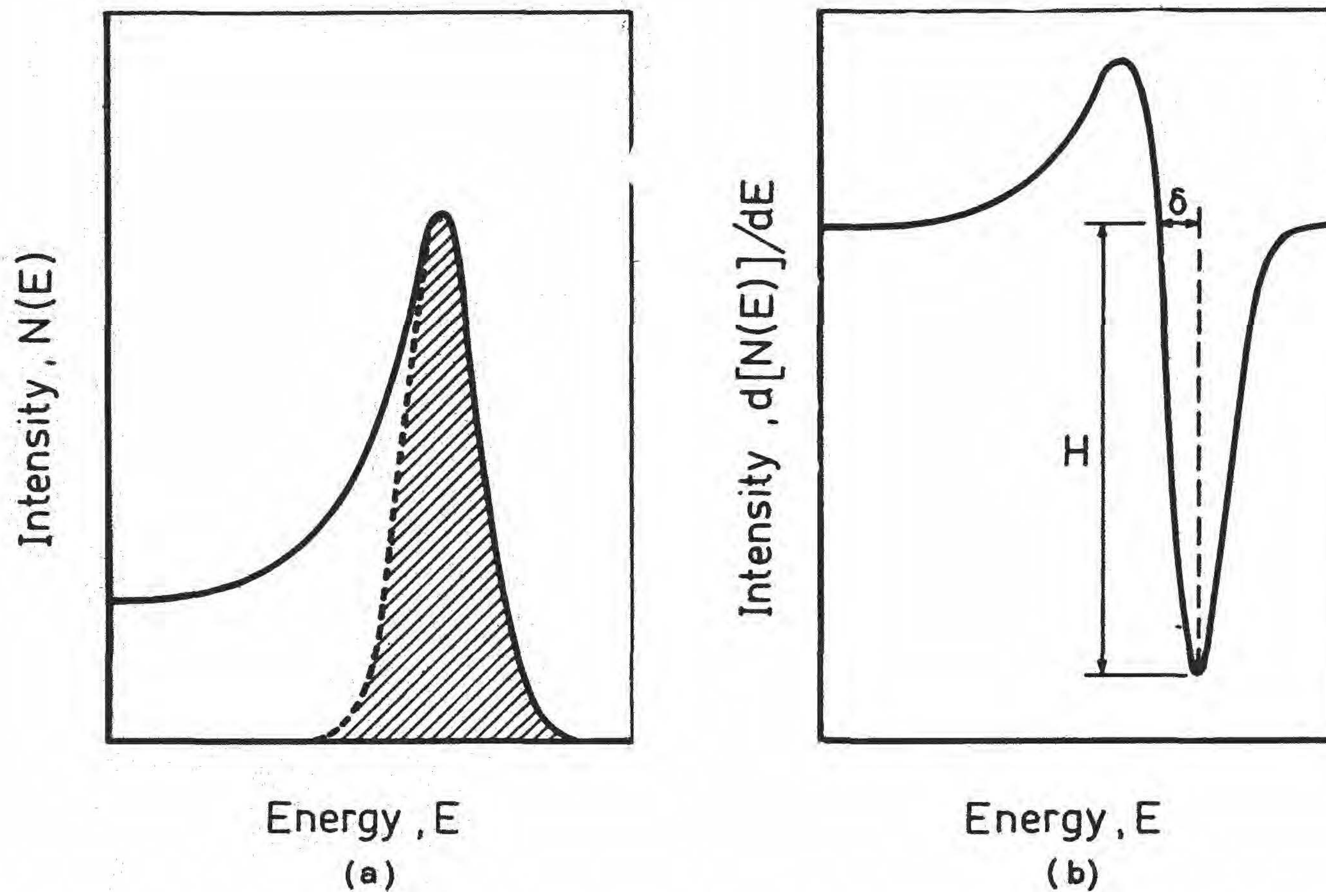


Fig. 14. The shape of the Auger electron feature in the energy spectra. (a) The integral spectrum; the shaded area corresponds to the Auger electron current emitted from the outer layers. (b) The differential spectrum; the distance H is recommended as a measure of the Auger electron current.



http://rcin.org.pl

## 6.3. Experimental procedures

Let us denote by $S^o$ the function relating the Auger intensity to the Auger electron current collected by the analyser. We have

$$H = S^o I_A \tag{6.1}$$

In general, the function $S^o$ depends on the energy of a chosen Auger transition, the analyser, and the spectrometer settings. Introducing eq (4.17) or eq (4.18) into eq (6.1) we obtain

$$H = k^o M^s r d X^s \tag{6.2}$$

where $k^o$ is the spectrometer constant. This constant is given by

$$k^o = \frac{1}{4\pi} P_A I_o \sigma(E_o) S^o \int_{\Delta\Omega} \cos\alpha \, d\Omega \tag{6.3}$$

or

$$k^o = \frac{\Delta\Omega}{4\pi} P_A I_o \sigma(E_o) S^o \cos\alpha \tag{6.4}$$

depending on the acceptance angle of the analyser. Similarly as $S^o$, the spectrometer constant depends on the energy of Auger transition, the kind of the analyser and the spectrometer settings. Eq (6.2) relates the measured Auger electron intensity to the concentration of a given element in the surface region for the case of uniform composition in the region sampled by Auger electrons. From eqs (4.20) and (6.1) we obtain similar relation for the case of segregation limited to the first monolayer

http://rcin.org.pl

$$H = k^{o}\, r\, d \left\{ M^{s} X^{s} \left[ 1 - \exp(-t/d \cos\alpha) \right] + M^{b} X^{b} \exp(-t/d \cos\alpha) \right\} \tag{6.5}$$

with $k^{o}$ given by eq (6.4).

The constant $k^{o}$ comprises a number of parameters independent of a matrix, and its value is unknown. For this reason the quantitative AES, similarly as EPMA, is a technique of relative measurements. Determination of the surface concentration $X^{s}$ involves comparison of Auger electron intensity from a given sample with Auger electron intensity from a standard, i.e. from a surface with known concentration of an element under consideration. The standard in quantitative AES is usually a carefully cleaned surface of a pure element. In few papers the surface of fractured alloy was postulated as a standard, under assumption that this surface has the composition of the bulk (Bouwman et al., 1973a,b, 1976a,b). This method, called the internal calibration method, involves more complicated experimental procedure than the analysis with pure metal as a standard.

The most frequently used experimental procedures are described below.

### 6.3.1. Relative sensitivity factor approach

The quantitative analysis using the so-called relative sensitivity factors seems to be the most convenient experimental procedure. The analysis consists in measuring the intensities of two Auger signals from two components of a given sample of binary alloy. Measurements provide a set of ratios $H_i/H_j$ corresponding to a set of alloys under investigation. Then, in separate experiment, the ratio of intensities of the same signals from pure

http://rcin.org.pl

metals, $H_i^i/H_j^j$ , is measured. The ratio $H_i^i/H_j^j$ is necessary to determine the so called relative sensitivity factor. The latter quantity is defined as (Hall and Morabito, 1977, 1979)

$$P_{i,j} = (H_i/X_i^s)/(H_j/X_j^s) \tag{6.6}$$

The relation between the correcting factors and the relative sensitivity factor depends on the model of the surface region.

(i) Uniform composition of the surface region within the sampling depth of Auger electrons.

Substitution of eq (6.2) into eq (6.6) gives

$$P_{i,j} = \frac{k_i^o \; r_i \; d_i}{k_j^o \; r_j \; d_j} = (H_i^i/H_j^j) \; F_{i,j} \tag{6.7}$$

where

$$F_{i,j} = \frac{M^j \; r_j^j \; d_j^j}{M^i \; r_i^i \; d_i^i} \; \frac{r_i \; d_i}{r_j \; d_j} \tag{6.7a}$$

In the limit of pure i-th component eq (6.7a) transforms into (Hall and Morabito, 1979)

$$F_{i,j}^i = \frac{M^j \; r_i^j \; d_i^j}{M^i \; r_j^i \; d_j^i} \tag{6.8}$$

Similarly, in the limit of pure j-th component we have (Hall and Morabito, 1979)

$$F_{i,j}^j = \frac{M^j \; r_i^j \; d_i^j}{M^i \; r_i^i \; d_i^i} \tag{6.9}$$

The values of the parameters $F_{i,j}^i$ and $F_{i,j}^j$ are similar in majority of binary alloys (Hall and Morabito, 1979). This

http://rcin.org.pl

indicates that the parameter $F_{i,j}$ (and the relative sensitivity factor) is a weak function of composition. The weak dependence of $P_{i,j}$ on composition was established experimentally (Hall et al., 1977) and theoretically (Jabłoński, 1980a) for a number of binary alloys.

From the definition of the relative sensitivity factor we obtain

$$X_i^s = \frac{X_j^s}{H_j} \frac{H_i}{P_{i,j}} \tag{6.10}$$

The sum of atom fractions extended over all elements present should be equal to unity

$$\frac{X_j^s}{H_j} \sum_i \frac{H_i}{P_{i,j}} = 1 \tag{6.11}$$

Eq (6.11) can be transformed into (Hall and Morabito, 1979)

$$X_j^s = \frac{H_j}{\sum_i H_i/P_{i,j}} \tag{6.12}$$

In the case of a binary alloy eq (6.12) has the form

$$X_j^s = \frac{1}{(H_i/H_j)/P_{i,j} + 1} \tag{6.13}$$

or, taking into account eq (6.7)

$$X_j^s = \frac{1}{(H_i/H_j)/\left[(H_i^i/H_j^j)\ \ F_{i,j}\right] + 1} \tag{6.14}$$

The surface concentration can be calculated directly from eq (6.14) provided the parameter $F_{i,j}$ given by eq (6.8) is known.

http://rcin.org.pl

However, the mean free paths, $d_i$ and $d_j$, may be functions of composition in the surface region. In that case eq (6.14) becomes more sophisticated equation in one unknown. The root of this equation is the sought surface composition $X_j^s$.

(ii) Surface segregation limited to the first monolayer.

The following formalism is limited to analysers with narrow range of acceptance angles, e.g. the CMA. The Auger electron intensity is described then by eq (6.5). Let the definition of the relative sensitivity factor be the same as in the case of the model of uniform composition within the escape depth [eq (6.6)]. From eqs (6.5) and (6.6) we obtain

$$P_{i,j} = (H_i^i/H_j^j) \; F_{i,j} \; W_{i,j} \; (X_j^s/X_i^s) \tag{6.15}$$

where

$$W_{i,j} = \frac{M^s X_i^s (1 - Y_i) + M^b X_i^b Y_i}{M^s X_j^s (1 - Y_j) + M^b X_j^b Y_j} \tag{6.15a}$$

$$Y_i = \exp(-t/d_i \cos\alpha)$$

$$Y_j = \exp(-t/d_j \cos\alpha)$$

and $F_{i,j}$ is given by eq (6.8).

The relative sensitivity factor is a function of surface composition. Eqs (6.13) and(6.15) form an equation in one unknown. Solution of this equation provides the value of $X_j^s$.

It is possible that eq (6.13) does not have a root in the range $0 < X_j^s < 1$. In that case the monolayer enrichment model is not valid. The segregation is considerable and the segregation

http://rcin.org.pl

region is extended over the distance of several monolayers. The segregation thickness can be estimated under assumption that the surface is covered by the pure i-th or j-th component (section 7.2).

6.3.2. Direct comparison with a standard

The most obvious experimental procedure of quantitative AES analysis consists in recording the Auger electron intensity from a given sample and, subsequently, from the pure component. Both recordings should be made as close in time as possible to avoid drifts in electronics gain. The experiment provides in that case the ratios $H_i/H_i^i$ . These ratios are sometimes denoted by $\xi_i$ (McDavid and Fain, 1975, Overbury and Somorjai, 1976, Jabłoński et al., 1977). Similarly as in the case of the relative sensitivity factor approach, we will briefly discuss calculations of the surface composition for both models of the surface region.

(i) Uniform composition of the surface region within the sampling depth of Auger electrons

The ratio $H_i/H_i^i$ can be derived from eq (6.2).

$$H_i/H_i^i = G_i\, X_i^s \tag{6.16}$$

where

$$G_i = \frac{M\, r_i\, d_i}{M^i\, r_i^i\, d_i^i} \tag{6.16a}$$

The surface concentration $X_i^s$ is calculated from the above equation. In general, the parameter $G_i$ may be a function of the surface composition (through factors $M$ and/or $d_i$ ) . In that

http://rcin.org.pl

case the surface composition $X_i^s$ is the root of eq (6.16).

(ii) Surface segregation limited to the first monolayer

The following relation results from eq (6.5).

$$H_i/H_i^i = [r_i\, d_i/(r_i^i\, d_i^i\, M^i)][M^s\, X_i^s(1 - Y_i) + M^b\, X_i^b\, Y_i] \qquad (6.17)$$

where

$$Y_i = \exp(- t/d_i \cos\alpha)$$

Solution of eq (6.17) provides the surface concentrations $X_i^s$. Eq (6.17) does not have the root in the range $0 < X_i^s < 1$ when the strong surface segregation exceeds one monolayer. The thickness of the segregated layer can be estimated assuming the presence of pure alloy constituent in the surface region (section 7.4).

http://rcin.org.pl

## 7. Proposition of an universal algorithm for calculating the surface composition of binary alloys

The material presented in sections 4, 5, and 6 makes possible the construction of an universal algorithm for calculations of quantitative AES (Jabłoński, 1981b, 1982). The proposed algorithm may be used in connection with experimental procedures discussed in section 6.3., i.e. the direct comparison with a standard or the relative sensitivity factor approach. The calculations of the surface concentration are performed for both models of the surface region discussed in section 4.2.

The correcting factors are calculated according to the following rules:

(i) The backscattering factor for pure elements is calculated from the formula of Love et al. (1978b) [eq (5.25)] . The linear dependence of the backscattering factor on the mass fraction of a given element is assumed to be generally valid (section 5.1.6). Thus, the backscattering factor for an alloy is calculated from the formula

$$r_i = r_i^j + (r_i^i - r_i^j)\, c_i^b \qquad (7.1)$$

where

$$c_i^b = A_i^o x_i^b / (A_i^o x_i^b + A_j^o x_j^b)$$

As it was discussed in section 5.1, the variation of the composition in the surface region should not affect the value of the backscattering factor, therefore the backscattering factor for an alloy is calculated for the bulk composition only.

http://rcin.org.pl

(ii) The total number of atoms in unit volume and the monolayer thickness for pure elements are calculated from eqs (5.37) and (5.38). Eq (5.41) was used to determine the total number of atoms in unit volume of the alloy, separately for the bulk composition and for the composition of the surface region

$$(1/M^s)^{1/3} = (1/M^j)^{1/3} + \left[(1/M^i)^{1/3} - (1/M^j)^{1/3}\right] X_i^s \qquad (7.2a)$$

$$(1/M^b)^{1/3} = (1/M^j)^{1/3} + \left[(1/M^i)^{1/3} - (1/M^j)^{1/3}\right] X_i^b \qquad (7.2b)$$

Similarly, the alloy monolayer thickness is calculated from eq (5.42) for the surface region and for the bulk

$$t^s = t^j + (t^i - t^j) X_i^s \qquad (7.3a)$$

$$t^b = t^j + (t^i - t^j) X_i^b \qquad (7.3b)$$

(iii) The inelastic mean free path for pure components is determined from the equation of Seah and Dench [eq (5.30)] . The dependence of the inelastic mean free path on the material enters eq(5.30) through the monolayer thickness $t$ (or the number of atoms in unit volume). Let us postulate that the inelastic mean free path for an alloy can be still calculated from eq (5.30) where monolayer thickness is given by eq (7.3a) or eq (7.3b). The inelastic mean free path is calculated for the surface composition when the extent of the surface segregation is comparable with the sampling depth of Auger electrons. It is reasonable to assume that the inelastic mean free path is then determined by the composition of the surface layer. When the mean free path is larger than the thickness of the segregated layer, the value of $d$ is determined by the bulk composition and is calculated from eqs (5.30) and (7.3b).

http://rcin.org.pl

The calculations are made for two experimental procedures and for two models of the surface region, so the algorithm consists of four sections, denoted by A, B, C and D. These sections are described below.

## 7.1. Section A

Section A calculates the surface composition when the experimental procedure of the relative sensitivity factor approach has been used and the model of uniform composition within sampling depth is assumed. The surface composition is determined then from eq (6.14). The inelastic mean free path is determined by the surface composition because the composition is assumed to be uniform within the depth comparable with $d$ . As a result, the factor $F_{i,j}$ in eq (6.14) is a function of the surface concentration

$$F_{i,j} = \frac{M^j \; r_j^j \; d_j^j}{M^i \; r_i^i \; d_i^i} \; \frac{r_i \; d_i^s}{r_j \; d_j^s} \qquad (7.4)$$

The parameters $H_i/H_j$ , $H_i^i/H_j^j$ and $F_{i,j}$ are always greater than zero, so

$$0 < \frac{1}{(H_i/H_j)/[(H_i^i/H_j^j)\; F_{i,j}] + 1} < 1$$

Thus, eq (6.14) has always a root in the range $0 < X_j^s < 1$ , and this root can be easily found. The half-interval method is used in the presented algorithm (Arden and Astill, 1970).

## 7.2. Section B

When the model of monolayer enrichment is assumed, the experi-

http://rcin.org.pl

mental data from the experimental procedure of the relative sensitivity factor approach are entered to the section B of the program. The surface composition is determined from eq (6.13) with $P_{i,j}$ given by eq (6.15). In the considered case the mean free path is supposed to be larger than the monolayer thickness, so the mean free paths are calculated for the bulk composition of the alloy. The parameter $F_{i,j}$ given by eq (6.7a) is then independent of the surface composition

$$F_{i,j} = \frac{M^j \; r^j_j \; d^j_j}{M^i \; r^i_i \; d^i_i} \; \frac{r_i \; d^b_i}{r_j \; d^b_j} \tag{7.5}$$

Substitution of eq (6.15) into eq (6.13) gives

$$B_{i,j} = W_{i,j} \tag{7.6}$$

where the parameter

$$B_{i,j} = (H_i/H_j)/[(H^i_i/H^j_j) \; F_{i,j}]$$

comprises all factors independent of the surface composition. The parameter $W_{i,j}$, given by eq (6.15a) is a function of composition because the number of atoms in unit volume, $M^s$, and the first monolayer thickness, $t^s$, depend on $X^s_i$. Thus, the surface concentration $X^s_i$ is obtained on solving eq (7.6).

When eq (7.6) does not have a root in the range $0 < X^s_i < 1$ the model of the monolayer enrichment is not valid. The extent of the strong surface segregation exceeds one monolayer. It is possible to estimate the thickness T of the surface region assuming that i-th or j-th pure component segregated to the surface. We have from eq (6.15a)

http://rcin.org.pl

$W_{i,j}(X_i^s=0) =$

$$= \frac{M^b\, X_i^b \exp(-t^j/d_i\cos\alpha)}{M^j[1-\exp(-t^j/d_j\cos\alpha)] + M^b\, X_j^b \exp(-t^j/d_j\cos\alpha)} \qquad (7.7)$$

and

$W_{i,j}(X_i^s=1) =$

$$= \frac{M^i[1-\exp(-t^i/d_i\cos\alpha)] + M^b\, X_i^b \exp(-t^i/d_i\cos\alpha)}{M^b\, X_j^b \exp(-t^i/d_j\cos\alpha)} \qquad (7.8)$$

(i) If $W_{i,j}(X_i^s=0) > B_{i,j}$ , the surface is enriched with j-th component. We shall choose such $t^j = T^j$ that $W_{i,j}(X_i^s=0) = B_{i,j}$ . This is equivalent to solving the following equation with respect to $T^j$

$$B_{i,j} = \frac{M^b\, X_i^b \exp(-T^j/d_i\cos\alpha)}{M^j[1-\exp(-T^j/d_j\cos\alpha)] + M^b\, X_j^b \exp(-T^j/d_j\cos\alpha)} \qquad (7.9)$$

(ii) If $W_{i,j}(X_i^s=1) < B_{i,j}$ , the surface is enriched with i-th component. The thickness of the segregated layer, $T^i$ , is determined from the equation

$$B_{i,j} = \frac{M^i[1-\exp(-T^i/d_i\cos\alpha)] + M^b\, X_i^b \exp(-T^i/d_i\cos\alpha)}{M^b\, X_j^b \exp(-T^i/d_j\cos\alpha)} \qquad (7.10)$$

7.3. Section C

The section C determines the surface composition in the case of the direct comparison with a standard, and for a model of uniform composition within the sampling depth. Similarly as in section A, the mean free path in the surface region is assumed

http://rcin.org.pl

to be determined by the surface composition. Also, the total number of atoms in unit volume is calculated for the surface composition. The parameter $G_i$ given by eq (6.16a) is a function of $X_i^s$

$$G_i = \frac{M^s \; r_i \; d_i^s}{M^i \; r_i^i \; d_i^i} \tag{7.11}$$

The surface composition is obtained from eq (6.16) with $G_i$ given by eq (7.11). Eq (6.16) does not have a root when $X_i^s < (H_i/H_i^i)/G_i$ for $0 < X_i^s < 1$. This occurs when the surface is strongly enriched with i-th component, and the parameters $H_i/H_i^i$ and/or $G_i$ are subjects to large errors.

## 7.4. Section D

The calculations of the surface composition in the case of the direct comparison with a standard for the model of monolayer enrichment take place in section D. As in section B, the mean free path of Auger electrons in the surface region is calculated for the bulk composition. The parameters M and t in the surface region are assumed to be functions of the surface composition. Eq (6.17) can be transformed to the form

$$L_i = V_i(X_i^s) \tag{7.12}$$

where the parameter

$$L_i = (H_i/H_i^i)[r_i^i \; d_i^i \; M^i/(r_i \; d_i^b)]$$

is independent of the surface composition, and

http://rcin.org.pl

$$V_i(X_i^s) = M^s X_i^s [1 - \exp(- t^s/d_i^b \cos\alpha)] + \tag{7.13}$$
$$+ M^b X_i^b \exp(- t^s/d_i^b \cos\alpha)$$

The surface concentration $X_i^s$ is calculated from eq (7.12).

When the root of eq (7.12) cannot be found in the region $0 < X_i^s < 1$ , the monolayer enrichment model is not valid. Similarly as in section B, the thickness of the segregation region can be estimated under assumption that the surface is covered by pure i-th or j-th component

(i) If $V_i(X_i^s=0) > L_i$ we have strong segregation of j-th component. In that case such value of $t^j=T^j$ is selected that the equation

$$L_i = V_i(X_i^s=0) = M^b X_i^b \exp(- T^j/d_i^b \cos\alpha)$$

is satisfied. This equation may be transformed to the form

$$T^j = - d_i^b \cos\alpha \ln(L_i/M^b X_i^b) \tag{7.14}$$

(ii) If $V_i(X_i^s=1) < L_1$ strong segregation of i-th component occurs. The thickness of the overlayer under assumption of pure i-th component at the surface is calculated from the equation

$$L_i = V_i(X_i^s=1) = M^i[1 - \exp(- T^i/d_i^b \cos\alpha)] +$$
$$+ M^b X_i^b \exp(- T^i/d_i^b \cos\alpha)$$

or

$$T^i = - d_i^b \cos\alpha \ln[(L_i - M^i)/(M^b X_i^b - M^i)] \tag{7.15}$$

It may be derived from eq (5.41) that the denominator in eq (7.15), $M^b X_i^b - M^i$ , is negative if $M^i > (8/27) M^j$ . This

http://rcin.org.pl

inequality is practically always valid. Thus, the thickness $T^i$ can be calculated from eq (7.15) if $L_i < M^i$. When the parameter $L_i$ is greater than $M^i$, the overlayer thickness cannot be determined and the respective information is printed.

## 7.5. The input and output data

The first group of parameters entered to the program specify the experimental procedure and the model of the surface region. The set of the remaining input data depends on the experimental procedure.

(i) The direct comparison with a standard

The list of the data is the following:

$n$ - Number of alloys.

$A_i^o$ - Atomic mass of i-th element, g/mole.

$A_j^o$ - Atomic mass of j-th element, g/mole.

$\rho^i$ - Density of pure i-th element, $g/cm^3$.

$\rho^j$ - Density of pure j-th element, $g/cm^3$.

$Z_i$ - Atomic number of i-th element.

$Z_j$ - Atomic number of j-th element.

$E_o$ - Primary energy, eV.

$E_A$ - Auger electron energy corresponding to a chosen Auger transition, eV.

$E_c$ - Ionization energy associated with a chosen Auger transition, eV.

$X_i^b$ - Table of bulk concentrations, atom fractions.

$H_i/H_i^i$ - Table of Auger electron intensity ratios.

When the monolayer enrichment model is selected, the acceptance angle of the analyser, $\alpha$, is additionally entered (degrees).

http://rcin.org.pl

(ii) The relative sensitivity factor approach

The list of input data begins with the same eight parameters as in the case of direct comparison with a standard, i.e. $n$, $A_i^o$, $A_j^o$, $\rho^i$, $\rho^j$, $Z_i$, $Z_j$ and $E_o$. Remaining data are the following:

$E_{A,i}$ - Auger electron energy corresponding to Auger transition in i-th element, eV.

$E_{A,j}$ - Auger electron energy corresponding to Auger transition in j-th element, eV.

$E_{c,i}$ - Ionization energy associated with Auger transition in i-th element, eV.

$E_{c,j}$ - Ionization energy associated with Auger transition in j-th element, eV.

$X_i^b$ - Table of bulk concentrations, atom fractions.

$H_i/H_j$ - Table of Auger electron intensity ratios.

$H_i^i/H_j^j$ - Auger electron intensity ratio for pure elements.

Assumption of the monolayer enrichment model requires also entering the acceptance angle of the analyser, $\alpha$ (degrees).

The details of the input data preparation are shown in Appendix (fig. A-1).

Similarly as in the case of input, the set of the output data depends also on the experimental procedure.

(i) The direct comparison with a standard

The list of the output parameters for a given alloy has the form:

$X_i^b$ - Bulk concentration of i-th element, atom fraction.

$t^i$ - Monolayer thickness for pure i-th element, nanometers.

$t^j$ - Monolayer thickness for pure j-th element, nanometers.

$t^s$ - Monolayer thickness in the surface region, nanometers.

http://rcin.org.pl

$d_i^i$ - Mean free path of Auger electron associated with i-th Auger transition in a matrix of pure i-th element, nanometers.

$d_i^j$ - Mean free path of Auger electron associated with i-th Auger transition in a matrix of almost pure j-th element, nanometers.

$d_i^s$ or $d_i^b$ - Mean free path of Auger electron associated with i-th Auger transition in the surface region, nanometers.

$M^i$ - Total number of atoms in unit volume of pure i-th element, $1/cm^3$.

$M^j$ - Total number of atoms in unit volume of pure j-th element, $1/cm^3$.

$M^s$ - Total number of atoms in unit volume of the surface region, $1/cm^3$.

$r_i^i$ - Backscattering factor for i-th Auger transition in pure i-th element.

$r_i^j$ - Backscattering factor for i-th Auger transition in the matrix of almost pure j-th element.

$r_i$ - Backscattering factor for i-th Auger transition in the alloy.

$G_i$ - Total correction given by eq (7.11). It is printed when the model of uniform composition in the sampling depth is selected.

$H_i/H_i^i$ - Auger electron intensity ratio.

$X_i^s$ - Surface concentration of i-th element, atom fraction.

To complete the output data, the comments are printed that specify the experimental procedure and the selected model of the surface region. When the monolayer enrichment model is not valid

http://rcin.org.pl

the diagnostics is also printed, in addition to the estimated thickness of the surface region.

(ii) The relative sensitivity factor approach

The output parameters $X_i^b$ , $t^i$ , $t^j$ , $t^s$ and $d_i^i$ are the same as in the previous case. Furthermore, we have

$d_j^j$ - Mean free path of Auger electron associated with j-th Auger transition in a matrix of pure j-th element, nanometers.

$d_i^s$ or $d_i^b$ - Mean free path of Auger electron associated with i-th Auger transition in the surface region, nanometers.

$d_j^s$ or $d_j^b$ - Mean free path of Auger electron associated with j-th Auger transition in the surface region, nanometers.

The parameters $M^i$ , $M^j$ , $M^s$ and $r_i^i$ are the same as in the case (i).

$r_j^j$ - Backscattering factor for j-th Auger transition in pure j-th element.

$r_i$ - Backscattering factor for i-th Auger transition in the alloy.

$r_j$ - Backscattering factor for j-th Auger transition in the alloy.

$F_{i,j}$ - Parameter given by eq (7.4) or eq (7.5).

$H_i^i/H_j^j$ - Auger electron intensity ratio for pure elements.

$X_i^s$ - Surface concentration of i-th element, atom fraction.

The comments specifying the experimental procedure and the model of surface region are also printed. Similarly as in the previous case, the thickness of the surface region is estimated when the model of monolayer enrichment is not valid.

http://rcin.org.pl

Examples of the output data are shown in Appendix in figs A-2, A-3 and A-4.

The program based on the described algorithm has been developed in the Institute of Physical Chemistry, Polish Academy of Sciences. The program is written in FORTRAN EXTENDED and consists of about 1100 computer cards. In addition to the described possibilities, the program has also a facility of plotting the calculated surface concentration versus the bulk concentrations (Appendix, fig. A-5).

http://rcin.org.pl

## 8. Examples of calculations

To illustrate the application of the proposed algorithm we shall calculate the surface composition of chosen binary alloys. The data for calculations were obtained from both experimental procedures described in sections 6.3.1 and 6.3.2.

Example 1 [taken from Jabłoński (1982)]. The results of quantitative AES analysis of equilibrated and extensively sputtered gold-palladium alloy surfaces have been published by Jabłoński et al. (1977). The experimental data were obtained from the procedure of the relative sensitivity factor approach. The authors recorded the ratios of 69 eV Au Auger intensity ( $N_7O_{4,5}O_{4,5}$ Auger transition ) to 330 eV Pd Auger intensity ( $M_5N_{4,5}N_{4,5}$ Auger transition ) and the ratios of 2024 eV Au Auger intensity ( $M_5N_7N_7$ Auger transition ) to 330 eV Pd Auger intensity. The published calculations of the surface composition did not account for the concentration dependence of the backscattering factors and the mean free paths. Let us recalculate the surface compositions using the presented algorithm.

The values of ionization energies associated with Auger transitions chosen for analysis are taken from Sevier (1972b). The $N_7O_{4,5}O_{4,5}$ Auger transition in gold was ascribed the ionization energy of $N_4$ subshell for reasons discussed in section 5.1.5. Thus, the input data are the following

$A_i^o$ = 196.9665 g/mole

$A_j^o$ = 106.4 g/mole

$\rho^i$ = 19.32 g/cm$^3$

$\rho^j$ = 12.02 g/cm$^3$

$Z_i$ = 79

$Z_j$ = 46

http://rcin.org.pl

$E_o$ = 4000 eV

$E_{A,i}$ = 69 eV or 2024 eV

$E_{A,j}$ = 330 eV

$E_{c,i}$ = 352 eV or 2205 eV

$E_{c,j}$ = 334.7 eV

The bulk concentrations, $X_i^b$ , and the ratios $H_i/H_j$ and $H_i^i/H_j^j$ are taken from table 1 of Jabłoński et al. (1977). Several examples of the output list are shown in Appendix (fig. A-2). The results of calculations are listed in tables 8 and 9. They are also shown in figs 15 and 16. The equilibrated surfaces are substantially enriched with gold, while the sputtered alloys seem to be enriched with palladium. The surface concentrations, $X_{Au}^s$ , calculated by the proposed program turned out to be close to these published by Jabłoński et al. (1977). The alloy components differ considerably in atomic number (46 as compared with 79), and therefore the strong concentration dependence of the backscattering factors is expected. However, all the three corrections, M , r and d, compensate, so the total correction $F_{i,j}$ is practically constant in the whole concentration range and is close to unity. The concentrations $X_{Au}^s$ calculated for the model of uniform composition within the sampling depth are practically identical with the uncorrected results (method 1 of Jabłoński et al., 1977). More pronounced differences are found between surface concentrations calculated for the model of monolayer enrichment (method 2 of Jabłoński et al., 1977). However, these differences are mainly due to the different values of the inelastic mean free paths used in the present calculations.

http://rcin.org.pl

Table 8. The surface and bulk compositions of the Au Pd binary alloy. The experimental intensity ratios were obtained from the relative sensitivity factor approach with 69 eV gold transition and 330 eV palladium transition chosen for analysis. (1) The model of uniform composition within the sampling depth of Auger electrons; (2) The model of the monolayer enrichment.

| $X^b_{Au}$ | After equilibration | | | After sputtering | | |
|---|---|---|---|---|---|---|
| | $H_{Au}/H_{Pd}$ | $X^s_{Au}$ (1) | $X^s_{Au}$ (2) | $H_{Au}/H_{Pd}$ | $X^s_{Au}$ (1) | $X^s_{Au}$ (2) |
| 0.0099 | 0.0400 | 0.0682 | 0.124 | | | |
| 0.0990 | 0.247 | 0.311 | 0.579 | 0.0487 | 0.0803 | 0.0621 |
| 0.3051 | 0.499 | 0.478 | 0.732 | 0.186 | 0.250 | 0.187 |
| 0.5976 | 1.28 | 0.701 | 0.887 | 0.788 | 0.585 | 0.566 |
| 0.8965 | 7.42 | 0.931 | 1.000 | 3.48 | 0.862 | 0.792 |
| 0.9897 | 67.3 | 0.992 | 0.997 | 30.0 | 0.982 | 0.964 |
| Pure metals | 0.549 | | | 0.561 | | |



http://rcin.org.pl

Table 9. The surface and bulk compositions of the Au Pd binary alloy. The experimental intensity ratios were obtained from the relative sensitivity factor approach with 2024 eV gold transition and 330 eV palladium transition chosen for analysis. (1) The model of uniform composition within the sampling depth of Auger electrons; (2) The model of the monolayer enrichment.

| $X^{b}_{Au}$ | After equilibration | | | After sputtering | | |
|---|---|---|---|---|---|---|
| | $H_{Au}/H_{Pd}$ | $X^{s}_{Au}$ (1) | $X^{s}_{Au}$ (2) | $H_{Au}/H_{Pd}$ | $X^{s}_{Au}$ (1) | $X^{s}_{Au}$ (2) |
| 0.0990 | 0.00507 | 0.132 | 0.304 | 0.00269 | 0.0724 | 0.0 |
| 0.3051 | 0.0172 | 0.339 | 0.478 | 0.0112 | 0.244 | 0.0 |
| 0.5976 | 0.0693 | 0.673 | 0.901 | 0.0527 | 0.603 | 0.618 |
| 0.8965 | 0.457 | 0.931 | 1.000 | 0.238 | 0.872 | 0.811 |
| 0.9897 | 4.44 | 0.992 | 0.999 | 1.94 | 0.982 | 0.965 |
| Pure metals | 0.0340 | | | 0.0351 | | |



http://rcin.org.pl

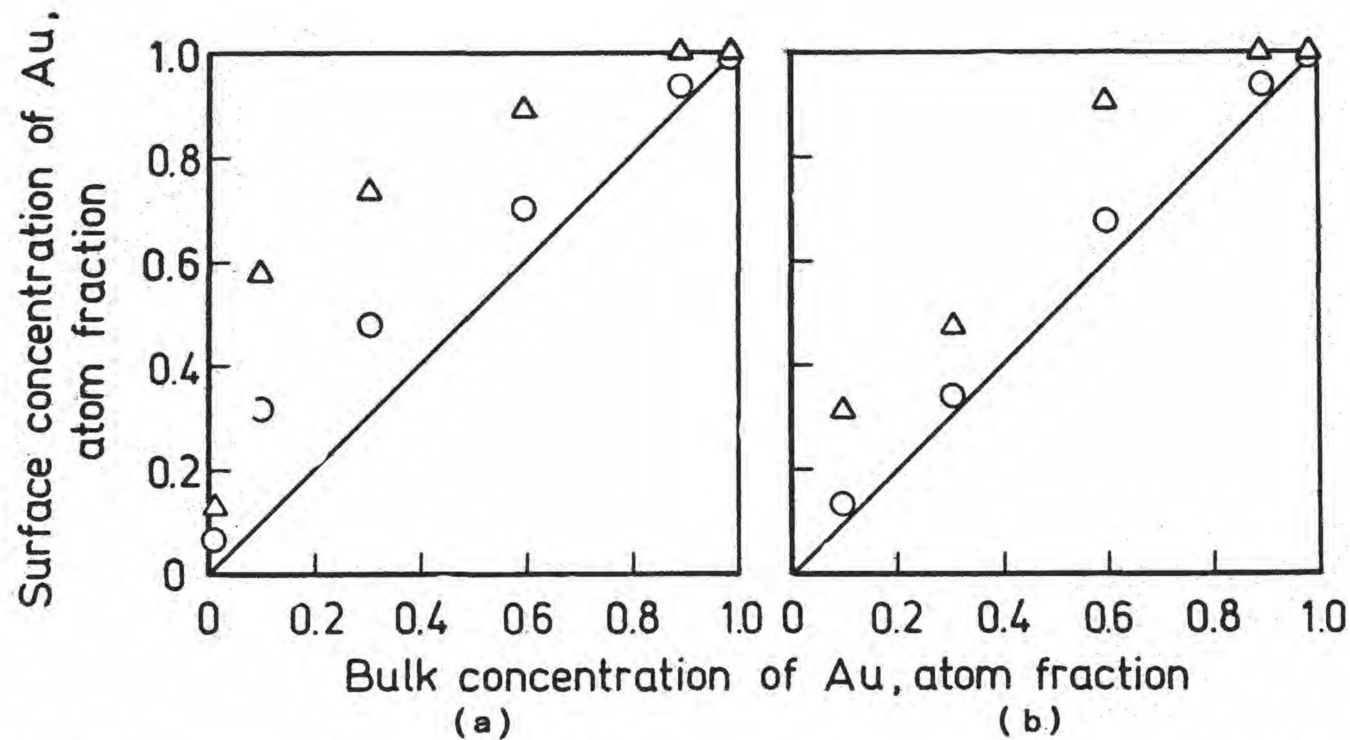


Fig. 15. The surface composition as a function of the bulk composition calculated for the equilibrated AuPd alloys. Circles: the assumption of uniform composition within the sampling depth of Auger electrons; triangles: the assumption of monolayer enrichment. (a) The surface composition calculated from the intensity ratios of 69 eV Au transition to 330 eV Pd transition. (b) The surface composition calculated from the intensity ratio of 2024 eV Au transition to 330 eV Pd transition [figure taken from Jabłoński (1982)].

http://rcin.org.pl

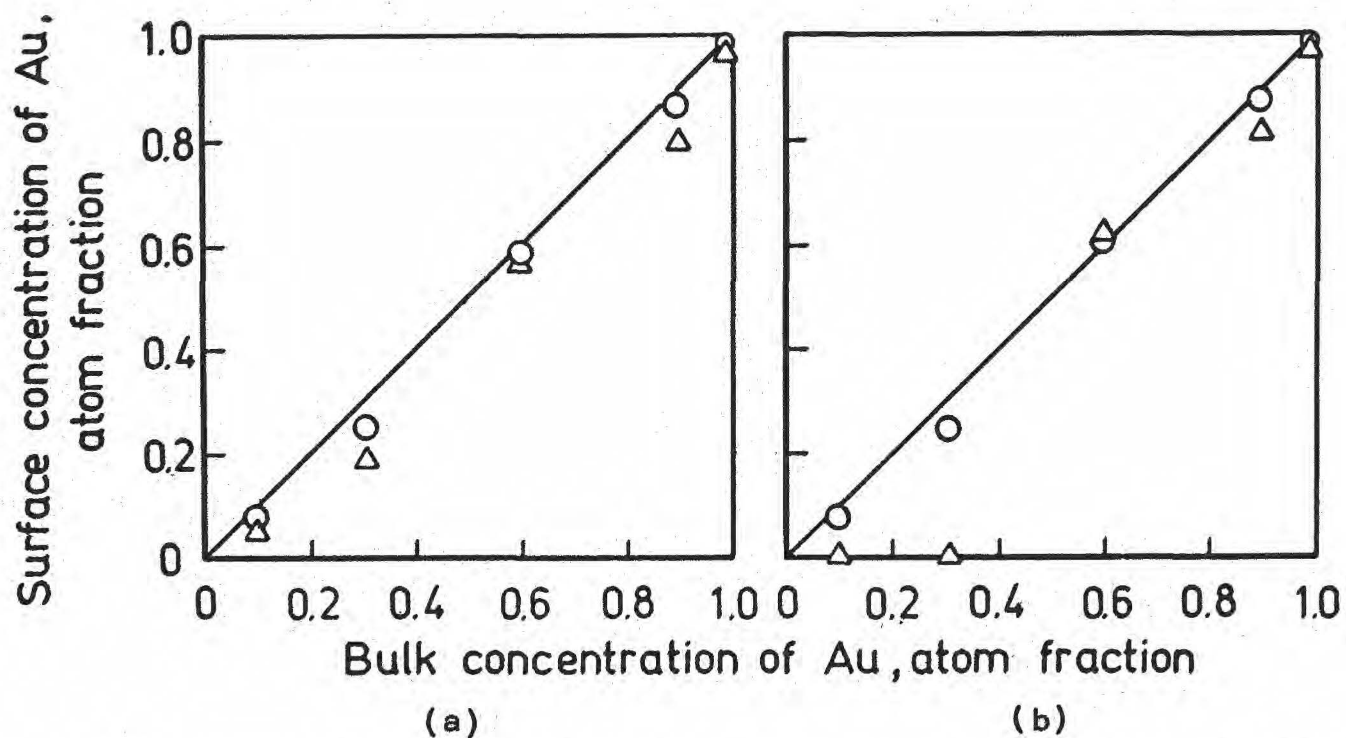


Fig. 16. The surface composition as a function of the bulk composition calculated for the AuPd alloys after extensive sputtering. Circles: the assumption of uniform composition within the sampling depth of Auger electrons; triangles: the assumption of monolayer enrichment. (a) The surface composition calculated from the intensity ratios of 69 eV Au transition to 330 eV Pd transition. (b) The surface composition calculated from the intensity ratio of 2024 eV Au transition to 330 eV Pd transition [figure taken from Jabłoński (1982)].



http://rcin.org.pl

Example 2 [ taken from Jabłoński (1981b)]. The neglect of one or more correcting factors in quantitative analysis may affect significantly the calculated surface composition. It has been shown that the apparent surface enrichment with an element of lower atomic number can be observed when the backscattering correction is neglected, no matter which Auger transition is taken for analysis (Jabłoński, 1978). As an example, the NiPd binary alloy has been considered (Jabłoński, 1978). Mathieu and Landolt (1975) have found the nickel enrichment of extensively sputtered NiPd alloys. The $M_5N_{4,5}N_{4,5}$ Pd Auger transition (330 eV) and $L_3M_{4,5}M_{4,5}$ Ni Auger transition (848 eV) were chosen for analysis. The authors calculated the surface composition assuming the uniform composition within the sampling depth of Auger electrons [eq (6.16)]. The results were corrected only for the changes in the total number of atoms in unit volume. In that case the total correction $G_i$ defined by eq (6.16a) has the form

$$G_i = M^b/M^i$$

Similarly as Mathieu and Landolt (1975), let us calculate the surface composition of NiPd alloy from relative intensities of $M_5N_{4,5}N_{4,5}$ Pd transition, so the index "i" is equivalent with Pd, and index "j" with Ni. The following input data were entered to the program

$A_i^o$ = 106.4 g/mole

$A_j^o$ = 58.71 g/mole

$\rho^i$ = 12.02 g/cm$^3$

$\rho^j$ = 8.902 g/cm$^3$

$Z_i$ = 46

$Z_j$ = 28

http://rcin.org.pl

$E_o$ = 5000 eV

$E_A$ = 330 eV

$E_c$ = 334.7 eV

The bulk concentrations, $X_i^b$ , and the ratios $H_i/H_i^i$ are taken from fig. 3 of the paper by Mathieu and Landolt (1975). An example of the output data for the procedure of direct comparison with a standard is shown in Appendix (fig. A-3). The present results of calculations are compared with the results of Mathieu and Landolt (1975) in fig. 17. One can see that the calculated surface composition is noticeably affected by taking into account all three corrections. The present results indicate that there is practically no surface enrichment in extensively sputtered NiPd binary alloys.

**Example 3.** Holloway (1975b) suggested the possibility of using Auger electron spectroscopy for measuring the thickness of one material evaporated on top of the other. This application of AES necessitates knowledge of the accurate expression relating the inelastic mean free path to the Auger electron energy and the atomic number of an element. The algorithm presented in section 7, using the expression of Seah and Dench (1979) to determine the inelastic mean free paths, offers also a possibility of calculating the overlayer thickness.

The proposed algorithm will be used in calculations of the thicknesses of tungsten overlayer on molybdenum and molybdenum overlayer on tungsten from the experimental data of Tarng and Wehner (1973). They monitored the relative intensity ratios $H_i/H_i^i$ for different Auger transitions as a function of the experimentally determined overlayer thickness. The authors recorded

http://rcin.org.pl

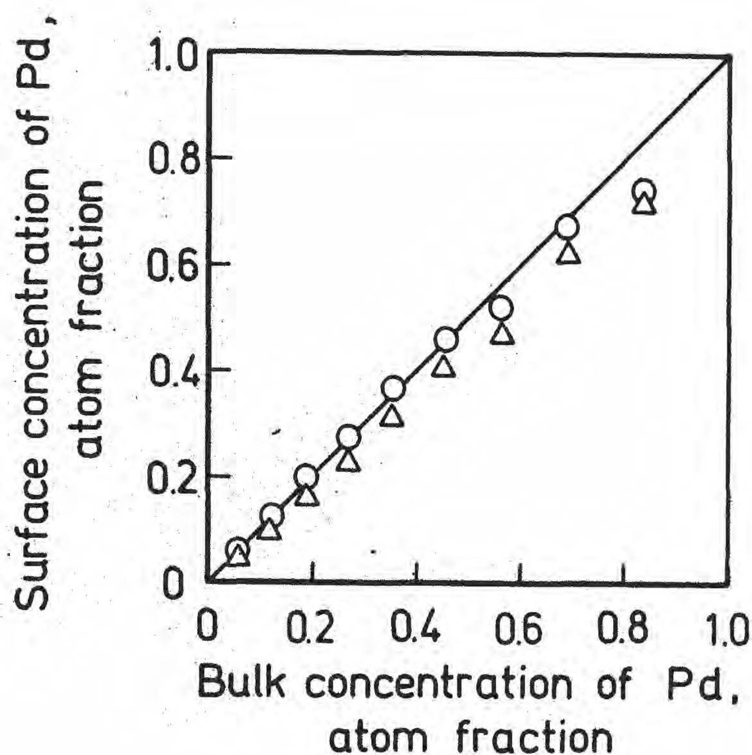


Fig. 17. The surface composition as a function of the bulk composition calculated for NiPd alloys after extensive sputtering from the relative intensity of the 330 eV Pd transition. Circles: present results obtained for the model of uniform composition within the sampling depth of Auger electrons; triangles: the surface concentrations calculated by Mathieu and Landolt (1975) [figure taken from Jabłoński (1981b)].

http://rcin.org.pl

the tungsten Auger electron peaks at 1736 eV, 350 eV and 48 eV, and the molybdenum peak at 120 eV. These Auger peaks may be assigned on energetic grounds the $M_5N_7N_7$, $N_3O_3O_3$, $O_2VV$ and $M_5N_1N_{2,3}$ Auger transitions, respectively. We will determine the overlayer thicknesses for each of these transitions. The calculations are performed for the model of the monolayer enrichment. The input data for the W overlayer on Mo are the following.

(i) The Auger transition in tungsten

The indexes "i" and "j" are ascribed to tungsten and molybdenum respectively.

$A_i^o$ = 183.85 g/mole
$A_j^o$ = 95.94 g/mole
$\rho^i$ = 19.3 g/cm$^3$
$\rho^j$ = 10.22 g/cm$^3$
$Z_i$ = 74
$Z_j$ = 42
$E_o$ = 5000 eV
$E_A$ = 1736 eV or 350 eV or 48 eV
$E_c$ = 1809.2 eV or 425.3 eV or 46.8 eV
$X_i^b$ = 0.0

$H_i/H_i^i$ is the ratio of the intensity recorded from the tungsten overlayer to the intensity recorded from the pure tungsten. These ratios are taken from fig. 2 of Tarng and Wehner (1973). Examples of the output data for 350 eV Auger transition are shown in Appendix (fig. A-4).

(ii) The Auger transition in molybdenum

The indexes "i" and "j" refer to molybdenum and tungsten, respectively.

http://rcin.org.pl

$A_i^o$ = 95.94

$A_j^o$ = 183.85

$\rho^i$ = 10.22

$\rho^j$ = 19.3

$Z_i$ = 42

$Z_j$ = 74

$E_o$ = 5000 eV

$E_A$ = 120 eV

$E_c$ = 227 eV

$X_i^b$ = 1.0

$H_i/H_i^i$ is the ratio of the intensity recorded from the substrate to the intensity recorded from pure molybdenum. These ratios are taken from fig. 2 of Tarng and Wehner (1973).

In table 10 the experimental thicknesses are compared with thicknesses calculated by the proposed program. Similar results calculated for the molybdenum overlayer on tungsten are listed in table 11. As follows from both tables, the calculated and experimental values agree within 70%. Thus, the present algorithm gives only the rough estimation of the overlayer thickness. The deviations of the calculated thicknesses from the experimental values are due to the differences between inelastic mean free paths determined experimentally by Tarng and Wehner (1973) for tungsten and molybdenum and the mean free paths resulting from the expression of Seah and Dench (1979). These differences reach 20-30%.

http://rcin.org.pl

Table 10. Comparison of experimental and calculated thicknesses of tungsten overlayer on molybdenum substrate. $m_{exp}$ and $m_{calc}$ denote the experimental and calculated number of monolayers, respectively. The ratios of Auger electron intensities, $H_i/H_i^i$ , for 1736 eV, 350 eV and 48 eV Auger transitions in W and 120 eV Auger transition in Mo are taken from the plot reported by Tarng and Wehner (1973).

| $m_{exp}$ | $H_W/H_W^W$ 1736 eV | $m_{calc}$ | $H_W/H_W^W$ 350 eV | $m_{calc}$ | $H_W/H_W^W$ 48 eV | $m_{calc}$ | $H_{Mo}/H_{Mo}^{Mo}$ 120 eV | $m_{calc}$ |
|---|---|---|---|---|---|---|---|---|
| 0.5 | 0.089 | 0.68 | 0.159 | 0.58 | 0.192 | 0.37 | 0.820 | 0.40 |
| 1.0 | 0.168 | 1.3 | 0.296 | 1.1 | 0.382 | 0.74 | 0.640 | 0.80 |
| 2.0 | 0.316 | 2.7 | 0.508 | 2.3 | 0.665 | 1.6 | 0.389 | 1.6 |
| 3.0 | 0.460 | 4.6 | 0.682 | 3.9 | 0.826 | 2.7 | 0.210 | 2.6 |



http://rcin.org.pl

Table 11. Comparison of experimental and calculated thicknesses of molybdenum overlayer on tungsten substrate. $m_{exp}$ and $m_{calc}$ denote the experimental and calculated number of monolayers, respectively. The ratios of Auger electron intensities, $H_i/H_i^i$, for 1736 eV, 350 eV and 48 eV Auger transitions in W and 120 eV Auger transition in Mo are taken from the plot reported by Tarng and Wehner (1973).

| $m_{exp}$ | $H_W/H_W^W$ 1736 eV | $m_{calc}$ | $H_W/H_W^W$ 350 eV | $m_{calc}$ | $H_W/H_W^W$ 48 eV | $m_{calc}$ | $H_{Mo}/H_{Mo}^{Mo}$ 120 eV | $m_{calc}$ |
|---|---|---|---|---|---|---|---|---|
| 0.5 | 0.877 | 0.84 | 0.791 | 0.71 | 0.736 | 0.48 | 0.219 | 0.45 |
| 1.0 | 0.769 | 1.7 | 0.649 | 1.2 | 0.556 | 0.80 | 0.395 | 0.82 |
| 2.0 | 0.702 | 2.3 | 0.453 | 2.3 | 0.274 | 1.6 | 0.643 | 1.5 |
| 3.0 | 0.660 | 2.6 | 0.270 | 3.7 | 0.100 | 2.8 | 0.861 | 2.6 |



http://rcin.org.pl

## 9. Concluding remarks

In the present work an attempt has been made to summarize the present status in the quantitative Auger electron spectroscopy, the considerations being limited to two-component polycrystalline systems. The recent progress in this technique enables the construction of the universal algorithm for calculating the surface composition of binary alloys from Auger electron intensity ratios. However, the accuracy of such calculations is much lower than in the case of electron probe microanalysis, despite similarities between both techniques. Large part of errors in determining the surface composition has origin in present methods for calculating the correcting factors.

The backscattering factor for pure elements calculated from the formula of Love et al. (1978b) deviates from published values of $r$ by up to 15%. The deviations seem to be smaller at relatively high primary electron energies, higher than 5000 eV. For this reason such energies are recommended for quantitative analysis. The concentration dependence of the backscattering factor awaits more attention in the literature. The linear dependence of $r$ on the mass fraction of a given element proposed in this work results from theoretical considerations (Jabłoński, 1978, 1980a). The published experimental data are too scarce to verify the postulate of linearity.

Much experimental and theoretical work has been devoted to determine the inelastic mean free path of electrons in elements and compounds. The formula of Seah and Dench (1979) resulting from the statistical analysis of the published experimental data provides the values of the inelastic mean free path with rather

http://rcin.org.pl

limited accuracy, even though it is considered to be the best at present. The expected difference between the experimental data and the values resulting from formula of Seah and Dench is equal to about 36% (Hall and Morabito, 1979). There is an obvious need for more accurate expression. To author's knowledge, no experimental or theoretical data on the composition dependence of the inelastic mean free path are available in the literature. The linear dependence of d on the atom fraction assumed by Holloway (1977) and Berndt et al. (1980), or the generalization of the Seah and Dench formula postulated in the present work, has no or little physical sense. Fortunately, the inelastic mean free path seems to be a weak function of composition and the above assumptions may have insignificant effect on results of calculations.

As one can see, a knowledge of accurate concentration dependence of the correcting factors is one of the largely unsolved problems of the quantitative analysis. This problem may be somewhat simplified when one considers the product of all matrix dependent parameters i.e. the backscattering factor, the inelastic mean free path and the total number of atoms in unit volume. In a number of binary systems the product r d M seems to be a weak function of concentration and the linear dependence of this product on atom fraction may be postulated with sufficient accuracy (Hall et al., 1977, Hall and Morabito, 1979).

The next step in development of the quantitative formalism of AES should be the extension of the correction procedure for the multicomponent systems. The relative sensitivity factor approach has already been published for multicomponent systems with considerable prevalence of one of the components (Hall and Morabito,

http://rcin.org.pl

1979). In that case the corrections may be calculated for pure element being in excess.

A number of other problems, already mentioned in the present work, should be met with attention in the future:

(i) The accuracy of the measurements of the Auger electron intensity should be further improved. The question of the proper definition for the measure of the Auger electron current still seems to be open.

(ii) The Coster-Kronig transitions need to be taken into account in quantitative analysis. In addition to the effect discussed in section 5.1.5, the Coster-Kronig transitions may influence the Auger electron yield due to changes in the ionization cross-section (DuCharme and Gerlach, 1974).

(iii) An effort should be made to estimate the effect of the surface roughness on the Auger electron intensity.

(iv) Accounting for the actual spatial distribution of Auger electrons would certainly improve the accuracy of the method, especially in cases when the diffraction effects are expected, i.e. the quantitative analysis of single crystals.

(v) The surface composition calculated from the ratios of Auger electron intensities depends considerably on the model of the surface region. A more realistic model of the surface region is necessary that accounts for actual concentration variations in vicinity of the surface.

Thus, much more work is still necessary to improve the accuracy of the quantitative Auger electron spectroscopy. However, the usefulness of this techniques in solid surface studies and, on the other hand, a great number of laboratories interested in quantification of AES, assure rapid progress in this field.

http://rcin.org.pl

# Appendix

http://rcin.org.pl

```
      PROGRAM SURCOM(INPUT,OUTPUT)
      DIMENSION X(100),R(100),XS(100)
      COMMON ZI,ZJ /AAA/ AI,AJ /BBB/ ROI,ROJ
C
C     ******************************************************************
C     ******************************************************************
C
C     GENERAL INPUT DATA .
C
C     ******************************************************************
C
C     L    - EXPERIMENTAL TECHNIQUE
C            L = 0  DIRECT COMPARISON WITH A STANDARD .
C            L = 1  RELATIVE SENSITIVITY FACTOR APPROACH .
C     K    - MODEL OF THE SURFACE REGION
C            K = 0  UNIFORM COMPOSITION OF THE SURFACE REGION WITHIN THE
C                   SAMPLING DEPTH OF AUGER ELECTRONS .
C            K = 1  UNIFORM COMPOSITION OF THE SURFACE REGION LIMITED TO
C                   THE FIRST MONOLAYER .
C     J    - PLOTTING THE RESULTS
C            J = 0  NO .
C            J = 1  YES .
C
C     ******************************************************************
C
C     FORMAT
C
C     ******************************************************************
C
      READ 10,L,K,J
   10 FORMAT(3I4)
      IF (L .EQ. 1) GO TO 100
C
C     ******************************************************************
C     ******************************************************************
C
C     DIRECT COMPARISON WITH A STANDARD
C
C     ******************************************************************
C
C     EXPERIMENT PROVIDED THE RATIOS OF AUGER ELECTRON INTENSITY FROM
C     THE ALLOY TO AUGER ELECTRON INTENSITY FROM PURE ELEMENT. THE AUGER
C     TRANSITION CHOSEN FOR ANALYSIS IS ASSOCIATED WITH I-TH ELEMENT .
C
C     INPUT DATA
C
C     N    - NUMBER OF ALLOYS .
C     AI   - ATOMIC MASS OF I-TH ELEMENT, G/MOLE .
C     AJ   - ATOMIC MASS OF J-TH ELEMENT, G/MOLE .
C     ROI  - DENSITY OF PURE I-TH ELEMENT, G/CM**3 .
C     ROJ  - DENSITY OF PURE J-TH ELEMENT, G/CM**3 .
C     ZI   - ATOMIC NUMBER OF I-TH ELEMENT .
C     ZJ   - ATOMIC NUMBER OF J-TH ELEMENT .
C     EO   - PRIMARY ENERGY, ELECTRONVOLTS .
C     EA   - AUGER ELECTRON ENERGY CORRESPONDING TO AUGER TRANSITION
C            IN I-TH ELEMENT, ELECTRONVOLTS .
C     EC   - IONIZATION ENERGY ASSOCIATED WITH A CHOSEN AUGER
```

Fig. A - 1. The descriptive part of the universal program specifying the input data preparation

http://rcin.org.pl

```
C             TRANSITION, ELECTRONVOLTS .
C       X(M) - TABLE OF BULK CONCENTRATIONS, ATOM FRACTIONS.
C             M = 1, 2, ... , N .
C       R(M) - TABLE OF AUGER ELECTRON INTENSITY RATIOS,
C             M = 1, 2, ... , N .
C
C       WHEN THE K = 1 OPTION IS CHOSEN .
C
C       AN    - ESCAPE ANGLE OF ELECTRONS ENTERING THE ANALYZER, DEGREES .
C
C       *****************************************************************
C
C       FORMAT
C
C       *****************************************************************
C
        READ 20,N
        READ 21,AI,AJ,ROI,ROJ,ZI,ZJ
        READ 22,EO,EA,EC
        READ 23,(X(I), I=1,N)
        READ 23,(R(I), I=1,N)
        IF (K .EQ. 1) READ 24,AN
   20   FORMAT(I4)
   21   FORMAT(4F10.5,2F4.0)
   22   FORMAT(3F8.1)
   23   FORMAT(F7.4)
   24   FORMAT(F6.1)
        GO TO 101
C
C       *****************************************************************
C       *****************************************************************
C
C       RELATIVE SENSITIVITY FACTOR APPROACH
C
C       *****************************************************************
C
C       EXPERIMENT PROVIDED THE RATIOS OF AUGER ELECTRON INTENSITY FROM
C       I-TH ELEMENT TO AUGER ELECTRON INTENSITY FROM J-TH ELEMENT .
C
C       INPUT DATA
C
C       N     - NUMBER OF ALLOYS .
C       AI    - ATOMIC MASS OF I-TH ELEMENT, G/MOLE .
C       AJ    - ATOMIC MASS OF J-TH ELEMENT, G/MOLE .
C       ROI   - DENSITY OF PURE I-TH ELEMENT, G/CM**3 .
C       ROJ   - DENSITY OF PURE J-TH ELEMENT, G/CM**3 .
C       ZI    - ATOMIC NUMBER OF I-TH ELEMENT .
C       ZJ    - ATOMIC NUMBER OF J-TH ELEMENT .
C       EO    - PRIMARY ENERGY, ELECTRONVOLTS .
C       EAI   - AUGER ELECTRON ENERGY CORRESPONDING TO AUGER TRANSITION IN
C               I-TH ELEMENT, ELECTRONVOLTS .
C       EAJ   - AUGER ELECTRON ENERGY CORRESPONDING TO AUGER TRANSITION IN
C               J-TH ELEMENT, ELECTRONVOLTS .
C       ECI   - IONIZATION ENERGY ASSOCIATED WITH AUGER TRANSITION IN
C               I-TH ELEMENT, ELECTRONVOLTS .
C       ECJ   - IONIZATION ENERGY ASSOCIATED WITH AUGER TRANSITION IN
C               J-TH ELEMENT, ELECTRONVOLTS .
```

Fig. A - 1. Continued (i)

http://rcin.org.pl

```
C       X(M) - TABLE OF BULK CONCENTRATIONS, ATOM FRACTIONS,
C              M = 1, 2, ... , N .
C       R(M) - TABLE OF AUGER ELECTRON INTENSITY RATIOS,
C              M = 1, 2, ... , N .
C       RP   - AUGER ELECTRON INTENSITY RATIO FOR PURE ELEMENTS .
C
C       WHEN THE K = 1 OPTION IS CHOSEN
C
C       AN   - ESCAPE ANGLE OF ELECTRONS ENTERING THE ANALYZER, DEGREES .
C
C       *****************************************************************
C
C       FORMAT
C
C       *****************************************************************
C
  100   READ 20,N
        READ 21,AI,AJ,ROI,ROJ,ZI,ZJ
        READ 32,EO,EAI,EAJ,ECI,ECJ
        READ 23,(X(I), I=1,N)
        READ 33,(R(I), I=1,N)
        READ 33,RP
        IF (K .EQ. 1) READ 24,AN
   32   FORMAT(5F8.1)
   33   FORMAT(E10.4)
        GO TO 102
C
C       *****************************************************************
C       *****************************************************************
```

Fig. A - 1. Continued (ii)

http://rcin.org.pl

INPUT DATA

| | | | |
|---|---|---|---|
| PRIMARY ENERGY | = | 4000.0 | ELECTRONVOLTS |
| ATOMIC MASS OF I-TH ELEMENT | = | 196.96650 | G/MOLE |
| ATOMIC MASS OF J-TH ELEMENT | = | 106.40000 | G/MOLE |
| DENSITY OF PURE I-TH ELEMENT | = | 19.32000 | G/CM**3 |
| DENSITY OF PURE J-TH ELEMENT | = | 12.02000 | G/CM**3 |
| ATOMIC NUMBER OF I-TH ELEMENT | = | 79. | |
| ATOMIC NUMBER OF J-TH ELEMENT | = | 46. | |
| AUGER ELECTRON ENERGY CORRESPONDING TO I-TH ELEMENT | = | 69.0 | ELECTRONVOLTS |
| AUGER ELECTRON ENERGY CORRESPONDING TO J-TH ELEMENT | = | 330.0 | ELECTRONVOLTS |
| IONIZATION ENERGY ASSOCIATED WITH AUGER TRANSITION IN I-TH ELEMENT | = | 352.0 | ELECTRONVOLTS |
| IONIZATION ENERGY ASSOCIATED WITH AUGER TRANSITION IN J-TH ELEMENT | = | 334.7 | ELECTRONVOLTS |

(a)

Fig. A - 2. The list of the output data for chosen AuPd alloys after surface equilibration:

(a) The input data.

(b) The assumption of the uniform composition within the sampling depth of Auger electrons;bulk atom fraction of gold equal to 0.5976.

(c) The assumption of the monolayer enrichment; bulk atom fraction of gold equal to 0.5976.

(d) The assumption of the monolayer enrichment; bulk atom fraction of gold equal to 0.8965.

http://rcin.org.pl

```
RELATIVE SENSITIVITY FACTOR APPROACH

UNIFORM COMPOSITION OF THE SURFACE REGION WITHIN SAMPLING DEPTH
  OF AUGER ELECTRONS

NUMBER OF THE ALLOY                              =   1
BULK CONCENTRATION OF I-TH ELEMENT               =   .5976       ATOM FRACTION

MONOLAYER THICKNESS FOR PURE I-TH ELEMENT        =   .257        NANOMETERS
MONOLAYER THICKNESS FOR PURE J-TH ELEMENT        =   .245        NANOMETERS
MONOLAYER THICKNESS IN SURFACE REGION            =   .253        NANOMETERS
MEAN FREE PATH OF AUGER ELECTRON FROM
  AUGER TRANSITION IN PURE I-TH ELEMENT          =   .472        NANOMETERS
MEAN FREE PATH OF AUGER ELECTRON FROM
  AUGER TRANSITION IN PURE J-TH ELEMENT          =   .904        NANOMETERS
MEAN FREE PATH OF AUGER ELECTRON FROM
  I-TH AUGER TRANSITION IN SURFACE REGION        =   .463        NANOMETERS
MEAN FREE PATH OF AUGER ELECTRON FROM
  J-TH AUGER TRANSITION IN SURFACE REGION        =   .950        NANOMETERS
TOTAL NUMBER OF ATOMS
  IN UNIT VOLUME OF PURE I-TH ELEMENT            =  .5907E+23    1/CM**3
TOTAL NUMBER OF ATOMS
  IN UNIT VOLUME OF PURE J-TH ELEMENT            =  .6803E+23    1/CM**3
TOTAL NUMBER OF ATOMS
  IN UNIT VOLUME OF SURFACE REGION               =  .6157E+23    1/CM**3
BACKSCATTERING FACTOR FOR
  AUGER TRANSITION IN PURE I-TH ELEMENT          =  1.980
BACKSCATTERING FACTOR FOR
  AUGER TRANSITION IN PURE J-TH ELEMENT          =  1.837
BACKSCATTERING FACTOR FOR
  I-TH AUGER TRANSITION IN THE ALLOY             =  1.941
BACKSCATTERING FACTOR FOR
  J-TH AUGER TRANSITION IN THE ALLOY             =  1.945

TOTAL CORRECTION F                               =   .9942

AUGER ELECTRON INTENSITY RATIO                   =  1.280

THE RATIO FOR PURE ELEMENTS                      =  .5490

SURFACE CONCENTRATION OF I-TH ELEMENT            =  .7011        ATOM FRACTION
```

(b)

Fig. A - 2. Continued (i)

http://rcin.org.pl

```
RELATIVE SENSITIVITY FACTOR APPROACH

UNIFORM COMPOSITION OF THE SURFACE REGION LIMITED TO THE FIRST MONOLAYER

NUMBER OF THE ALLOY                              =    2
BULK CONCENTRATION OF I-TH ELEMENT               =   .5976      ATOM FRACTION

MONOLAYER THICKNESS FOR PURE I-TH ELEMENT        =   .257       NANOMETERS
MONOLAYER THICKNESS FOR PURE J-TH ELEMENT        =   .245       NANOMETERS
MONOLAYER THICKNESS IN SURFACE REGION            =   .255       NANOMETERS
MEAN FREE PATH OF AUGER ELECTRON FROM
  AUGER TRANSITION IN PURE I-TH ELEMENT          =   .472       NANOMETERS
MEAN FREE PATH OF AUGER ELECTRON FROM
  AUGER TRANSITION IN PURE J-TH ELEMENT          =   .904       NANOMETERS
MEAN FREE PATH OF AUGER ELECTRON FROM
  I-TH AUGER TRANSITION IN SURFACE REGION        =   .459       NANOMETERS
MEAN FREE PATH OF AUGER ELECTRON FROM
  J-TH AUGER TRANSITION IN SURFACE REGION        =   .944       NANOMETERS
TOTAL NUMBER OF ATOMS
  IN UNIT VOLUME OF PURE I-TH ELEMENT            =  .5907E+23   1/CM**3
TOTAL NUMBER OF ATOMS
  IN UNIT VOLUME OF PURE J-TH ELEMENT            =  .6803E+23   1/CM**3
TOTAL NUMBER OF ATOMS
  IN UNIT VOLUME OF SURFACE REGION               =  .6000E+23   1/CM**3
BACKSCATTERING FACTOR FOR
  AUGER TRANSITION IN PURE I-TH ELEMENT          =  1.980
BACKSCATTERING FACTOR FOR
  AUGER TRANSITION IN PURE J-TH ELEMENT          =  1.837
BACKSCATTERING FACTOR FOR
  I-TH AUGER TRANSITION IN THE ALLOY             =  1.941
BACKSCATTERING FACTOR FOR
  J-TH AUGER TRANSITION IN THE ALLOY             =  1.945

TOTAL CORRECTION F                               =   .9944

AUGER ELECTRON INTENSITY RATIO                   =  1.280

THE RATIO FOR PURE ELEMENTS                      =  .5490

SURFACE CONCENTRATION OF I-TH ELEMENT            =  .8873       ATOM FRACTION
```

(c)

**Fig. A - 2. Continued (ii)**

http://rcin.org.pl

RELATIVE SENSITIVITY FACTOR APPROACH

UNIFORM COMPOSITION OF THE SURFACE REGION LIMITED TO THE FIRST MONOLAYER

```
NUMBER OF THE ALLOY                           =   1
BULK CONCENTRATION OF I-TH ELEMENT            =  .8965       ATOM FRACTION

MONOLAYER THICKNESS FOR PURE I-TH ELEMENT     =  .257        NANOMETERS
MONOLAYER THICKNESS FOR PURE J-TH ELEMENT     =  .245        NANOMETERS
MONOLAYER THICKNESS IN SURFACE REGION         =  .257        NANOMETERS
MEAN FREE PATH OF AUGER ELECTRON FROM
  AUGER TRANSITION IN PURE I-TH ELEMENT       =  .472        NANOMETERS
MEAN FREE PATH OF AUGER ELECTRON FROM
  AUGER TRANSITION IN PURE J-TH ELEMENT       =  .904        NANOMETERS
MEAN FREE PATH OF AUGER ELECTRON FROM
  I-TH AUGER TRANSITION IN SURFACE REGION     =  .469        NANOMETERS
MEAN FREE PATH OF AUGER ELECTRON FROM
  J-TH AUGER TRANSITION IN SURFACE REGION     =  .963        NANOMETERS
TOTAL NUMBER OF ATOMS
  IN UNIT VOLUME OF PURE I-TH ELEMENT         = .5907E+23    1/CM**3
TOTAL NUMBER OF ATOMS
  IN UNIT VOLUME OF PURE J-TH ELEMENT         = .6803E+23    1/CM**3
TOTAL NUMBER OF ATOMS
  IN UNIT VOLUME OF SURFACE REGION            = .5907E+23    1/CM**3
BACKSCATTERING FACTOR FOR
  AUGER TRANSITION IN PURE I-TH ELEMENT       = 1.980
BACKSCATTERING FACTOR FOR
  AUGER TRANSITION IN PURE J-TH ELEMENT       = 1.837
BACKSCATTERING FACTOR FOR
  I-TH AUGER TRANSITION IN THE ALLOY          = 1.972
BACKSCATTERING FACTOR FOR
  J-TH AUGER TRANSITION IN THE ALLOY          = 1.975

TOTAL CORRECTION F                            =  .9941

AUGER ELECTRON INTENSITY RATIO                = 7.420

THE RATIO FOR PURE ELEMENTS                   = .5490

SURFACE CONCENTRATION OF I-TH ELEMENT         = 1.000        ATOM FRACTION


THE MODEL OF ONE MONOLAYER SEGREGATION IS NOT VALID, OR THE CORRECTIONS
  ARE SUBJECT TO LARGE SYSTEMATIC ERRORS .
UNDER ASSUMPTION THAT SURFACE IS COVERED
  BY PURE I-TH ELEMENT, THE THICKNESS
  OF THE SEGREGATED LAYER IS EQUAL TO         =  .283        NANOMETERS
  WHICH CORRESPONDS TO                        =  1.1         MONOLAYERS
```

(d)

Fig. A - 2. Continued (iii)

http://rcin.org.pl

INPUT DATA

| | | | |
|---|---|---|---|
| PRIMARY ENERGY | = | 5000.0 | ELECTRONVOLTS |
| ATOMIC MASS OF I-TH ELEMENT | = | 106.40000 | G/MOLE |
| ATOMIC MASS OF J-TH ELEMENT | = | 58.71000 | G/MOLE |
| DENSITY OF PURE I-TH ELEMENT | = | 12.02000 | G/CM**3 |
| DENSITY OF PURE J-TH ELEMENT | = | 8.90200 | G/CM**3 |
| ATOMIC NUMBER OF I-TH ELEMENT | = | 46. | |
| ATOMIC NUMBER OF J-TH ELEMENT | = | 28. | |
| AUGER ELECTRON ENERGY CORRESPONDING TO I-TH ELEMENT | = | 330.0 | ELECTRONVOLTS |
| IONIZATION ENERGY ASSOCIATED WITH A CHOSEN AUGER TRANSITION | = | 334.7 | ELECTRONVOLTS |

(a)

Fig. A - 3. The list of the output data for a chosen NiPd alloy after extensive sputtering:

(a) The input data.

(b) The assumption of the uniform composition of the surface region within sampling depth of Auger electrons; bulk mass fraction of Pd equal to 0.6.

http://rcin.org.pl

```
DIRECT COMPARISON WITH A STANDARD

UNIFORM COMPOSITION OF THE SURFACE REGION WITHIN SAMPLING DEPTH
  OF AUGER ELECTRONS

NUMBER OF THE ALLOY                           =    1
BULK CONCENTRATION OF I-TH ELEMENT            =   .4529      ATOM FRACTION

MONOLAYER THICKNESS FOR PURE I-TH ELEMENT     =   .245       NANOMETERS
MONOLAYER THICKNESS FOR PURE J-TH ELEMENT     =   .222       NANOMETERS
MONOLAYER THICKNESS IN SURFACE REGION         =   .233       NANOMETERS
MEAN FREE PATH
  OF AUGER ELECTRON IN PURE I-TH ELEMENT      =   .904       NANOMETERS
MEAN FREE PATH
  OF AUGER ELECTRON IN PURE J-TH ELEMENT      =   .781       NANOMETERS
MEAN FREE PATH
  OF AUGER ELECTRON IN SURFACE REGION         =   .837       NANOMETERS
TOTAL NUMBER OF ATOMS
  IN UNIT VOLUME OF PURE I-TH ELEMENT         =  .6803E+23   1/CM**3
TOTAL NUMBER OF ATOMS
  IN UNIT VOLUME OF PURE J-TH ELEMENT         =  .9131E+23   1/CM**3
TOTAL NUMBER OF ATOMS
  IN UNIT VOLUME OF SURFACE REGION            =  .7944E+23   1/CM**3
BACKSCATTERING FACTOR FOR PURE I-TH ELEMENT   =  1.854
BACKSCATTERING FACTOR FOR PURE J-TH ELEMENT   =  1.671
BACKSCATTERING FACTOR FOR THE ALLOY           =  1.781

TOTAL CORRECTION G                            =  1.0380

AUGER ELECTRON INTENSITY RATIO                =  .4787

SURFACE CONCENTRATION OF I-TH ELEMENT         =  .4612       ATOM FRACTION
```

(b)

Fig. A - 3. Continued

http://rcin.org.pl

INPUT DATA

| | | | |
|---|---|---|---|
| PRIMARY ENERGY | = | 5000.0 | ELECTRONVOLTS |
| ATOMIC MASS OF I-TH ELEMENT | = | 183.85000 | G/MOLE |
| ATOMIC MASS OF J-TH ELEMENT | = | 95.94000 | G/MOLE |
| DENSITY OF PURE I-TH ELEMENT | = | 19.30000 | G/CM**3 |
| DENSITY OF PURE J-TH ELEMENT | = | 10.22000 | G/CM**3 |
| ATOMIC NUMBER OF I-TH ELEMENT | = | 74. | |
| ATOMIC NUMBER OF J-TH ELEMENT | = | 42. | |
| AUGER ELECTRON ENERGY CORRESPONDING TO I-TH ELEMENT | = | 350.0 | ELECTRONVOLTS |
| IONIZATION ENERGY ASSOCIATED WITH A CHOSEN AUGER TRANSITION | = | 425.3 | ELECTRONVOLTS |
| ESCAPE ANGLE OF ELECTRONS ENTERING THE ANALYZER | = | 42.3 | DEGREES |

(a)

Fig. A - 4. The list of the output data for the tungsten overlayer on molybdenum. The overlayer thickness is calculated from the relative intensity of 350 eV Auger transition in tungsten.
(a)The input data.
(b)The calculated thickness of 0.58 monolayer corresponding to the relative intensity ratio of 0.159.
(c)The calculated thickness of 1.1 monolayer corresponding to the relative intensity ratio of 0.296.

http://rcin.org.pl

```
DIRECT COMPARISON WITH A STANDARD

UNIFORM COMPOSITION OF THE SURFACE REGION LIMITED TO THE FIRST MONOLAYER

NUMBER OF THE ALLOY                              =    1
BULK CONCENTRATION OF I-TH ELEMENT               =  0.0000      ATOM FRACTION

MONOLAYER THICKNESS FOR PURE I-TH ELEMENT        =   .251       NANOMETERS
MONOLAYER THICKNESS FOR PURE J-TH ELEMENT        =   .250       NANOMETERS
MONOLAYER THICKNESS IN SURFACE REGION            =   .251       NANOMETERS
MEAN FREE PATH
  OF AUGER ELECTRON IN PURE I-TH ELEMENT         =   .966       NANOMETERS
MEAN FREE PATH
  OF AUGER ELECTRON IN PURE J-TH ELEMENT         =   .959       NANOMETERS
MEAN FREE PATH
  OF AUGER ELECTRON IN SURFACE REGION            =   .959       NANOMETERS
TOTAL NUMBER OF ATOMS
  IN UNIT VOLUME OF PURE I-TH ELEMENT            =  .6322E+23   1/CM**3
TOTAL NUMBER OF ATOMS
  IN UNIT VOLUME OF PURE J-TH ELEMENT            =  .6415E+23   1/CM**3
TOTAL NUMBER OF ATOMS
  IN UNIT VOLUME OF SURFACE REGION               =  .6360E+23   1/CM**3
BACKSCATTERING FACTOR FOR PURE I-TH ELEMENT      =  1.966
BACKSCATTERING FACTOR FOR PURE J-TH ELEMENT      =  1.805
BACKSCATTERING FACTOR FOR THE ALLOY              =  1.805

AUGER ELECTRON INTENSITY RATIO                   =  .1590

SURFACE CONCENTRATION OF I-TH ELEMENT            =  .5825       ATOM FRACTION
```

(b)

Fig. A - 4. Continued (i)

http://rcin.org.pl

```
DIRECT COMPARISON WITH A STANDARD

UNIFORM COMPOSITION OF THE SURFACE REGION LIMITED TO THE FIRST MONOLAYER

NUMBER OF THE ALLOY                            =    2
BULK CONCENTRATION OF I-TH ELEMENT             =  0.0000      ATOM FRACTION

MONOLAYER THICKNESS FOR PURE I-TH ELEMENT      =   .251       NANOMETERS
MONOLAYER THICKNESS FOR PURE J-TH ELEMENT      =   .250       NANOMETERS
MONOLAYER THICKNESS IN SURFACE REGION          =   .251       NANOMETERS
MEAN FREE PATH
  OF AUGER ELECTRON IN PURE I-TH ELEMENT       =   .966       NANOMETERS
MEAN FREE PATH
  OF AUGER ELECTRON IN PURE J-TH ELEMENT       =   .959       NANOMETERS
MEAN FREE PATH
  OF AUGER ELECTRON IN SURFACE REGION          =   .959       NANOMETERS
TOTAL NUMBER OF ATOMS
  IN UNIT VOLUME OF PURE I-TH ELEMENT          =  .6322E+23   1/CM**3
TOTAL NUMBER OF ATOMS
  IN UNIT VOLUME OF PURE J-TH ELEMENT          =  .6415E+23   1/CM**3
TOTAL NUMBER OF ATOMS
  IN UNIT VOLUME OF SURFACE REGION             =  .6322E+23   1/CM**3
BACKSCATTERING FACTOR FOR PURE I-TH ELEMENT    =  1.966
BACKSCATTERING FACTOR FOR PURE J-TH ELEMENT    =  1.805
BACKSCATTERING FACTOR FOR THE ALLOY            =  1.805

AUGER ELECTRON INTENSITY RATIO                 =  .2961

SURFACE CONCENTRATION OF I-TH ELEMENT          =  1.000       ATOM FRACTION


THE MODEL OF ONE MONOLAYER SEGREGATION IS NOT VALID, OR THE CORRECTIONS
  ARE SUBJECT TO LARGE SYSTEMATIC ERRORS .
UNDER ASSUMPTION THAT SURFACE IS COVERED
  BY PURE I-TH ELEMENT, THE THICKNESS
  OF THE SEGREGATED LAYER IS EQUAL TO          =   .279       NANOMETERS
  WHICH CORRESPONDS TO                         =   1.1        MONOLAYERS
```

(c)

**Fig. A - 4. Continued (ii)**

http://rcin.org.pl

Fig. A - 5. The rough plot of the surface composition versus the bulk composition calculated for the equilibrated AuPd alloy from the intensity ratio of 69 eV Au transition to 330 eV Pd transition.

(a) The assumption of uniform composition within the sampling depth of Auger electrons.

(b) The assumption of monolayer enrichment.

http://rcin.org.pl

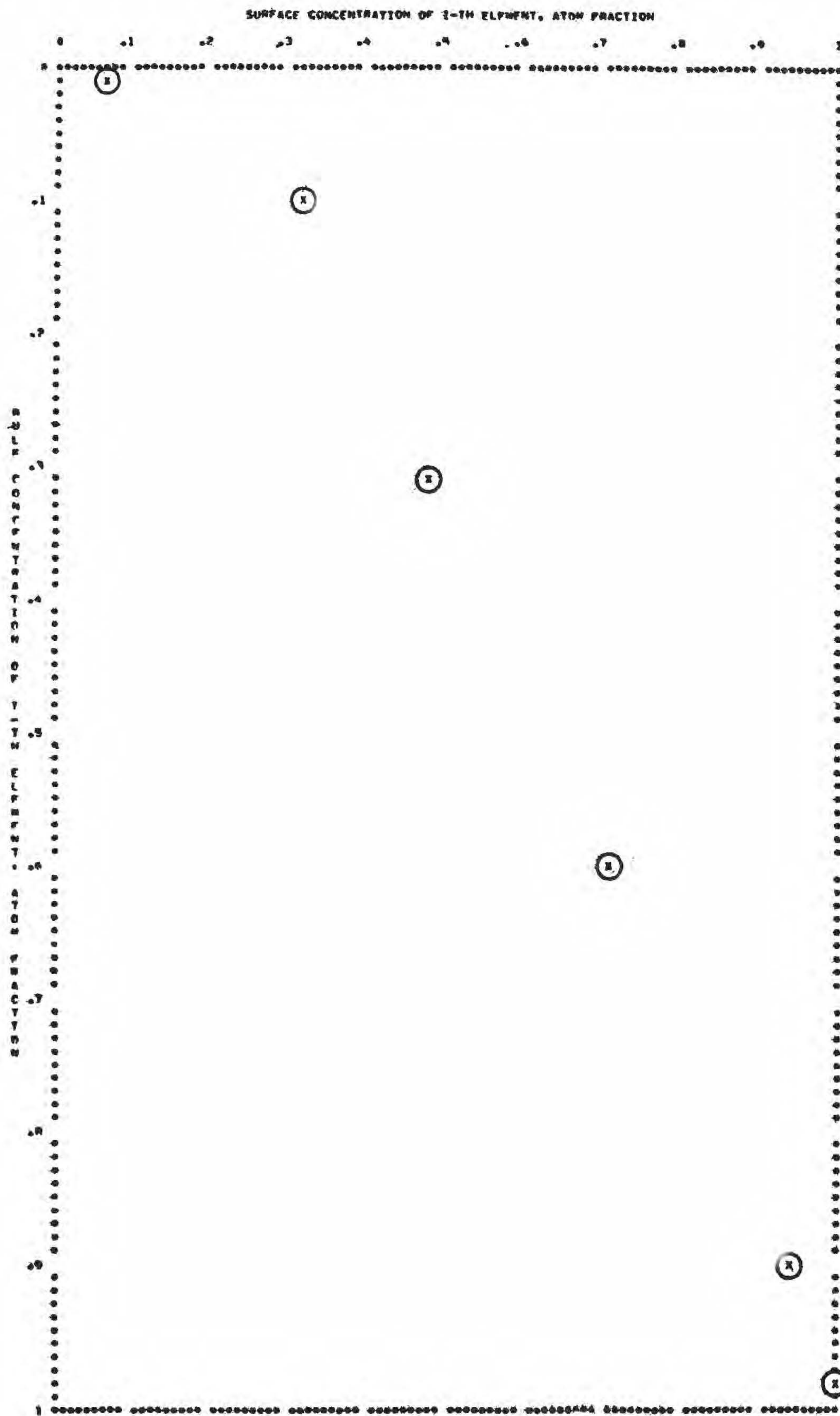


(a)

Fig. A - 5. Continued (i)

http://rcin.org.pl

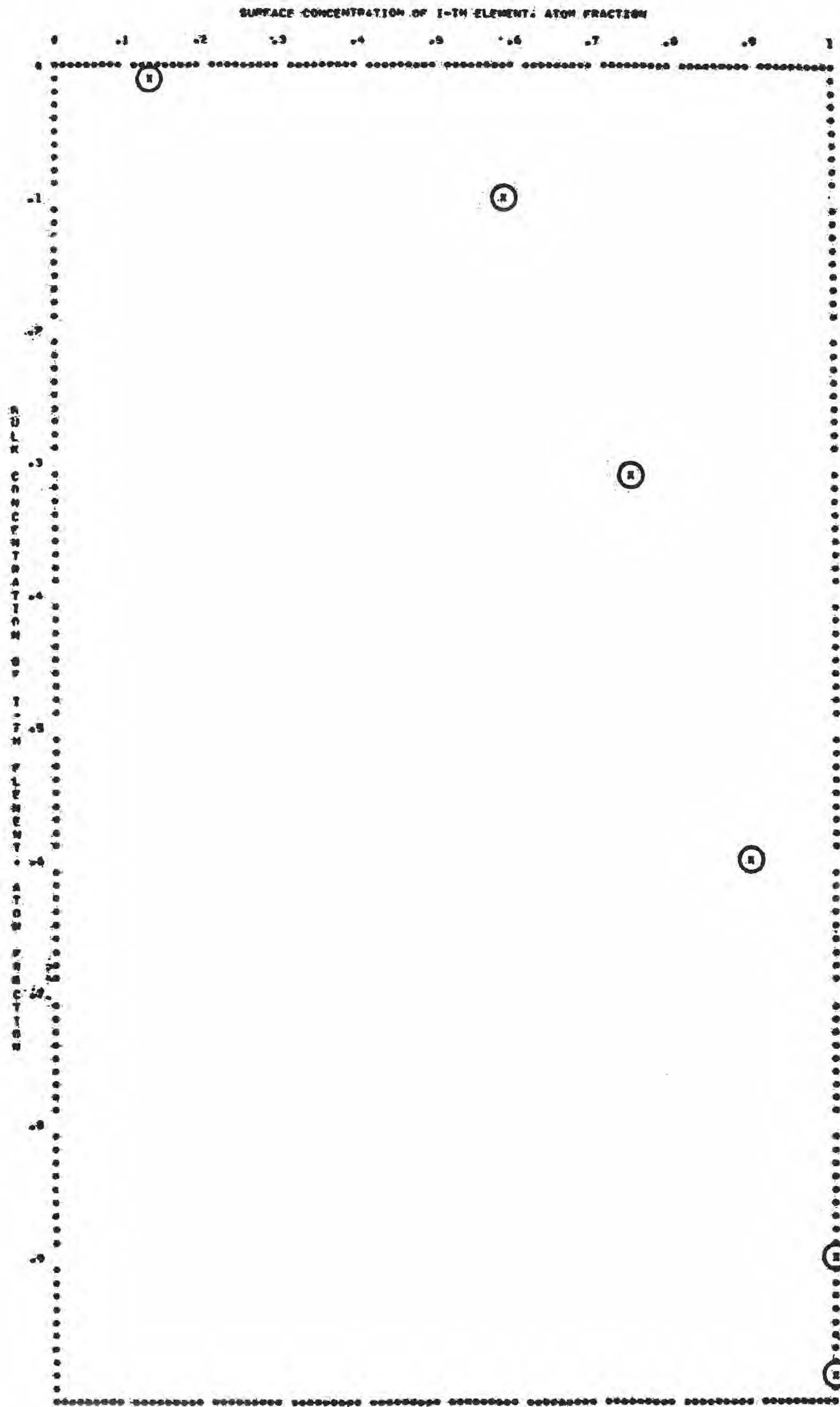


(b)

Fig. A - 5, Continued (ii)

http://rcin.org.pl

References

Aksela, S., Karras, M., Pessa, M. and Suoninen, E. (1970). Rev. Sci. Instrum. 41, 351.

Allié, G., Blanc, E. and Dufayard, D. (1976). Surface Sci. 57,293.

Archard, G.D. (1961). J. Appl. Phys. 32, 1505.

Arden, B.W. and Astill, K.N. (1970). Numerical Algorithms: Origins and Applications, Addison-Wesley Publishing Co., Reading, p. 71.

Ashley, J.C., Tung, C.J. and Ritchie, R.H. (1979). Surface Sci. 81, 409.

Auger, P. (1925a). Comptes Rendus, 180, 65.

Auger, P. (1925b). J. Phys. Radium, 6, 205.

Berndt, H., Streubel, P. and Meisel, A. (1980). Kristall und Technik 15, 1433.

Bishop, H.E. (1965). Proc. Phys. Soc. London. 85, 855.

Bishop, H.E. (1966). In Castaing et al., p. 153.

Bishop, H.E. (1967). Brit. J. Appl. Phys. 18, 703.

Bishop, H.E. (1968). J. Phys. D. 1, 673.

Bishop, H.E., Coad, J.P. and Rivière, J.C. (1973). J. Electron Spectrosc. 1, 389.

Bishop, H.E. and Rivière, J.C. (1969). J. Appl. Phys. 40, 1740.

Bouwman, R., Toneman, L.H. and Holscher, A.A. (1973a). Vacuum 23, 163.

Bouwman, R., Toneman, L.H. and Holscher, A.A. (1973b). Surface Sci. 35, 8.

Bouwman, R., Van Mechelen, J.B. and Holscher, A.A. (1976a). Surface Sci. 57, 441.

Bouwman, R., Toneman, L.H., Boersma, M.A.M. and Van Santen, R.A. (1976b). Surface Sci. 59, 72.

http://rcin.org.pl

Brundle, C.R. (1974). J. Vac. Sci. Technol. 11, 212.

Burton, J.J., Helms, C.R. and Polizzotti, R.S. (1976). Surface Sci. 57, 425.

Castaing, R., Deschamps, P. and Philibert, J. eds, (1966). X-Ray Optics and Microanalysis, Hermann, Paris.

Castaing, R. and Henoc, J. (1966). In Castaing et al., p. 120.

Chang, C.C. (1974). In Characterization of Solid Surfaces. Kane, P.F. and Larrabee, G.R., eds, Plenum Press, New York--London, p. 509.

Chang, C.C. (1975). Surface Sci. 48, 9.

Chattarji, D. (1976). The Theory of Auger Transitions, Academic Press, London.

Colby, J.W., Wise, W.N. and Conley, D.K. (1967). Adv. X-Ray Anal. 10, 447.

Darlington, E.H. and Cosslett, V.E. (1972). J. Phys. D. 5, 1969.

Dejardin-Horgues, C., Ganachaud, J.P. and Cailler, M. (1976). J. Phys. C. 9, L 633.

Drescher, H., Reimer, L. and Seidel, H. (1970). Z. Angew. Physik, 29, 331.

DuCharme, A.R. and Gerlach, R.L. (1974). J. Vac. Sci. Technol. 11, 281.

Duncumb, P. and Melford, D.A. (1966). In Castaing et al., p. 240.

El Gomati, M.M., Janssen, A.P., Prutton, M. and Venables, J.A. (1979). Surface Sci. 85, 309.

El Gomati, M.M. and Prutton, M. (1978). Surface Sci. 72, 485.

Ertl, G. and Küppers, J. (1974a). Low Energy Electrons and Surface Chemistry, Verlag Chemie, Weinheim, p. 7.

Ertl, G. and Küppers, J. (1974b). Ibid., pp. 17-51.

Everhart, T.E. (1960). J. Appl. Phys. 31, 1483.

http://rcin.org.pl

Fink, R.W., Jopson, R.C., Mark, H. and Swift, C.D. (1966). Rev. Mod. Phys. 38, 513.

Frank, L. (1976). J. Phys. E. Sci. Instrum. 9, 670.

Fujinaga, Y. (1977). Surface Sci. 64, 751.

Gallon, T.E. (1972). J. Phys. D. 5, 822.

Gergely, G., Gruzza, B. and Menyhárd, M. (1980a). Proceedings of the Fourth International Conference on Solid Surfaces and the Third European Conference on Surface Science, Cannes, 1980, Degras, D.A. and Costa, M., eds, p. 1392.

Gergely, G., Gruzza, B. and Menyhárd, M. (1980b). Acta Phys. Acad. Sci. Hungar. 48, 337.

Gergely, G. (1981). Surface Interface Anal., in press.

Gerlach, R.L. (1972). J. Vac. Sci. Technol. 9, 1043.

Gerlach, R.L. and DuCharme, A.R. (1972). Surface Sci. 32, 329.

Glupe, G. and Mehlhorn, W. (1967). Phys. Letters, A 25, 274.

Glupe, G. and Mehlhorn, W. (1971). J. Phys. Paris Colloq. C4, 40.

Goto, K., Ishikawa, K., Koshikawa, T. and Shimizu, R. (1975). Surface Sci. 47, 477.

Grant, J.T., Haas, T.W. and Houston, J.E. (1973a). Phys. Letters, A 45, 309.

Grant, J.T., Haas, T.W. and Houston, J.E. (1973b). J. Vac. Sci. Technol. 11, 227.

Grant, J.T., Hooker, M.P. and Haas, T.W. (1974). Surface Sci. 46, 672.

Green, M. (1963). Proc. Phys. Soc. London, 82, 204.

Gryziński, M. (1965). Phys. Rev. A 138, 336.

Gschneidner, K.A. and Vineyard, G.H. (1962). J. Appl. Phys. 33, 3444.

Haas, T.W., Dooley, G.J., Grant, J.T., Jackson, A.G. and Hooker, M.P. (1971). In Progress in Surface Science.

http://rcin.org.pl

Jabłoński, A. (1980b). Proceedings of the Fourth International Conference on Solid Surfaces and the Third European Conference on Surface Science, Cannes, 1980. Degras, D.A. and Costa, M., eds, p. 1307.

Jabłoński, A. (1981a). J. Phys. B. 14, 281.

Jabłoński, A. (1981b). Proceedings of International Seminar on X-Ray and Electron Spectroscopy, Jabłonna, 1981, in press.

Jabłoński, A. (1982). Surface Interface Anal., in press.

Jabłoński, A. and Hartweck, W. (1981). Surface Sci. 110, L593.

Jabłoński, A., Overbury, S.H. and Somorjai, G.A. (1977). Surface Sci. 65, 578.

Joshi, A., Davis, L.E. and Palmberg, P.W. (1975). In Methods of Surface Analysis, Czanderna, A.W. ed., Elsevier Scientific Publishing Co., Amsterdam.

Janssen, A.P., Harland, C.J. and Venables, J.A. (1977). Surface Sci. 62, 277.

Kanter, H. (1957). Ann. Physik (Leipz.). 20, 144.

Kirschner, J. (1977). Appl. Phys. 14, 351.

Koval, I.P., Krynko, Yu.N., Melnik, P.V. and Nakhodkin, N.G. (1978). Surface Sci. 77, 40.

Kuijers, F.J., Tieman, B.M. and Ponec, V. (1978). Surface Sci. 75, 657.

Lander, J.J. (1953). Phys. Rev. 91, 1382.

Leroux, J. (1961). Adv. X-Ray Anal. 5, 153.

Leygraf, C., Hultquist, G., Ekelund, S. and Eriksson, J.C. (1974). Surface Sci. 46, 157.

Lindau, I. and Spicer, W.E. (1974). J. Electron Spectrosc. 3,409.

Love, G., Cox, M.G.C. and Scott, V.D. (1974). J. Phys. D. 7,2131.

Love, G., Cox, M.G.C. and Scott, V.D. (1978a). J. Phys. D. 11, 7.

Love, G., Cox, M.G.C. and Scott, V.D. (1978b). J. Phys. D. 11,23.

http://rcin.org.pl

Love, G. and Scott, V.D. (1978). J. Phys. D. 11, 1369.

McAfee, W.S. (1976). J. Appl. Phys. 47, 1179.

McDavid, J.M. and Fain, S.C. Jr. (1975). Surface Sci. 52, 161.

McDonnell, L., Woodruff, D.P. and Holland, B.W. (1975). Surface Sci. 51, 249.

McGuire, G.E. (1979). Auger Electron Spectroscopy Reference Manual, Plenum Press, New York, London.

Mathieu, H.J. and Landolt, D. (1975). Surface Sci. 53, 228.

Matsudaira, T. and Onchi, M. (1978). Surface Sci. 72, 53.

Matsukawa, T., Murata, K. and Shimizu, R. (1973). Phys. Status Solidi (b), 55, 371.

Meyer, F. and Vrakking, J.J. (1972). Surface Sci. 33, 271.

Meyer, F. and Vrakking, J.J. (1973). Phys. Letters, A 44, 511.

Meyer, F. and Vrakking, J.J. (1974). Surface Sci. 45, 409.

Murata, K. (1974). J. Appl. Phys. 45, 4110.

Murata, K. (1976). Phys. Status Solidi (a), 36, 197.

Murata, K., Matsukawa, T. and Shimizu, R. (1971). Japanese J. Appl. Phys. 10, 678.

Murata, K., Matsukawa, T. and Shimizu, R. (1972). In Shinoda et al., p. 105.

Noonan, J.R., Zehner, D.M. and Jenkins, L.H. (1976). J. Vac. Sci. Technol. 13, 183.

Overbury, S.H., Bertrand, P.A. and Somorjai, G.A. (1975). Chem. Rev. 75, 547.

Overbury, S.H. and Somorjai, G.A. (1976). Surface Sci. 55, 209.

Palmberg, P.W. (1967). J. Appl. Phys. 38, 2137.

Palmberg, P.W. (1968). Appl. Phys. Letters, 13, 183.

Palmberg, P.W. (1973). Anal. Chem. 45, 549 A.

Palmberg, P.W. (1976). J. Vac. Sci. Technol. 13, 214.

http://rcin.org.pl

Palmberg, P.W., Bohn, G.K. and Tracy, J.C. (1969). Appl. Phys. Letters, 15, 254.

Palmberg, P.W. and Rhodin, T.N. (1968). J. Appl. Phys. 39, 2425.

Palmberg, P.W., Riach, G.E., Weber, R.E. and MacDonald, N.C. (1972). Handbook of Auger Electron Spectroscopy, Physical Electronics Industries, Inc., Edina, Minnesota.

Pearson, W.B. (1958). A Handbook of Lattice Spacing and Structures of Metals and Alloys, Pergamon Press, London, New York, p. 24.

Penn, D.R. (1976a). Phys. Rev. B 13, 5248.

Penn, D.R. (1976b). J. Vac. Sci. Technol. 13, 221.

Penn, D.R. (1976c). J. Electron Spectrosc. 9, 29.

Pons, F., Le Héricy, J. and Langeron, J.P. (1977a). Surface Sci. 69, 547.

Pons, F., Le Héricy, J. and Langeron, J.P. (1977b). Surface Sci. 69, 565.

Powell, C.J. (1974). Surface Sci. 44, 29.

Powell, C.J. (1976). Rev. Mod. Phys. 48, 33.

Reed, S.J.B. (1975a). Electron Microprobe Analysis, Cambridge University Press, Cambridge, p. xv.

Reed, S.J.B. (1975b). Ibid., pp. 198-260.

Reed, S.J.B. (1975c). Ibid., p. 202.

Reimer, L. (1968). Optik, 27, 86.

Reuter, W. (1972). In Shinoda et al., p. 121.

Ritchie, R.H., Garber, F.W., Nakai, M.Y. and Birkhoff, R.D. (1969). Adv. Radiation Biology, 3, 1.

Ruste, J. and Gantois, M. (1975). J. Phys. D. 8, 872.

Sar-El, H.Z. (1967). Rev. Sci. Instrum. 38, 1210.

http://rcin.org.pl

Scheibner, E.J. and Tharp, L.N. (1967). Surface Sci. 8, 247.

Seah, M.P. (1979a). Surface Interface Anal. 1, 86.

Seah, M.P. (1979b). Surface Interface Anal. 1, 91.

Seah, M.P. and Dench, W.A. (1979). Surface Interface Anal. 1, 2.

Sevier, K.D. (1972a). Low Energy Electron Spectrometry, Wiley--Interscience, New York, p. 112.

Sevier, K.D. (1972b). Ibid., pp. 356-373.

Shaw, C.G. and Fain, S.C. (1977). Proc. 7th Vacuum Congress, 3rd Int. Conf. on Solid Surfaces, Vienna, p. 2315.

Shelton, J.C. (1974). Surface Sci. 44, 305.

Shimizu, R. and Ichimura, S. (1981). Quantitative Analysis by Auger Electron Spectroscopy, Toyota Foundation Research Report.

Shimizu, R., Ikuta, T. and Murata, K. (1972a). J. Appl. Phys. 43, 4233.

Shimizu, R., Nishigori, N. and Murata, K. (1972b). In Shinoda et al., p. 95.

Shimizu, R., Kataoka, Y., Ikuta, T., Koshikawa, T. and Hashimoto, H. (1976). J. Phys. D. 9, 101.

Shimizu, R., Kataoka, Y., Matsukawa, T., Ikuta, T., Murata, K. and Hashimoto, H. (1975). J. Phys. D. 8, 820.

Shimizu, R. and Murata, K. (1971). J. Appl. Phys. 42, 387.

Shinoda, G., Kohra, K. and Ichinokawa, T. eds (1972). Proc. 6th Int. Conf. on X-ray Optics and Microanalysis, University of Tokyo Press, Tokyo.

Smith, D.M. and Gallon, T.E. (1974). J. Phys. D. 7, 151.

Sommerkamp, P. (1970). Z. Angew. Physik. 28, 220.

Staib, P. and Kirschner, J. (1974). Appl. Phys. 3, 421.

Sternglass, E.J. (1954). Phys. Rev. 95, 345.

Streubel, P., Berndt, H. and Meisel, A. (1978). Kristall und

http://rcin.org.pl

Davison, S.G., ed., Pergamon Press, Oxford, Vol. 1, p. 155.

Hafner, H., Simpson, J.A. and Kuyatt, C.E. (1968). Rev. Sci. Instrum. 39, 33.

Hall, P.M. and Morabito, J.M. (1977). Surface Sci. 67, 373.

Hall, P.M. and Morabito, J.M. (1979). Surface Sci. 83, 391.

Hall, P.M., Morabito, J.M. and Conley, D.K. (1977). Surface Sci. 62, 1.

Harrower, G.A. (1956). Phys. Rev. 102, 340.

Harris, L.A. (1968). J. Appl. Phys. 39, 1419.

Harris, L.A. (1969). Surface Sci. 15, 77.

Heinrich, K.F.J. (1966). In Castaing et al., p. 159.

Holloway, P.H. (1975a). J. Electron Spectrosc. 7, 215.

Holloway, P.H. (1975b). J. Vac. Sci. Technol. 12, 1418.

Holloway, P.H. (1976). Solid State Comm. 19, 729.

Holloway, P.H. (1977). Surface Sci. 66, 479.

Holloway, P.H. (1978). In Scanning Electron Microscopy I, Johari, O. ed., O'Hare, p. 361.

Houston, J.E. (1973). Surface Sci. 38, 283.

Hunger, R.-J. and Köhler, L. (1979). Phys. Status Solidi (a), 56, K 45.

Iafrate, G.J., McAfee, W.S. and Ballato, A. (1976). J. Vac. Sci. Technol. 13, 843.

Ishikawa, K. and Tomida, Y. (1978). J. Vac. Sci. Technol. 15, 1123.

Jabłoński, A. (1977). Adv. Interface Colloid Sci. 8, 213.

Jabłoński, A. (1978). Surface Sci. 74, 621.

Jabłoński, A. (1979a). Surface Sci. 87, 539.

Jabłoński, A. (1979b). Surface Interface Anal. 1, 122.

Jabłoński, A. (1980a). Surface Interface Anal. 2, 39.

http://rcin.org.pl

Technik, 13, 441.

Tarng, M.L. and Wehner, G.K. (1973). J. Appl. Phys. 44, 1534.

Taylor, N.J. (1969). Rev. Sci. Instrum. 40, 792.

Tharp, L.N. and Scheibner, E.J. (1967). J. Appl. Phys. 38, 3320.

Tokutaka, H., Nishimori, K. and Takashima, K. (1977). Surface Sci. 66, 659.

Tung, C.J., Ashley, J.C. and Ritchie, R.H. (1979). Surface Sci. 81, 427.

Vašina, P. and Frank, L. (1979). J. Phys. E. Sci. Instrum. 12, 744.

Vignes, A. and Dez, G. (1968). J. Phys. D. 1, 1309.

Vrakking, J.J. and Meyer, F. (1973). Phys. Rev. A 9, 1932.

Vrakking, J.J. and Meyer, F. (1975). Surface Sci. 47, 50.

Weber, R.E. and Peria, W.T. (1967). J. Appl. Phys. 38, 4355.

Weeks, S.P. and Liebsch, A. (1977). Surface Sci. 62, 197.

Weinryb, E. and Philibert, J. (1964). Comptes Rendus Acad. Sci. Paris, 258, 4535.

Williams, F.L. and Nason, D. (1974). Surface Sci. 45, 377.

Wittry, D.B. (1966). In Castaing et al., p. 168.

Wood, B.J. and Wise, H. (1975). Surface Sci. 52, 151.

Zashkvara, V.V., Korsunskii, M.I. and Kosmachev, O.S. (1966). Zh. Tekh. Fiz. 36, 132; English transl. (1966). Sov. Phys.-Tech. Phys. 11, 96.

zam.346/o/82 n.300

B 229/83

http://rcin.org.pl

Biblioteka Instytutu Chemii Fizycznej PAN
F-B.229/83
70000000012576

http://rcin.org.pl